

**Isolation and characterization of novel
biomolecules during the mutualistic
interaction between *Piriformospora indica*
and *Arabidopsis thaliana***

Dissertation

**zur Erlangung des akademischen Grades
„doctor rerum naturalium“ (Dr. rer. nat.)**

**vorgelegt dem Rat der Fakultät für Biowissenschaften
der Friedrich-Schiller- Universität Jena**

**von Diplom-Agrarbiologe Johannes Thürich
geboren am 02.01.1986 in Karlsburg**

Gutachter

1. Prof. Dr. Erika Kothe

Lehrstuhl für Mikrobielle Kommunikation, Institut für Mikrobiologie,
Friedrich-Schiller-Universität Jena

2. Prof. Dr. Philipp Franken

Lehrstuhl für Molekulare Phytopathologie, Institut für Mikrobiologie,
Friedrich-Schiller-Universität Jena

3. Prof. Dr. Alga Zuccaro

Institut für Pflanzenwissenschaften
Universität zu Köln

Tag der öffentlichen Verteidigung: 18.06.2020

Table Of Contents

Table Of Contents	i
List Of Abbreviations	ii
List Of Tables And Graphs.....	iv
Chapter 1: General Introduction	1
I. Mycorrhiza	2
II. Tit For Tat.....	3
III. Plant-Microbial Communication	4
IV Endophytes.....	6
V. <i>Piriformospora indica</i>	7
Chapter 2: Manuscripts	12
Manuscript 1 A Poly(A) Ribonuclease controls the cellotriose-based interaction between <i>Piriformospora indica</i> and its host Arabidopsis.....	13
Manuscript 2 <i>Arabidopsis thaliana</i> responds to colonisation of <i>Piriformospora indica</i> by secretion of symbiosis-specific proteins	14
Manuscript 3 How does AtPARN connect RNA metabolism with Calcium signalling?.....	15
Chapter 3: General Discussion And Conclusion	16
I. General Discussion.....	17
II. Cellotriose And PARN	17
III. Secretome Analysis	22
Chapter 4: Summary & Zusammenfassung	27
I Summary	28
II Zusammenfassung	29
References	30
Supplementary Material	45
Acknowledgment.....	46
Ehrenwörtliche Erklärung	47

List Of Abbreviations

%	Percent
ABA	Absciscic Acid
AM	Arbuscular Mycorrhiza
AMF	Arbuscular Mycorrhiza Fungus
At	<i>Arabidopsis thaliana</i>
bp	Base Pair
[Ca ²⁺] _{cyt}	Cytosolic calcium
CCaMK	Calcium- and Calmodulin-dependent Protein Kinase
CERK1	Chitin Elicitor Receptor Kinase 1
CK	Cytokinin
CT	Cellotriose
CWE	Cell Wall Extract
Cycam	Cytosolic calcium mutant
CO	Chitooligosaccharides
DIP1	DELLA Interacting Protein 1
DNA	Deoxyribonucleic Acid
DPI	Days Post Inoculation
EMS	Ethyl Methane Sulfonate
ER	Endoplasmic Reticulum
ERF19	Ethylene Response Factor 19
ET	Ethylene
F6'H1	Feruloyl CoA Ortho-Hydroxylase 1
GA	Gibberellic Acid
GFP	Green Fluorescent Protein
GO-term	Gene Ontology-Term
HPLC	High Performance Liquid Chromatography
JA	Jasmonic Acid
JAZ	Jasmonate Zim-domain
K	Elemental Potassium

L135F	Substitution of Leucine at Position 135 with Phenylalanine
LCO	Lipo-Chitooligosaccharides
LRS	Legume-Rhizobium Symbiosis
LysM-RLK	(Lysin Motif) domain-containing Receptor Like Kinase
LPc	Lysophosphatidylcholine
MAMP	Microbial Associated Molecular Pattern
miRNA	micro RNA
MiSSP7	Mycorrhiza-Induced Small Secreted Protein 7
MYC	Mycorrhiza
N	Elemental Nitrogen
ncRNA	Non-Coding RNA
NFP	NOD factor perception
Nod	Nodulation
NSP2	Nodulation Signalling Pathway 2
P	Elemental Phosphorous
PIIN	<i>Piriformospora indica</i>
PLAT1	Polycystin, Lipoxygenase, Alpha-toxin and Triacylglycerol lipase 1
pMAQ2	Cytosolic Apoaquorin Construct
PARN	Poly(A) Specific Ribonuclease
RAM1	Reduced Arbuscular Mycorrhization 1
RNA	Ribonucleic Acid
ROS	Reactive Oxygen Species
RuBisCo	Ribulose-1,5-Bisphosphate Carboxylase/Oxygenase
SA	Salicylic Acid
SBT	Subtilisin-Like Protease
SNP	Single-Nucleotide Polymorphisms
SP7	Secreted Protein 7
SPE	Solid-Phase-Extraction

Abbreviations that were used in the manuscripts and units defined by the International System of Units are not given. The one letter code is used for amino acids (e.g. RXLR for arginine, unknown, leucine, arginine). *Genes* are written in italic and with lower case letters (with the exception of the first letter). **PROTEINS** are written with capitalized letters, *mnas* are written in italic and with lower case letters.

List Of Tables And Graphs

Table 1 Reported effects of <i>P. indica</i> on plant fitness	10
Table 2 Differentially regulated miRNA in <i>cycam</i>	21
Figure 1 <i>P. indica</i> grown in axenic culture	8
Figure 2 Alignment of PIIN_04111 and CEL3A	18
Figure 3 Parental lines and <i>cycam</i> and plants complemented with the PARN construct	19
Figure 4 Liquid culture of <i>A. thaliana</i> without and with <i>P. indica</i>	23
Figure 5 Impact of <i>P. indica</i> on the secretome of <i>A. thaliana</i>	24

Chapter 1:

General Introduction

I. Mycorrhiza

The term mycorrhiza was first coined by A.B. Frank, in 1885, to describe the widespread coating of tree roots with fungal mycelium (Trappe, 2005). Since the end of the 19th century a lot of studies on this mutualistic interaction between fungi and plants were performed. This form of symbiosis has been proven to exist for at least 460 million years and is found in 80-90% of all plant species both in monocotyledons and dicotyledons (Remy et al., 1994; Redecker, 2000; Bonfante and Genre, 2010; van der Heijden et al., 2015). Most of the fungal partners belong to the phyla *Glomeromycota* but several Basidiomycetes and Ascomyces can form mycorrhiza as well (Bonfante and Genre, 2010). Depending on the colonisation structure, mycorrhizal interaction can be classified into endomycorrhiza and ectomycorrhiza (Bonfante and Genre, 2015; van der Heijden et al., 2015). Fungi in an ectomycorrhizal interaction grow intercellularly and do not penetrate root cells. The main morphological characteristic of an ectomycorrhizal interaction is the Hartig net. This structure forms around and within the roots of the host and consists of fungal hyphae and plant cells (Tedersoo et al., 2010). An example for ectomycorrhizal symbiosis is the well-studied interaction between the Basidiomycete *Laccaria bicolor* and its host *Populus trichocarpa* (Martin and Nehls, 2009). In contrast to ectomycorrhizal fungi, endomycorrhizal fungi penetrate cells of the host. Endomycorrhiza can be classified into ericoidal, orchidial, and arbuscular mycorrhiza. Ericoidal and orchidial mycorrhizal symbioses occur only in a small number of plant species, whereas arbuscular mycorrhiza (AM) is the most prevalent type of symbiosis (van der Heijden et al., 2015). In natural communities, more than 100 metres of AM hyphae can be found per square centimetre of soil (Miller et al., 1995). Approximately 80% of all terrestrial plants can form an AM with fungi of the phylum *Glomeromycota*. In this interaction the fungi form tree-like structures (arbuscules) inside the inner cortical cells (Bonfante and Genre, 2010). All *Glomeromycota* are obligate biotroph and depend on a plantal partner to complete their lifecycle (Parniske, 2008).

II. Tit For Tat

As a result of their symbiosis, mycorrhizal plants can overcome unfavourable conditions. For example, abiotic stress such as drought, salinity, or heavy metal conditions can be counteracted (González-Guerrero et al., 2005; Miransari, 2010; Lenoir et al., 2016; Mariotte et al., 2018). But the main advantage for both partners in a mycorrhiza is the exchange of nutrients, mainly carbon and phosphorus (P). Up to 70% of the P acquired by mycorrhizal fungi is transported to its plantal partner and up to 90% of the total P which is found in the plant is derived from the fungal partner (Chiapello et al., 2015). Phosphate transporters such as MtPT4 from *Medicago truncatula* are specifically induced in the presence of arbuscular mycorrhiza fungi (AMF) (Javot et al., 2007a). In addition to phosphate transporters, mycorrhizal fungi possess transporters for the active uptake of ammonium from the soil and its subsequent transfer to the host plant (Govindarajulu et al., 2005; Guether et al., 2009). The transport of nutrients is constantly monitored by the plant. Lysophosphatidylcholine (LPC), a product of the phospholipid metabolism, can act as a signalling molecule and activates expression of phosphate transporter genes in plants (Parniske, 2008). The level of LPC and other substances can be measured by the plant cell (Javot et al., 2007b). Thus, a reduced transfer of nutrients from the fungal partner can cause a premature end of the symbiotic interaction (Javot et al., 2007b). Agricultural practices such as fertilization increase the amount of plant-available nutrients and subsequently reduce the level of mutualistic fungi in the soil significantly (Bakhshandeh et al., 2017; Mariotte et al., 2018).

In turn, 10%-50% of the plant's photoassimilates are transported to the fungal partner (van der Heijden et al., 2015). These photoassimilates are transferred to the fungus mainly as carbohydrates and fatty acids (Rich et al., 2017). These transfers of carbon and other molecules are sink-based and might be controlled by jasmonic acid (JA) (Hause et al., 2002). Interestingly, a single fungus can connect several different plants, creating the so called "wood wide web" (Simard et al., 1997; van der Heijden et al., 2015). In addition to nutrient exchange, mycorrhizal interactions have been shown to reduce the damage and infection rate of biotrophic and necrotrophic pathogens, as well as aphids, nematodes, fungi, and bacteria (Pinochet et al., 1996; Bruisson et al., 2016; Mustafa et al., 2017; Volpe et al., 2018). For example, wheat plants which are colonised by the AMF *Rhizophagus irregularis* (formerly known as *Glomus intraradices*), show a higher expression of defence-related genes as well as an increased production of defence compounds (Mustafa et al., 2017). Furthermore, the infection rate of *Blumeria graminis* f. sp. *tritici* in wheat plants can be reduced by almost 80% (Mustafa et al., 2017). Interestingly, it was reported that *Astragalus adsurgens* plants show a growth

promotional effect when grown in a mycorrhizal interaction but these plants are more susceptible against powdery mildew (Liu et al., 2018).

Mutualism, commensalism, and parasitism require a sophisticated communication between fungi and plants. Especially during the establishment of a mutualistic symbiosis, the release and exchange of different compounds into the rhizosphere and to the respective partner can be observed (Besserer et al., 2006; Bonfante and Anca, 2009; Schmitz and Harrison, 2014).

III. Plant-Microbial Communication

Plants secrete molecules which have an broad impact on the diversity and quantity of microorganisms in the rhizosphere (Azcón-Aguilar and Barea, 1996; Mariotte et al., 2018; Stringlis et al., 2018). For example, amino acids, sugars, organic acids, flavonoids, terpenoids, vitamins, enzymes, and gaseous molecules are released by plants (Dakora and Phillips, 2002). One of the major chemical mediators are phenolic compounds, which comprise up to 40% of the total released organic carbon (Hirsch et al., 2003). Examples for phenolic compounds are strigolactones (Ruyter-Spira et al., 2013). Initially, these substances were found in the secretome of cotton plants, where small quantities of phytohormones induce germination of the root-parasitic witchweed *Striga lutea* (Cook et al., 1966; Musselman, 1980). Strigolactones are produced under low P condition, play a role in auxin transport, and induce root growth (Ruyter-Spira et al., 2013; Shinohara et al., 2013). In addition, strigolactones and other phenolic compounds can act as attractants for AMF and nitrogen (N)-fixing *Rhizobiaceae* bacteria (Besserer et al., 2006; Parniske, 2008; Mandal et al., 2010). In AMF, strigolactones activate mitochondrial genes which in turns stimulate both germination of spores and branching of hyphae (Besserer et al., 2006).

In addition to plants, microbes secrete compounds which induce responses in plants as well. For example, plants which grow in the proximity of AMF or which are treated with germinating spore extracts from AMF, activate symbiosis-specific genes (Kosuta et al., 2003; Oláh et al., 2005). Furthermore, the germinating spore extracts from *Gigaspora margarita* induce a specific calcium signal in the host plant *Glycine max* but not in non-host plants such as *Arabidopsis thaliana* (Navazio et al., 2007).

In *Rhizobiaceae*, plant-derived phenolic compounds such as flavonoids or strigolactones act as direct promotor for *nod* (*nodulation*) genes (Peck et al., 2006; Mandal et al., 2010). *Nod* genes are involved in the production of lipo-chitooligosaccharides (LCOs), so called NOD factors. In general, LCOs have a chitooligosaccharide backbone that consists of four to five N-acetylglucosamine residues with

β 1–4 linkages. Depending on the species of *Rhizobiaceae*, different substitutions on the reducing and nonreducing end of the LCOs can be added (Liang et al., 2014).

LCOs were also found in AMF upon treatment with root extracts (Maillet et al., 2011; Liang et al., 2014). These fungal LCOs are called MYC (mycorrhiza) factors and increase colonisation, alter root architecture, and induce the expression of symbiosis marker genes in different plants such as *M. truncatula*, *G. max*, or *Oryza sativa* (Maillet et al., 2011; Schmitz and Harrison, 2014).

It is likely that the legume-rhizobium symbiosis (LRS) has evolved from the more ancient mycorrhizal interaction (Liang et al., 2014). Thus, it is not surprising that bacterial NOD factors and fungal MYC factors have a similar structure and activate similar genes as well as symbiotic pathways (Oldroyd, 2013). The respective host plant has to distinguish mutualistic bacteria and fungi from pathogens. LysM (Lysin Motif) domain-containing Receptor Like Kinases (LysM-RLKs) are involved all three symbiotic interactions (Oldroyd, 2013; Gough et al., 2018). LysM domains are found in the extracellular region of the host cell where they bind NOD and MYC factors at nanomolar concentrations (Oldroyd, 2013). LysM-RLKs are essential for the formation of nodules but only have a supporting role in mycorrhiza (Gough et al., 2018). It therefore seems likely that additional fungal signal and perception systems must exist in order to establish mycorrhiza.

Calcium signalling is a quick response pathway often used to link perception of external signals to the induction of specific genes (Vadassery and Oelmüller, 2009; Oldroyd, 2013; Edel et al., 2017). Upon stimulation by external stresses, the concentration of calcium in the cytosol ($[Ca^{2+}]_{cyt}$) increases drastically within seconds to minutes. Afterwards, the $[Ca^{2+}]_{cyt}$ binds to calcium binding proteins, is secreted from the cell, or is transported to internal storages such as mitochondria or the vacuole (Vadassery and Oelmüller, 2009). Depending on the amplitude, frequency, duration, and location of the calcium signal, a specific reaction for different stresses can be observed (Oldroyd, 2013; Zipfel and Oldroyd, 2017). Examples for substances which create a specific calcium signature are microbial associated molecular patterns (MAMPs) such as flagellin or chitin (Vadassery and Oelmüller, 2009), phytohormones (Meimoun et al., 2009), or LCOs (Genre et al., 2013).

Despite the structural similarity between fungal and bacterial LCOs, distinct calcium signals have been observed for the different organisms (Kosuta et al., 2008; Genre et al., 2013). One central protein for the decoding of the mutualistic calcium signalling is the Calcium- and Calmodulin-dependent Protein Kinase (CCaMK) (Oldroyd, 2013). CCaMK is essential for AM formation by phosphorylation and subsequent activation of the transcription factor CYCLOPS (Diédhiou and Diouf, 2018). Together with DELLA proteins and DIP1 (DELLA Interacting Protein 1), CYCLOPS forms a complex which promotes the expression of RAM1 (Reduced Arbuscular Mycorrhization 1)

(Diédhiou and Diouf, 2018). RAM1 and RAM2 are two transcription factors which are critically involved in colonisation of plants by AMF as well as pathogenic fungi (Gobbato et al., 2013). RAM1 induces the expression of different early symbiotic genes including RAM2. RAM2 has different roles including cell wall construction and promotion of hyphal formation (Diédhiou and Diouf, 2018).

CCaMK can decode and respond to calcium oscillation from NOD and MYC factors. Consequentially, additional signals must exist to help plants to differentiate between AMF and *Rhizobiaceae* (Oldroyd, 2013). Recently the central role of small ncRNAs (Non Coding RNAs) in the regulation of plant-microbial communication has emerged (Lelandais-Brière et al., 2016; Diédhiou and Diouf, 2018). Small ncRNAs can control gene expression on transcriptional and posttranscriptional level, and link phytohormones with gene regulation (Lelandais-Brière et al., 2016). Even transspecies acting small ncRNA have been reported (Cai et al., 2018). For example, after infection by the necrotrophic fungus *Botrytis cinerea*, *A. thaliana* secretes small ncRNAs which are transferred to the infection site. After uptake, the fungal pathogenicity genes are silenced (Cai et al., 2018).

In AM and LRS a central role of small ncRNAs has been reported as well (Lelandais-Brière et al., 2016). Exemplary, miR171h (microRNA 171h) silences NSP2 (Nodulation Signalling Pathway 2) which has diverse functions in AM and LRS (Lelandais-Brière et al., 2016). NSP2 is involved in strigolactone production prior to colonisation, formation of nodules, and the development of AMF (Diédhiou and Diouf, 2018). Furthermore, NSP2 interacts with RAM1 and *nsp2* mutants are colonised slower by AMF (Oldroyd, 2013). The exact interplay between perception of MYC factors, calcium signalling, miRNA-mediated gene regulation, and expression of symbiosis-specific genes is subject of ongoing research.

IV Endophytes

While a lot of work has been done on the ecological and agroeconomical impact of AMF, several limitations exist in studying this interaction. One major disadvantage is the obligate biotrophic lifestyle of AMF. With the exception of *R. irregularis*, *in vitro* cultivation of AMF is not easily possible (Hildebrandt et al., 2002; Parniske, 2008). This makes identification and characterization of signalling molecules from AMF and their respective host plants challenging. Furthermore, many genetic tools are not established for AMF and their respective host plants, and the model plant *A. thaliana* is not colonised by AMF (Veiga et al., 2013; Chiapello et al., 2015). In contrast to AMF, not so much data exists on mutualistic interactions between plants and endophytic fungi. Nonetheless,

endophytic fungi share similarities with AMF, can be cultivated *in vitro* on axenic media, and several genetic tools are available (Hilbert et al., 2012). In the present thesis an endophyte, called *Piriformospora indica* (also known as *Serendipita indica*) was used, to study beneficial traits in symbiotic interactions. Endophytic fungi have interacted with plants for 400 million years and depending on the environmental conditions, these interactions can shift from commensalism to parasitism, to mutualism (Lahrmann et al., 2015; Perotto et al., 2018). Endophytic fungi are a diverse group of organisms which have different taxonomic backgrounds but share a similar lifestyle. Endophytic fungi can inhabit different plant tissues as part of their life cycle, without necessarily causing harm to the host, but can live as soil saprophytes as well (Chiapello et al., 2015; Perotto et al., 2018). These diverse lifestyles are manifested in the genome of endophytes. For example, endophytic fungi have been shown to have enzymes required for degradation of plant cell walls or other plant components, as well as enzymes required for mutualism and parasitism (Schlegel et al., 2016; Perotto et al., 2018). Similar to AMF, mutualistic endophytic fungi improve plant growth, nutrient availability, and improve resistance against biotic and abiotic stresses (Perotto et al., 2018). Some endophytic fungi can have a broad host range and, depending on the environmental conditions or the respective host plant, the outcome of symbiosis can be changed (Petrini, 1991; Fesel and Zuccaro, 2016). For example, the Ascomycete *Meliniomyces variabilis* can form symbiotic interactions with Ericaceae and Brassicaceae plants (Ohtaka and Narisawa, 2008). In *Brassica campestris*, *M. variabilis* improves the plant fitness but when the endophyte colonises eucalyptus roots it does not have any impact on the plant fitness (Ohtaka and Narisawa, 2008).

V. *Piriformospora indica*

The endophytic fungus *P. indica* promotes plant growth and resistance against abiotic and biotic stress (Franken, 2012). *P. indica* belongs to the family Serendipitaceae (division Basidiomycota, class Agaricomycetes, order Sebaciniales) (Weiß et al., 2016). The endophyte was isolated in the Indian Thar Desert from the rhizosphere of the native bush *Zizyphus nummularia* and the invasive shrub *Prosopis juliflora* (Verma et al., 1998). Initial reports showed a growth promotional effect on different plant species such as maize or tobacco (Varma et al., 1999). *P. indica* can easily be cultivated *in vitro* (Johnson et al., 2011) and is used as a model organism to study mutualistic plant-symbiont interactions with different hosts (Figure 1) (Franken, 2012). *P. indica* forms mutualistic interactions with many plant species, including non-mycorrhizal plants such as *A. thaliana* (Table 1). In general,

the colonisation of plants by *P. indica* takes place in three phases during which the fungus manipulates various aspects of plant defences (Jacobs et al., 2011; Lahrman and Zuccaro, 2012; Xu et al., 2018). In the first phase, which can last between one to three days, the fungus grows around the root and on the root surface, initiating the first physical contact (Lahrman and Zuccaro, 2012). During this time an upregulation of fungal genes for hydrolytic enzymes and effector proteins can be observed (Lahrman and Zuccaro, 2012; Liu et al., 2019). At the same time an upregulation of plant genes associated with the production of lectins and hormones has been reported (Lahrman and Zuccaro, 2012). Furthermore, a higher level of different phytohormones can be observed (Vahabi et al., 2015; Xu et al., 2018). For example, *A. thaliana* plants show elevated levels of both salicylic acid (SA) and jasmonic acid (JA) two dpi (days post inoculation) with *P. indica* (Vahabi et al., 2015). The level of these two main plant-defence hormones is reduced once the mutualistic interaction is established (Vahabi et al., 2015). Another hormone, abscisic acid (ABA), which has been proposed to be a sensing mechanism for AMF (Stec et al., 2016), is also upregulated during *P. indica* colonisation (Peskan-Berghöfer et al., 2015). Higher level of exogenous ABA and drought stress enhances colonisation of the fungus, whereas ABA deficient plants are not as strongly colonised as wild-type plants (Peskan-Berghöfer et al., 2015).

In the second phase, after three to seven days, a biotrophic-like phase can be observed (Lahrman and Zuccaro, 2012). Fungal hyphae penetrate the outer layer of root cells with the help of cell wall degrading enzymes and grow inter- and intracellularly (Jacobs et al., 2011). The hyphae are especially present in the mature root, whereas they are only sparsely found in the elongation zone (Deshmukh et al., 2006). The vascular tissue and leaves of host plants are not regularly colonised (Schäfer et al., 2009). Interestingly, the fungal hyphae are surrounded by a plant-derived membrane which is similar to the AMF-plant periarbuscular membrane (Bonfante and Genre, 2010). During this second phase, genes and hormones associated with plant defence are downregulated (Lahrman and Zuccaro, 2012; Vahabi et al., 2015). For example, H_2O_2 accumulation and callose deposition is reduced and expression of cell-death-inducing genes is suppressed in colonised plants (Deshmukh and Kogel, 2007; Schäfer et al., 2009; Jacobs et al., 2011).

A third phase has been reported for barley seven to ten dpi (Lahrman and Zuccaro, 2012). During this “cell-death-associated-phase” several cortical and rhizodermal cells die and are filled with hyphae which later produce



Figure 1 *P. indica* grown for 28 days in axenic culture

chlamydospores (Deshmukh and Kogel, 2007). DELLA proteins are degraded by *P. indica* at the 7th dpi (Jacobs et al., 2011). This shows further similarities of *P. indica* to AMF, as DELLA proteins have been shown to be involved in RAM1 activation (Diédhiou and Diouf, 2018). DELLA proteins have been shown to act as negative regulators of gibberellic acid (GA) (Xu et al., 2018). GA is upregulated in the presence of *P. indica* and plants impaired in GA synthesis or GA perception showed reduced colonisation by the fungus (Xu et al., 2018).

In *A. thaliana*, this clear distinction between the three colonisation phases cannot be observed (Lahrmann and Zuccaro, 2012). For example, proteins associated with saprophytism and DELD effector proteins are upregulated in barley but not in *A. thaliana* at the late time point of colonisation (Lahrmann et al., 2013).

The aim of this thesis was to investigate the interaction between *P. indica* and *A. thaliana* with special focus on calcium signalling during the early phase of colonisation and the secretion of proteins during the establishment of symbiosis.

Table 1 Reported effects of *P. indica* on plant fitness

Impact on	Host plant	Main findings	Reference
Growth	<i>Artemisia annua</i> <i>Bacopa monnieri</i> <i>Nicotiana tabacum</i> <i>Petroselinum crispum</i> <i>Populus tremula</i> <i>Zea mays</i>	Increased biomass	(Varma et al., 1999)
Growth	<i>Adhatoda vasica</i>	Increased biomass	(Rai and Varma, 2005)
Growth	<i>A. thaliana</i>	Increased biomass	(Peskan-Berghofer et al., 2004)
Biotic stress resistance	<i>A. thaliana</i>	Increased resistance against <i>Golovinomyces oronii</i> (in dependence of JA and NPR1)	(Stein et al., 2008)
Biotic stress resistance	<i>A. thaliana</i>	Decreased fitness of root nematode <i>Heterodera schachtii</i>	(Daneskhah et al., 2013)
Growth	<i>A. thaliana</i>	Increased biomass (auxin transporter AUX1 plays a role in <i>B. campestris</i> but not in <i>A. thaliana</i>)	(Lee et al., 2011)
Biotic stress resistance	<i>B. campestris</i> sp. <i>chinensis</i>	Increased resistance against <i>Verticillium dahliae</i>	(Sun et al., 2014)
Growth	<i>A. thaliana</i>	Increased biomass	(Sharma and Agrawal, 2013)
Secondary metabolites	<i>A. annua</i>	Increased production of artemisinin	
Growth	<i>B. campestris</i> sp. <i>chinensis</i>	Increased biomass	(Sun et al., 2010)
Abiotic stress resistance		Increased resistance against drought Decreased production of reactive oxygen species (ROS) markers	
Abiotic	<i>Cassia angustifolia</i>	Increased resistance against copper	(Nanda and Agrawal, 2018)
Growth	<i>Centella asiatica</i>	Increased biomass	(Satheesan et al., 2012)
Secondary metabolites		Increased production of secondary metabolites	
Growth	<i>Cicer arietinum</i>	Increased biomass	(Nautiyal et al., 2010)
		Tripartite interaction with <i>Paenibacillus lentimorbus</i> showed strongest effect	
Growth	<i>C. arietinum</i>	Increased yield (independent of P uptake)	(Meena et al., 2010)
Biotic stress resistance	<i>C. arietinum</i>	Increased resistance against <i>B. cinerea</i>	(Narayan et al., 2017)
Growth	<i>Coleus forskohlii</i>	Increased biomass Higher survival rate of plants during the transfer from <i>in vitro</i> culture to the greenhouse	(Das et al., 2012)
Growth	<i>Foeniculum vulgare</i>	Increased biomass	(Dolatabadi et al., 2011)
Secondary metabolites		Increased production of secondary metabolites	
Growth Abiotic stress resistance	<i>Fragaria x ananassa</i>	Increased biomass in wild-type and growth impaired mutants Increased resistance against salt stress	(Husaini et al., 2012)
Growth	<i>G. max</i>	Increases biomass	(Rathod et al., 2011)
Abiotic stress resistance		Increased drought resistance (in dependence on the cultivar)	

Impact on	Host plant	Main findings	Reference
Growth	<i>Hordeum vulgare</i>	Increased yield	(Waller et al., 2005)
Abiotic stress resistance		Increased resistance against salt stress	
Biotic stress resistance		Increased resistance against <i>B. graminis</i> and <i>Fusarium culmorum</i>	
Biotic stress resistance	<i>H. vulgare</i>	Increased resistance against <i>Fusarium graminearum</i>	(Deshmukh and Kogel, 2007)
Biotic stress resistance	<i>H. vulgare</i>	Increased resistance against <i>B. graminis</i> f. sp. <i>hordei</i>	(Felle et al., 2009)
Biotic stress resistance	<i>Lens culinaris</i>	Decreased growth repression after infection with <i>Fusarium oxysporum</i> f. sp. <i>lentis</i>	(Kari Dolatabadi et al., 2012)
Growth	<i>Lycopersicon esculentum</i>	Increased biomass	(Fakhro et al., 2010)
Biotic stress resistance		Increased resistance against <i>V. dahliae</i>	
		Increased susceptibility against Pepino mosaic virus under low light	
Abiotic stress resistance	<i>M. truncatula</i>	Increased resistance against salt resistance	(Li et al., 2017)
Growth	<i>Nicotiana attenuate</i>	Increased biomass (independent of N and P)	(Barazani et al., 2005)
Growth promotion	<i>N. tabacum</i>	Increased biomass	(Sherameti et al., 2005)
Nutrient uptake		Increased uptake of N	
Abiotic stress resistance	<i>N. tabacum</i>	Increased resistance against cadmium stress	(Hui et al., 2015)
Abiotic stress resistance	<i>O. sativa</i>	Increased resistance against osmotic stress	(Saddique et al., 2018)
Growth	<i>Piper nigrum</i>	Increased biomass	(Anith et al., 2011)
Growth	<i>Populus</i> spp.	Increased biomass	(Kaldorf et al., 2005)
		Increased induction of necrosis in the presence of ammonium	
Growth	<i>Solanum lycopersicum</i>	Increased biomass and yield	(Sarma et al., 2011)
Nutrient uptake		Increased uptake of N, P, and potassium (K)	
Biotic stress resistance		Increased resistance against <i>F. oxysporum</i> f. sp. <i>lycopersici</i>	
Growth	<i>Triticum aestivum</i>	Increased biomass in nutrient depleted soil	(Serfling et al., 2007)
Biotic stress resistance		Increased resistance against <i>B. graminis</i> f. sp. <i>tritici</i> , <i>Pseudocercospora herpotrichoides</i> , and <i>F. culmorum</i> in vitro and (partially) in field trials	
Growth	<i>Vigna mungo</i>	Increased biomass	(Kumar et al., 2012)
Nutrient uptake		Increased uptake of N,P, and K	
Growth	<i>Withania somnifera</i>	Increased biomass	(Rai et al., 2001)
	<i>Spilanthes calva</i>		
Growth	<i>Z. mays</i>	Increased biomass	(Kumar et al., 2009)
Biotic stress resistance		Increased resistance against <i>Fusarium verticillioides</i>	
Nutrient uptake	<i>Z. mays</i>	Increased uptake of P	(Kumar et al., 2014)

Chapter 2: Manuscripts

Manuscript 1

A Poly(A) Ribonuclease controls the cellotriose-based interaction between *Piriformospora indica* and its host *Arabidopsis*

Joy M. Johnson, **Johannes Thürich**, Elena K. Petutschnig, Lothar Altschmied, Doreen Meichsner, Irena Sherameti, Julian Dindas, Anna Mrozinska, Christian Paetz, Sandra S. Scholz, Alexandra C.U. Furch, Volker Lipka, Rainer Hedrich, Bernd Schneider, Aleš Svatoš and Ralf Oelmüller

Published: Plant Physiology, March 2018, Vol. 176, pp. 2496–2514
www.plantphysiol.org/cgi/doi/10.1104/pp.17.01423

Summary

In this manuscript the role of cellotriose (CT) in the communication between *P. indica* and *A. thaliana* was described. CT was isolated in axenic culture of *P. indica* and induces a specific calcium signature which resembles signals from LCOs. *Cycam*, a mutant which is impaired in CT-induced calcium signalling, has a point mutation in the Poly(A) specific Ribonuclease (AtPARN). I complemented the *cycam* mutant plants and recovered the wild-type phenotype. Furthermore, I analysed the phenotype of the complemented plants.

A Poly(A) Ribonuclease Controls the Cellotriose-Based Interaction between *Piriformospora indica* and Its Host *Arabidopsis*^{1[OPEN]}

Joy M. Johnson,^a Johannes Thürich,^a Elena K. Petutschnig,^b Lothar Altschmied,^c Doreen Meichsner,^a Irena Sherameti,^a Julian Dindas,^d Anna Mrozinska,^a Christian Paetz,^e Sandra S. Scholz,^a Alexandra C.U. Furch,^a Volker Lipka,^b Rainer Hedrich,^d Bernd Schneider,^e Aleš Svatoš,^f and Ralf Oelmüller^{a,2}

^aDepartment of Plant Physiology, Matthias Schleiden Institute of Genetics, Bioinformatics, and Molecular Botany, Friedrich-Schiller-University, D-07743 Jena, Germany

^bDepartment of Plant Cell Biology, Albrecht von Haller Institute, Georg August University, 37077 Goettingen, Germany

^cLeibniz Institute of Plant Genetics and Crop Plant Research Gatersleben, 06466 Stadt Seeland, Germany

^dMolecular Plant Physiology and Biophysics, Julius-von-Sachs Institute for Biosciences, Biocenter, University of Würzburg, D-97082 Würzburg, Germany

^eResearch Group Biosynthesis/NMR, Max Planck Institute for Chemical Ecology, 07745 Jena, Germany

^fResearch Group Mass Spectrometry/Proteomics, Max Planck Institute for Chemical Ecology, 07745 Jena, Germany

ORCID IDs: 0000-0003-3383-0628 (J.M.J.); 0000-0002-0846-1878 (E.K.P.); 0000-0002-7692-2971 (L.A.); 0000-0002-3096-1844 (I.S.); 0000-0003-3224-1362 (R.H.); 0000-0003-4788-1565 (B.S.); 0000-0003-1032-7288 (A.S.); 0000-0002-3878-0044 (R.O.).

Piriformospora indica, an endophytic root-colonizing fungus, efficiently promotes plant growth and induces resistance to abiotic stress and biotic diseases. *P. indica* fungal cell wall extract induces cytoplasmic calcium elevation in host plant roots. Here, we show that cellotriose (CT) is an elicitor-active cell wall moiety released by *P. indica* into the medium. CT induces a mild defense-like response, including the production of reactive oxygen species, changes in membrane potential, and the expression of genes involved in growth regulation and root development. CT-based cytoplasmic calcium elevation in *Arabidopsis thaliana* roots does not require the BAK1 coreceptor or the putative Ca²⁺ channels TPC1, GLR3.3, GLR2.4, and GLR2.5 and operates synergistically with the elicitor chitin. We identified an ethyl methanesulfonate-induced mutant (*cytoplasmic calcium elevation mutant*) impaired in the response to CT and various other cellooligomers ($n = 2-7$), but not to chitooligomers ($n = 4-8$), in roots. The mutant contains a single nucleotide exchange in the gene encoding a poly(A) ribonuclease (AtPARN; At1g55870) that degrades the poly(A) tails of specific mRNAs. The wild-type PARN cDNA, expressed under the control of a 35S promoter, complements the mutant phenotype. Our identification of cellotriose as a novel chemical mediator casts light on the complex *P. indica*-plant mutualistic relationship.

Ca²⁺ signaling controls many processes in pathogenic and beneficial plant-microbe interactions (Oldroyd, 2013; Steinhorst and Kudla, 2014). In pathogenic interactions, cytoplasmic Ca²⁺ ([Ca²⁺]_{cyt}) elevation is initiated by cell surface receptors after activation by microbe-associated molecular patterns (MAMPs; like the bacterial flg22 for FLS2 and elf18 for the EF-Tu receptors or the fungal chitin for CERK1). Receptors activated by flg22 or elf18 bind to the coreceptor BRI1-ASSOCIATED RECEPTOR KINASE1 (BAK1), and the phosphorylated pattern recognition receptor (PRR) complexes associate with and phosphorylate BOTRYTIS-INDUCED KINASE1 and other signaling kinases to induce [Ca²⁺]_{cyt} elevation and downstream immune responses (Lu et al., 2010; Zhang et al., 2010; Shi et al., 2013; Li et al., 2014; Kadota et al., 2015). Besides local responses at the infection site, Ca²⁺, electric, and reactive oxygen species (ROS) waves transfer

threat information to distal tissues (Kiep et al., 2015; Gilroy et al., 2016). In interactions with biotrophic microbes, Ca²⁺ activates distinct CALCIUM-DEPENDENT PROTEIN KINASEs, which control host entry and facilitate the accommodation of pathogens in host cells by suppressing plant defense responses (Freymark et al., 2007; Chen et al., 2015). The different functions of Ca²⁺ in these pathogenic interactions are elicited by different Ca²⁺ signatures and decoded by a variety of Ca²⁺-binding proteins (Johnson et al., 2011a).

Colonization of legume roots by arbuscular mycorrhizal fungi is initiated by low-frequency Ca²⁺ spiking in epidermal cells induced by chitin tetramers and pentamers from exudates of germinating fungal spores (Kosuta et al., 2008; Chabaud et al., 2011; Genre et al., 2013; Gutjahr and Parniske, 2013). As soon as the fungus enters the cells, a shift from low- to high-frequency

Ca^{2+} spiking is observed (Sieberer et al., 2012), and the two types of Ca^{2+} spiking responses do not propagate to neighboring cells (Miwa et al., 2006; Sieberer et al., 2009; Capoen et al., 2011). The Ca^{2+} channels that mediate these responses have not yet been identified; however, activation of the potassium channels DMI1 from *Medicago truncatula* or CASTOR and POLLUX from *Lotus japonicus* could lead to the opening of putative voltage-gated Ca^{2+} channels (Peiter et al., 2007; Charpentier et al., 2008; Venkateshwaran et al., 2012). In contrast to pathogenic interactions, cytoplasmic Ca^{2+} elevation induced by beneficial microbes does not result in massive ROS production (Vadassery et al., 2009).

Besides pathogenic and mycorrhizal fungi, plants interact with numerous endophytes (Johnson et al., 2011a). The root-colonizing endophytic fungus *Piriformospora indica*, which was isolated originally from the rhizosphere of two woody shrubs in the Indian Thar Desert (Verma et al., 1998), colonizes the roots of a broad host range, including the model plant *Arabidopsis thaliana* (Franken, 2012; Lahrmann et al., 2013; Bakshi et al., 2015; Weiß et al., 2016). It does not cause pathogenic symptoms (Sherameti et al., 2005; Yadav et al., 2010; Johri et al., 2015) but promotes root and shoot biomass production (Peškan-Berghöfer et al., 2004; Camehl et al., 2011; Lee et al., 2011; Das et al., 2012), induces early flowering (Das et al., 2012), and enhances the plant's resistance to various biotic and abiotic stresses (Waller et al., 2005; Baltruschat et al., 2008; Sherameti et al., 2008; Schäfer et al., 2009; Achatz et al., 2010; Knecht et al., 2010; Das et al., 2012; Lahrmann and Zuccaro, 2012; Daneshkhah et al., 2013; Sun et al., 2014). The fungus releases a chemical compound into its environment that induces rapid (within 90 s) $[Ca^{2+}]_{cyt}$ elevation in *Arabidopsis* and tobacco (*Nicotiana tabacum*) roots (Vadassery et al., 2009). Here, we demonstrate that the Ca^{2+} -inducing compound

from *P. indica* is cellotriose (CT) and that the $[Ca^{2+}]_{cyt}$ response in *Arabidopsis* roots requires the poly(A) ribonuclease PARN.

RESULTS

CT Induces $[Ca^{2+}]_{cyt}$ Elevation

Cell wall extract (CWE) from *P. indica* induces $[Ca^{2+}]_{cyt}$ elevation in *Arabidopsis* and tobacco roots (Vadassery et al., 2009). To identify the compound triggering the elevation, we combined various chromatographic steps (see "Materials and Methods"; Supplemental Fig. S1). The structure of the purified compound was elucidated by high-resolution mass spectrometry as a trisaccharide ($C_{18}H_{32}O_{16}$; Fig. 1). NMR experiments (1H -NMR [Supplemental Fig. S2], selective total correlation [seTOCSY; Supplemental Fig. S3], and 1H , 1H -double quantum filtered correlation [1H , 1H -DQF-COSY; Supplemental Fig. S4]) at 700 MHz using a highly sensitive 1.7-mm microcryoprobe indicated the trisaccharide to consist of three hexopyranose units. Based on their characteristic coupling constants, all of these hexopyranose units were identified as Glcs. The low-field chemical shifts of the protons in the 4-positions suggested 1→4 linkage of the Glc units. According to these data, the structure of the trisaccharide was identified as CT. Comparison with the heteronuclear single quantum coherence-NMR spectrum of authentic CT (Fig. 1B) confirmed the suggested structure.

Chemically pure CT (Sigma-Aldrich) induces dose-dependent $[Ca^{2+}]_{cyt}$ elevations in *Arabidopsis* roots in the nanomolar range. After a lag phase of 15 to 20 s, the $[Ca^{2+}]_{cyt}$ level begins to rise, and a sharp peak of 507 ± 6 nM at 40 ± 5 s was observed (Fig. 2, A and B). The peak response is followed by a slow and gradual decrease of the $[Ca^{2+}]_{cyt}$ level. Besides roots, leaf $[Ca^{2+}]_{cyt}$ responded to CT too, although ~5 times weaker. To test whether the CT-inducing $[Ca^{2+}]_{cyt}$ activity shows refractory behavior, we initially activated the roots with the CWE and, 10 min later, applied a CT stimulus. When the $[Ca^{2+}]_{cyt}$ level induced by the first stimulus declined, the second stimulus was reduced strongly compared with the initial one (Fig. 2C). This indicates that both stimuli activate the same perception/signaling system.

To test the specificity of the sugar moiety, the $[Ca^{2+}]_{cyt}$ response to Glc and different cellooligomers ($n = 2-7$) was compared with CT (Fig. 2D). Glc (data not shown) and CWE or CT after acid hydrolysis (Fig. 2A) did not induce $[Ca^{2+}]_{cyt}$ elevation. This indicates that CT is an active compound of *P. indica* CWE that induces $[Ca^{2+}]_{cyt}$ elevation in *Arabidopsis* roots. We also identified $[Ca^{2+}]_{cyt}$ -inducing activity in concentrated culture medium after the removal of *P. indica* hyphae (Fig. 2E), which showed the same refractory behavior to a second application of CT but not to chitin (Fig. 2H). Since no response was obtained with the concentrated medium alone, CT is likely to be released by *P. indica* into the medium. Finally, various combinations of CT with pathogen-associated molecular patterns and

¹ The work was supported by the Deutsche Forschungsgemeinschaft (ChemBioSys; CRC1127).

² Address correspondence to ralf.oelmueller@uni-jena.de.

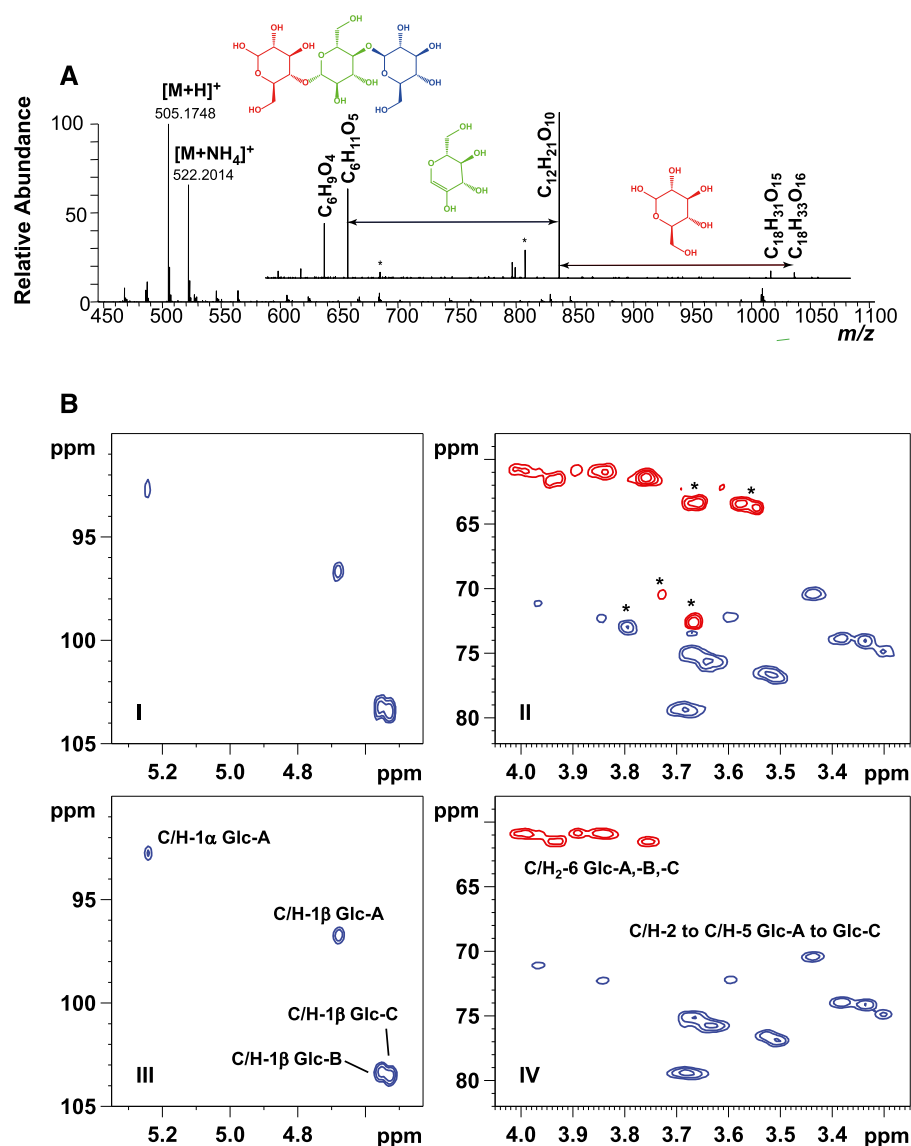
The author responsible for distribution of materials integral to the findings presented in this article in accordance with the policy described in the Instructions for Authors (www.plantphysiol.org) is: Ralf Oelmueller (ralf.oelmueller@uni-jena.de).

J.M.J. performed isolation of mutant, isolation of CT, and physiological Ca^{2+} experiments; J.T. performed complementation and analysis of mutant; E.K.P. performed SNP analyses; L.A. performed Illumina (100-bp paired-end) sequencing; D.M. performed microarrays and data analysis; I.S. performed ROS analyses and supervision of A.M., J.M.J., and J.T.; J.D. performed electrophysiology; A.M. performed cellooligomer, ABA, and RBOHD experiments; C.P. performed NMR analyses; S.S.S. performed physiological experiments and supervision of J.T.; A.C.U.F. performed supervision of J.T. and D.M.; V.L. performed SNP analyses; R.H. performed electrophysiology; B.S. performed NMR analysis; A.S. performed supervision of J.M.J. for purification of cellotriose and structural elucidation of cellotriose; R.O. devised the concept, supervised the work, and wrote the article; all authors read and approved of the article.

[OPEN] Articles can be viewed without a subscription.

www.plantphysiol.org/cgi/doi/10.1104/pp.17.01423

Figure 1. Purification of the fungal compound inducing $[Ca^{2+}]_{\text{cyt}}$ elevation from the *P. indica* CWE. The active compound was purified from the CWE based on its property to induce $[Ca^{2+}]_{\text{cyt}}$ elevation. Ultra-performance liquid chromatography/mass spectrometry, tandem mass spectrometry, and 2D-NMR data were used for structure elucidation. A, Mass spectrometry spectrum corresponding to the peak at 10.46 min. The inset graph is a fixed precursor (505.2 \pm 1 D). The collision-induced dissociation scan spectrum was obtained at 7 eV normalized fragmentation energy with the annotated molecular compositions and indicated neutral losses. B, NMR spectra of the CT-containing sample from *P. indica* (I and II) and CT standard sample (III and IV). I and III, Region of anomeric centers of Glc-A to Glc-C. II and IV, Region of C/H-2 to C/H-6 of Glc-A to Glc-C. Methylene signals (CH₂) are shown in red, and methine signals (CH) are shown in blue. *, Signals of contamination. Vertical axes, ΔC (175 MHz); horizontal axes, ΔH (700 MHz).



cellooligomers either as first or second stimulus confirmed that the tested pathogen-associated patterns operate independently of the cellooligomers for full induction of the Ca^{2+} response, while cellooligomers activate the same perception and/or early signaling system leading to $[Ca^{2+}]_{\text{cyt}}$ elevation (Supplemental Table S1).

Identification of Mutants Defective in CT-Dependent $[Ca^{2+}]_{\text{cyt}}$ Elevation

To identify Arabidopsis mutants impaired in the Ca^{2+} response to CWE from *P. indica*, an ethyl methanesulfonate population generated from the pMAQ2 aequorin line was screened. The screen was performed with roots from individual 18-d-old M2 seedlings, and generation of $[Ca^{2+}]_{\text{cyt}}$ luminescence signals induced by the CWE was monitored with a plate-reader luminometer.

Screening of ~75,000 individual M2 plants identified three mutants that did not induce any $[Ca^{2+}]_{\text{cyt}}$ elevation in response to the CWE (null mutants). Five mutants showed a reduced $[Ca^{2+}]_{\text{cyt}}$ response, along with variations in lag phase, peak, and decline to the resting $[Ca^{2+}]_{\text{cyt}}$ level. To confirm their impaired Ca^{2+} phenotype, all eight mutants were transferred to soil to obtain M3 and M4 seeds by self-fertilization. Genetic analyses of crosses documented that the three null mutants are allelic, and we named the mutant *cytoplasmic calcium elevation mutant* (*cycam*). The mutant also failed to induce $[Ca^{2+}]_{\text{cyt}}$ elevation in response to pure CT (Fig. 2F). After backcrossing to the wild type (Columbia-0 [Col-0] or Landsberg [La]), $[Ca^{2+}]_{\text{cyt}}$ elevation to CT was restored in ~25% of F2 progeny ($P < 0.05$), indicating that the mutation is recessive.

To test whether the loss of $[Ca^{2+}]_{\text{cyt}}$ elevation in the *cycam* mutant is specific for the *P. indica* CWE, we tested CWEs from other beneficial (e.g. *Mortierella hyalina* and

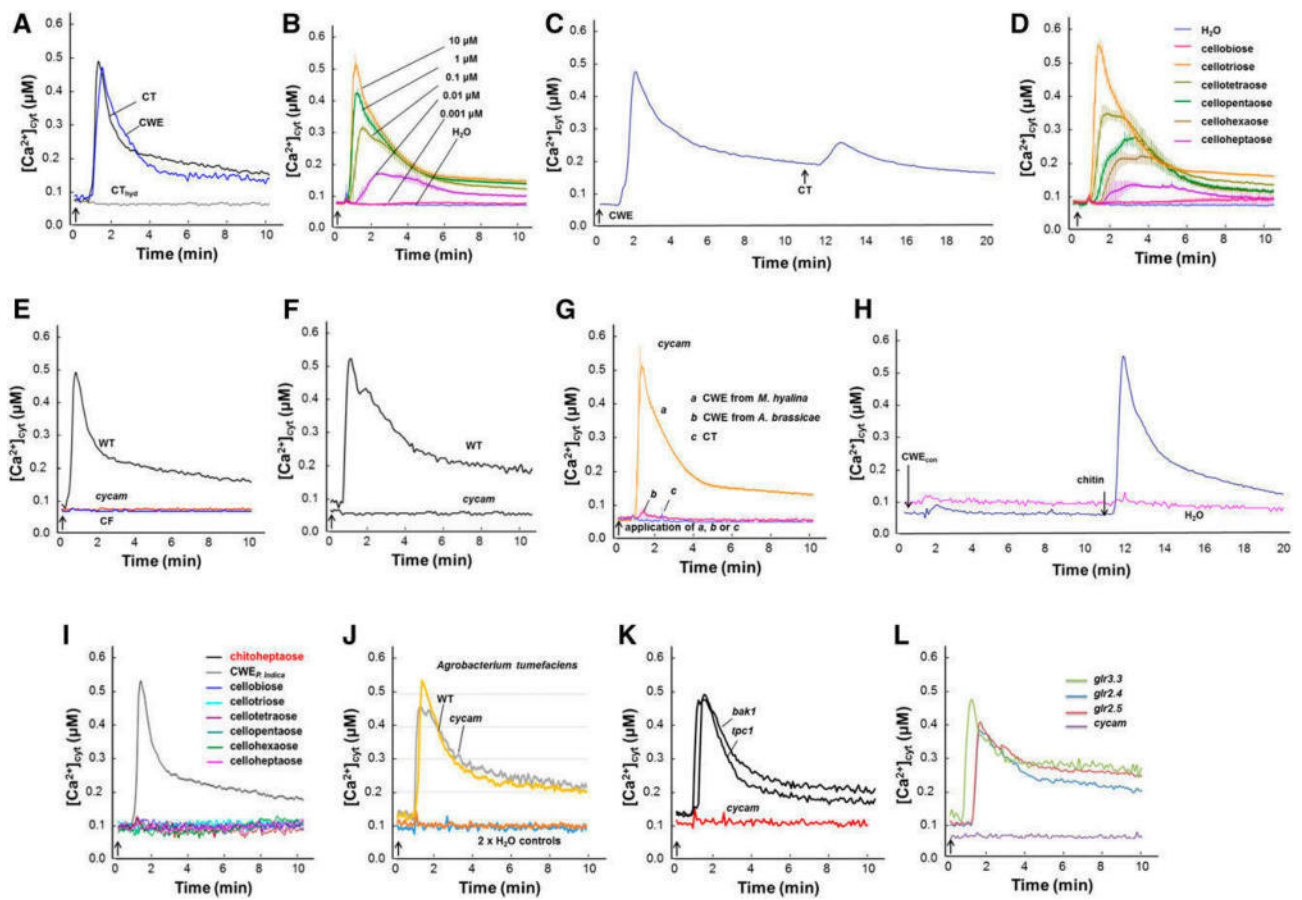


Figure 2. $[Ca^{2+}]_{cyt}$ elevation in the roots of 18-d-old wild-type (WT) or mutant *Arabidopsis* seedlings expressing cytosolic aequorin. Arrows indicate the application of CT, cellooligomers or chitooligomers, CWEs from fungi or *A. tumefaciens*, or an exudate fraction from *P. indica*. A, $[Ca^{2+}]_{cyt}$ elevation after the application of 50 μ L of CT (10 μ M), 50 μ L of CWE, or a CT solution after acid hydrolysis (CT_{hyd}), as described in "Materials and Methods." B, Dose-dependent increase in $[Ca^{2+}]_{cyt}$ elevation after CT application. C, Roots were first exposed to 50 μ L of CWE and, after 10 min, to 50 μ L of CT. D, $[Ca^{2+}]_{cyt}$ elevation induced by different cellooligomers (1 μ M). Error bars ($n = 40$) show significant differences between the triose form and the other oligomers. E, $[Ca^{2+}]_{cyt}$ elevation induced by a concentrated culture filtrate from *P. indica*. A 2-week-old culture filtrate of *P. indica* was clarified by high-speed centrifugation (30 min, 250,000g) and concentrated in a lyophilizer before $[Ca^{2+}]_{cyt}$ elevation was determined in the roots of wild-type and *cycam* seedlings. CF, Culture filtrate without the fungus. F, CT induces $[Ca^{2+}]_{cyt}$ elevation in the roots of wild-type, but not *cycam*, seedlings. G, A CWE from *M. hyalina*, but not from *A. brassicae*, induces $[Ca^{2+}]_{cyt}$ elevation in the roots of *cycam* seedlings. CT was used as a control. H, Chitin (chitoheptaose), but not the concentrated CWE from *P. indica* (CWE_{con}), induces $[Ca^{2+}]_{cyt}$ elevation in roots of *cycam* mutants. H₂O, Water control. I, Chitoheptaose, but not cellooligomers, induces $[Ca^{2+}]_{cyt}$ elevation in *cycam* roots. J, A CWE from *A. tumefaciens* induces $[Ca^{2+}]_{cyt}$ elevation in wild-type and *cycam* roots. K and L, CT induces $[Ca^{2+}]_{cyt}$ elevation in the *bak1* and *tpc1* (K), *glr3.3*, *glr2.4*, and *glr2.5* (L) knockout lines. Roots of *cycam* seedlings were used as a control.

Periconia macrospinosus) and pathogenic (e.g. *Alternaria brassicae* and *Verticillium dahliae*) fungi. Three extracts induce $[Ca^{2+}]_{cyt}$ elevation in the wild-type aequorin line and the *cycam* mutant. The CWE from *A. brassicae* induced $[Ca^{2+}]_{cyt}$ elevation in the wild type but not in the *cycam* mutant (Fig. 2G). Crosses between the *cycam* mutant and a previously described mutant not responding to the CWE from *A. brassicae* (Johnson et al., 2013) and analyses of the Ca^{2+} responses of the F1 seedlings demonstrate that they are allelic (see below). This demonstrates that the *cycam* mutation prevents $[Ca^{2+}]_{cyt}$ elevation in response to extracts from a beneficial and a pathogenic fungus. In an independent screen, we isolated

an *Arabidopsis* mutant with an altered $[Ca^{2+}]_{cyt}$ response to a CWE from *M. hyalina* (E. Seebald and R. Oelmüller, unpublished data). The $[Ca^{2+}]_{cyt}$ response of this mutant to CT is identical to that of the wild type. Furthermore, a Leu-rich-repeat protein (At1g13230) is required for the beneficial interaction of the two symbionts (Shahollari et al., 2007). However, a knockout line for this protein was not impaired in the Ca^{2+} response (Supplemental Table 1B), suggesting that the protein is not part of the early Ca^{2+} signaling system or located downstream of it. To further characterize the *cycam* mutant, we tested its response to flg22 and chitin. The Ca^{2+} signals triggered by both well-known

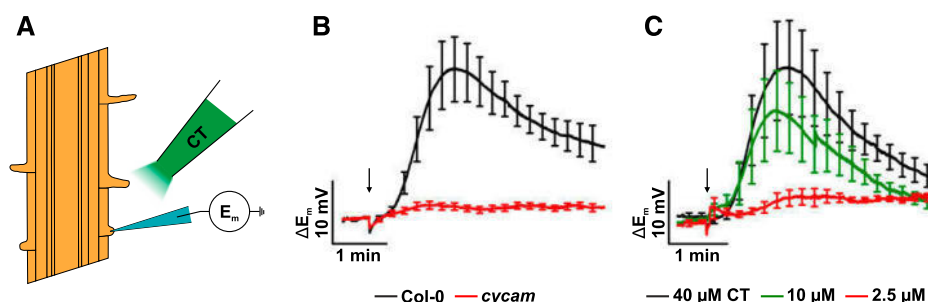


Figure 3. CT induces CYCAM-dependent root hair plasma membrane depolarization. A, Cartoon of the experimental setup. Microelectrodes, impaled into bulging root hair cells, measured the plasma membrane potential, while CT was applied locally via application pipettes. B, Average depolarization of the Col-0 and *cycam* root hair plasma membranes. CT was applied at a concentration of 40 μM for 1 s (arrow). Error bars show SE; $n = 8$. C, Average dose-dependent depolarization of the Col-0 root hair plasma membrane. CT was applied at the indicated concentrations for 1 s (arrow). Error bars show SE; $n = 5$.

elicitors in the *cycam* mutant were comparable with the wild type (Fig. 2H, shown for chitin). The *cycam* mutant also is defective in inducing $[\text{Ca}^{2+}]_{\text{cyt}}$ elevation in response to other cellooligomers ($n = 2\text{--}7$; Fig. 2I), whereas the responses to chitoooligomers ($n = 5\text{--}8$) were not affected (Fig. 2, H and I, shown for chitoheptaose). The differences in the CT/cellooligomer and chitoooligomer responses demonstrate that *cycam* is defective in cellooligomer recognition or signaling.

Sharma et al. (2008), Glaeser et al. (2016), and Guo et al. (2017) demonstrated that *P. indica* forms an intimate association with *Rhizobium radiobacter* F4, an α -proteobacterium. The endophytic bacterium shows a high degree of similarity to the plant pathogenic *R. radiobacter* (formerly, *Agrobacterium tumefaciens* C58), except for distinct differences in both the tumor-inducing and the accessory plasmids, which can explain the loss of its pathogenicity (Glaeser et al., 2016). A CWE from the disarmed *A. tumefaciens* GV3101 induced $[\text{Ca}^{2+}]_{\text{cyt}}$ elevation in both wild-type and *cycam* roots (Fig. 2J). This demonstrates that both Ca^{2+} -inducing activities are different and that CT is likely of fungal and not bacterial origin. The absence of Ca^{2+} -inducing activity in the *P. indica* CWE in *cycam* suggests that the amount of bacterial effector in this preparation is either too low for detection or not present.

Exploration of the Signaling Pathway Underlying the CT-Induced $[\text{Ca}^{2+}]_{\text{cyt}}$ Response

$[\text{Ca}^{2+}]_{\text{cyt}}$ elevation is induced by MAMP-activated receptor complexes in which BAK1 often functions as a coreceptor. CT induces $[\text{Ca}^{2+}]_{\text{cyt}}$ elevation in aequorin lines in the *bak1* knockout background similar to the wild type (Fig. 2K). Furthermore, the roots of mutants for the proposed calcium channel GLU-LIKE RECEPTORS (GLR2.4, GLR2.5, and GLR3.3) and vacuolar TWO PORE CHANNEL1 (TPC1) in the aequorin background also were not impaired in CT-induced $[\text{Ca}^{2+}]_{\text{cyt}}$ elevation (Fig. 2L). These data suggest that neither BAK1 as coreceptor nor the calcium channels tested are involved in CT signaling.

Early Downstream Responses to CT-Induced $[\text{Ca}^{2+}]_{\text{cyt}}$ Elevation

MAMP-triggered Ca^{2+} responses are associated with changes in plasma membrane potentials and the generation of ROS or H_2O_2 and interplay between the three responses is proposed to be involved in systemic signaling (Gilroy et al., 2016). When *Arabidopsis* roots were impaled with voltage-recording microelectrodes, resting potentials of -163 mV for the wild type ($\text{SE} = 3$ mV; $n = 23$) and -166 mV for *cycam* ($\text{SE} = 4$ mV; $n = 8$) were measured (Fig. 3). Following the application of CT stimulus, wild-type root cells depolarized in a dose- and time-dependent manner in the wild type. Membrane responses were elicited at CT concentrations of above 2.5 μM . Signals were transient in nature, and the delay time between stimulus onset and membrane response time decreased with increasing CT concentration. Local application of 40 μM CT to wild-type roots induced the plasma membrane depolarization of bulging root hair cells with average amplitudes of 27 mV ($\text{SE} = 4$; $n = 13$). Under the same conditions, CT in *cycam* roots did not trigger the depolarization of the plasma membrane (Fig. 3).

CT also induces H_2O_2 production in wild-type roots; however, compared with chitin, the response was low (Fig. 4). Since no ROS production is detectable in *cycam* roots, CT-induced generation of Ca^{2+} , ROS, and electrical signals is genetically linked (see "Discussion"). However, if both MAMPs are applied to the roots together (either simultaneously, as shown in Fig. 4, or successively in either sequence within 8 h), the initial H_2O_2 production is higher than that of the sum of the two individual treatments. This suggests a synergistic effect of the two elicitors on H_2O_2 production (see below). Furthermore, comparable to chitin, barely any H_2O_2 production can be induced by CT in *rbodD* roots (chitin, $3,111 \pm 451$ relative light units [RLU] in the wild type versus 155 ± 22 RLU in *rbodD*; CT, 988 ± 108 RLU in the wild type versus 81 ± 9 RLU in *rbodD* [$n = 5$]), suggesting that, as with chitin, NADH oxidase D is the major ROS producer in response to CT too.

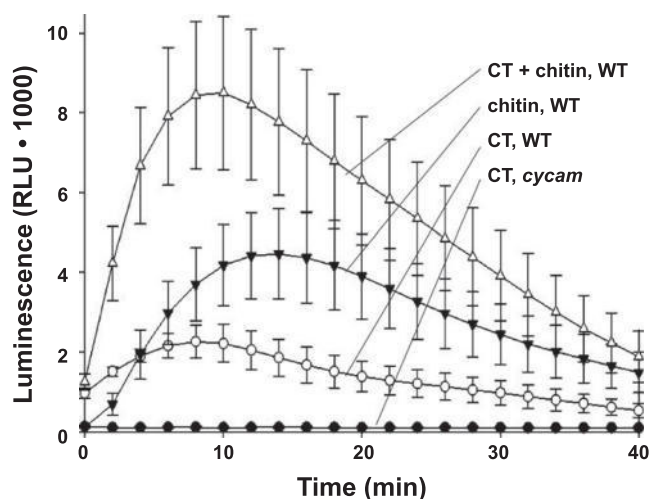


Figure 4. CT induces CYCAM-dependent H_2O_2 production in Arabidopsis roots and cooperates with chitin-induced H_2O_2 production. H_2O_2 production is shown in roots of 18-d-old wild-type (WT) and *cycam* seedlings challenged with 50 μ L of CT or chitin or CT + chitin (10 μ M; application at time 0). Data are based on eight independent experiments; error bars represent SE.

CT Promotes *RBOHD* and Defense Gene Expression

Since chitin-mediated H_2O_2 production is stimulated by CT application (Fig. 4), the *RBOHD* mRNA level is induced rapidly by CT and chitin (Fig. 5), and *RBOHD* is required for CT-induced H_2O_2 production, we investigated the interplay between CT and chitin on

RBOHD expression. CT was applied to Arabidopsis roots 8, 2, or 0 h before chitin application, and the accumulation of *RBOHD* mRNA was monitored within the first 30 min (Fig. 6). Simultaneous application of CT and chitin to the roots (time 0) had no significant effect on *RBOHD* mRNA accumulation within the first 10 min, whereas after 20 and 30 min, a comparable stimulation was observed for both elicitors. The effects of both elicitors on *RBOHD* mRNA accumulation was additive, which can be explained either by independent effects or a stimulating/amplifying effect of one elicitor on the action of the other elicitor. However, if CT was applied 2 or 8 h before chitin application, the chitin-induced *RBOHD* mRNA level was much higher after 10 min compared with the treatment with chitin alone. This suggests that CT cooperates with chitin to induce *RBOHD* expression and that a CT pretreatment to the roots establishes conditions that allow a faster and stronger accumulation of *RBOHD* mRNA in response to chitin. Downstream of the membrane-delimited steps addressed above, early elicitor responses can be seen at the level of the expression of genes that serve as defense markers, such as *MAPK3*, *ZAT12*, *NPR1*, and *LOX1*. Within 30 min, the mRNA levels of *RBOHD*, *MAPK3*, and *ZAT12* are up-regulated after CT application to wild-type, but not *cycam*, roots (Fig. 5). Chitin, however, induced the mRNAs in *cycam* roots too (Fig. 5). In contrast to H_2O_2 production (Fig. 4), which was less induced by CT compared with chitin in the wild type, the stimulatory effect of the two elicitors on these mRNA levels is comparable (Fig. 5). The mRNA levels for the hormone marker genes *NPR1* and *LOX1*

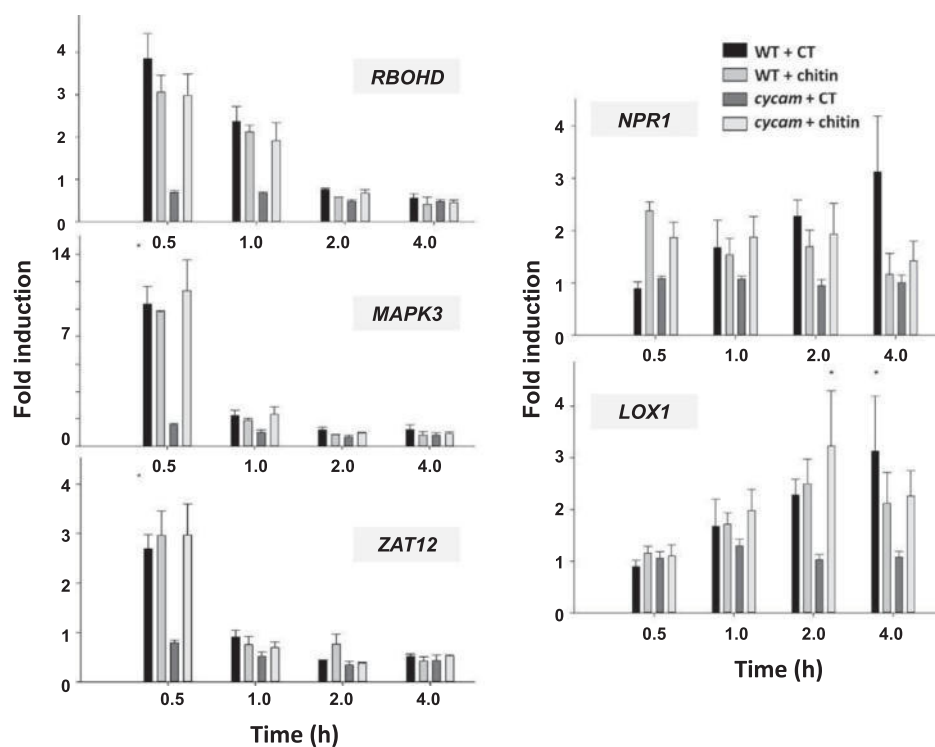


Figure 5. CT- or chitin-induced accumulation of transcripts in wild-type (WT) and *cycam* roots. The data show fold induction of the mRNA levels relative to the mock-treated controls with water. Samples were analyzed by quantitative real-time PCR (RT-qPCR). Data are based on four independent experiments; error bars represent SE.

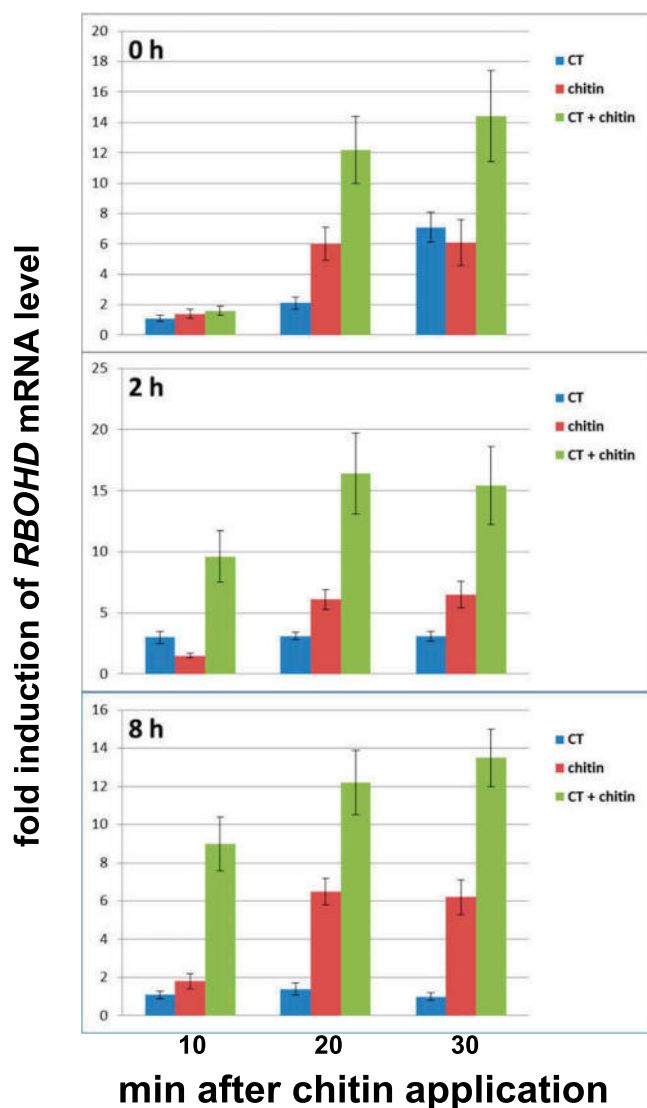


Figure 6. Accumulation of *RBOHD* mRNA in response to CT, chitin, and both elicitors. 0 h, CT, chitin, or CT + chitin was applied to Arabidopsis roots, and *RBOHD* mRNA accumulation was determined by RT-qPCR 10, 20, and 30 min after elicitor application. For the reference value, water was applied to the roots. 2 h and 8 h, CT was applied 2 and 8 h before chitin. The data show fold induction of the *RBOHD* mRNA levels relative to the mock-treated controls with water. Data are based on four independent experiments; error bars represent SE.

respond less and later to CT application, and significant differences can only be seen 2 to 4 h after elicitor application (Fig. 5). These results demonstrate the involvement of the *cycam* gene product in CT-induced defense gene activation.

cycam Is Defective in a PARN

CYCAM was mapped on chromosome 1 using the ARMS primer set (Schäffner, 1998) with 25 F2 mutant individuals of crosses between *cycam* (cytosolic

apoaquorin in the Col-0 background) and the wild type (in the La background). Backcrossing of *cycam* to the aequorin line used for mutagenesis (Col-0 background) followed by Illumina sequencing of two DNA pools from F2 individuals with and without the *cycam* phenotype identified a target interval on the lower arm of chromosome 1 containing two candidate genes (Supplemental Fig. S5), one of which encodes AtPARN. This nuclease is a eukaryotic poly(A)-degrading deadenylase that efficiently degrades poly(A) tails of selective mRNAs and, thus, reduces their translation efficiency (Virtanen et al., 2013).

As expected from a mutant defective in poly(A) tail degradation and compared with the wild type, the overall growth of *cycam* plants appeared less synchronized and adult plants showed a stunted phenotype, which was caused mainly by reduced stem lengths. The numbers of leaves of each adult *cycam* and wild-type plant, grown in the greenhouse, were the same, whereas the fresh weights of the mutant leaves were reduced by $18.8\% \pm 7.2\%$ ($n = 73$ plants). Full-length PARN cDNAs were isolated from wild-type and *cycam* plants. Sequence analyses demonstrated that a point mutation (C→T) at position 403 downstream of the A of the ATG start codon in the mutant resulted in a Leu-to-Phe amino acid exchange (L135F).

The wild-type cDNA sequence was expressed in *cycam* plants under the control of the 35S promoter, and four transformants were analyzed in more detail. The visible mutant phenotype was rescued by the transformation. After CT application to the roots, the $[Ca^{2+}]_{cyt}$ elevation response was recovered (Fig. 7A). Expression of the 35S::PARN construct in wild-type plants did not cause any visible phenotype, and the plants looked like the untransformed wild type. These transformants also showed the same Ca^{2+} responses after CT application as the untransformed wild type, suggesting that the Ca^{2+} response and the performance of the plant are not limited by the amount of PARN mRNA in the wild type. The *cycam* mutant contains elevated abscisic acid (ABA) levels (Johnson et al., 2013, and refs. therein for comparable *parn* mutants), and the ABA levels in seedlings of the four rescued mutant lines were reduced by ~50% (Fig. 7B). Again, no difference was observed for wild-type plants transformed or not transformed with the 35S::PARN construct. Interestingly, 1 mM chitin applied to the roots of wild-type seedlings resulted in stomata closure in the leaves, while the stomata in the *cycam* leaves remained closed due to the elevated ABA level. The stomata in the rescued mutants are open and closed after application of 1 mM chitin, comparable to the wild type (data not shown). Again, higher expression of PARN under the control of the 35S promoter in wild-type plants did not result in any change in stomata opening in comparison with the untransformed wild type. Thus, the single amino acid exchange in the mutant PARN protein appears to be responsible for the observed phenotype.

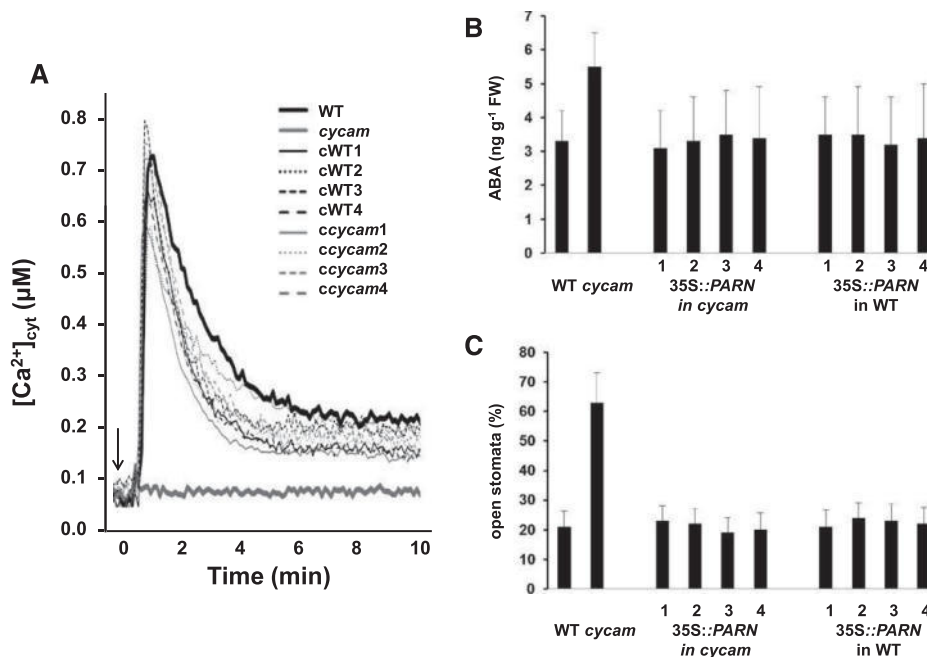


Figure 7. A 35S::PARN construct complements the mutant phenotype. A, Wild-type (WT) and *cycam* plants were transformed with the 35S::PARN construct, and $[Ca^{2+}]_{cyt}$ elevation after application of 50 μ L of CT (10 μ M) was measured in roots of wild-type and *cycam* seedlings as well as of four (1–4) wild-type and *cycam* seedlings that were independently transformed with the 35S::PARN construct. B and C, The same seed batches were used to determine ABA levels (B) and the percentage of open stomata (C). Data are based on four (Ca^{2+} measurement), 10 (ABA level), and five (stomatal opening) independent experiments; error bars represent SE. FW, Fresh weight.

PARN Is Required for *P. indica*-Mediated Benefits to Arabidopsis Seedlings

Our (Peřkan-Berghöfer et al., 2004) and other (Banhara et al., 2015) studies demonstrated that the growth of Arabidopsis seedlings in the presence of *P. indica* results in an ~30% increase (depending on the growth conditions) of biomass. The biomass of *cycam* seedlings is reduced by ~10% when they are cocultivated with *P. indica* (Table I).

We also demonstrated that *P. indica* confers drought stress tolerance to Arabidopsis seedlings. This can be quantified by the chlorophyll fluorescence parameter F_v/F_m , which describes the efficiency of the photosynthetic electron transfer after exposure of the seedlings to drought stress (Sherameti et al., 2008). Under drought stress, the F_v/F_m value is higher for *P. indica*-colonized wild-type seedlings compared with the uncolonized control, whereas no difference can be observed for colonized and uncolonized *cycam* seedlings (Table I). Finally, we have shown previously that *cycam* seedlings are more susceptible to *A. brassicae* infection and its toxin(s) than are wild-type seedlings and that a protective role of *P. indica* against the *A. brassicae* challenge can be detected in wild-type but not *cycam* seedlings

(Johnson et al., 2013). Taken together, *P. indica*-mediated benefits and defense against *A. brassicae* require functional PARN in Arabidopsis seedlings.

Expression Profiling Identified CT-Responsive Genes

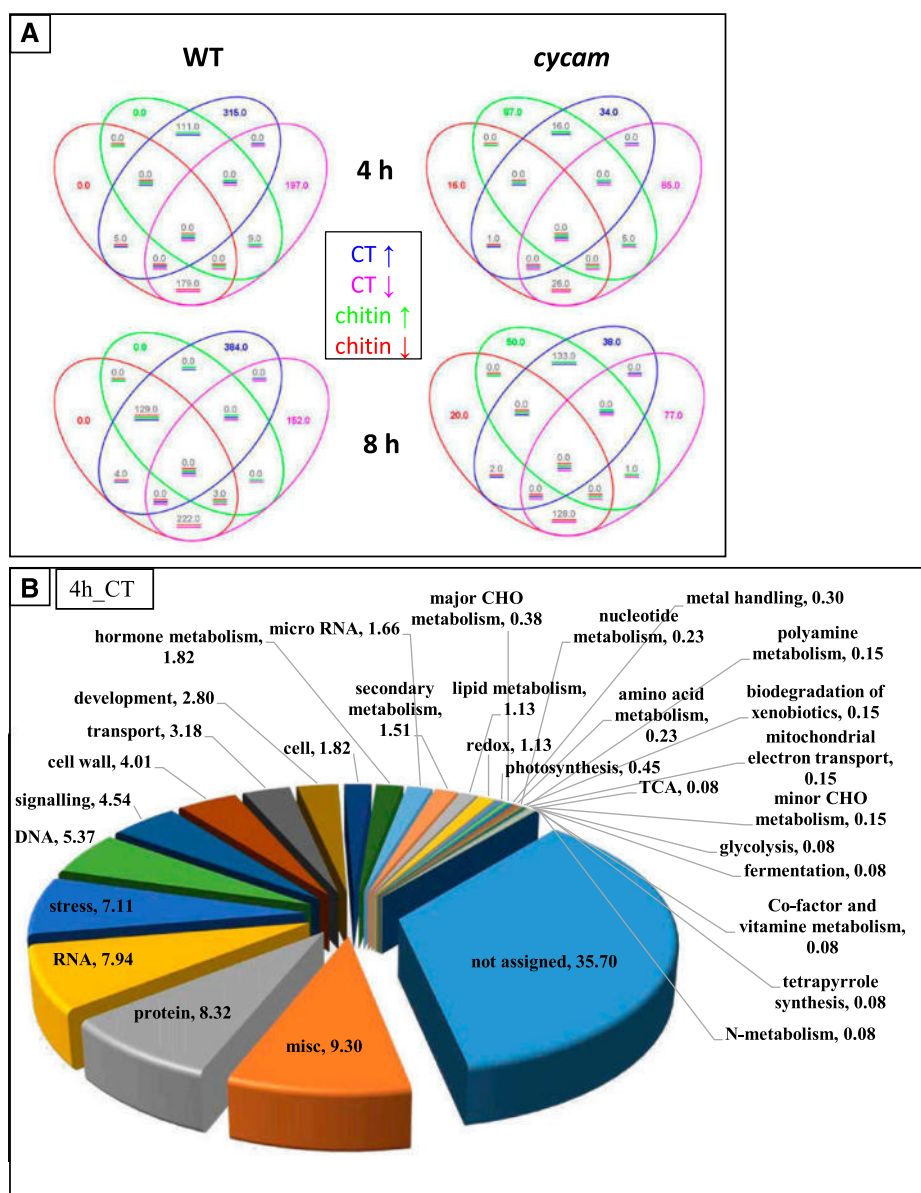
In initial studies, we observed that the number of genes responding to CT in Arabidopsis roots increased with longer (greater than 1 h) incubation periods. Therefore, we analyzed expression profiles 4 and 8 h after exposure of wild-type and *cycam* roots to CT and compared them with those obtained after chitin application. Chitin was used as a control because it is a well-characterized MAMP and also active in roots. Overall, 1,532 genes responded to either CT or chitin application greater than 2.5-fold 4 or 8 h after application (Fig. 8A; Supplemental Tables S2A and S2B). A total of 1,026 genes responded to CT but not to chitin. Interestingly, we did not identify any gene that was regulated in the opposite direction in response to CT or chitin treatments at a given time point. This suggests overlapping functions of both elicitors, whereas the CT response is normally lower and occurs later when compared with the response to chitin. In accordance with the ROS data

Table I. *P. indica* promotes biomass production and drought tolerance in wild-type, but not *cycam*, seedlings

The increase in biomass of Arabidopsis wild-type and *cycam* seedlings was determined 12 d after cocultivation with *P. indica*. The biomass of uncolonized wild-type seedlings was set as 100%. The chlorophyll fluorescence parameter F_v/F_m , representing the efficiency of the photosynthetic electron flow, was determined for *P. indica*-exposed and mock-treated wild-type and *cycam* seedlings 48 h after opening of the lid of the petri dishes (for experimental details, see Fig. 2 in Sherameti et al., 2008). Data are based on 120 seedlings of four independent experiments; errors are SE.

Parameter	Wild Type – <i>P. indica</i>	Wild Type + <i>P. indica</i>	<i>cycam</i> – <i>P. indica</i>	<i>cycam</i> + <i>P. indica</i>
Biomass (%)	100 ± 9	132 ± 15	89 ± 13	78 ± 6
F_v/F_m after 48 h of drought	0.49 ± 0.05	0.78 ± 0.06	0.51 ± 0.03	0.46 ± 0.06

Figure 8. Microarray analysis of differentially regulated genes after the application of CT or chitin. A, Venn diagrams of microarray data of wild-type (WT) and *cycam* roots 4 and 8 h after treatment with CT or chitin (10 μ M each). Genes responding to CT were analyzed from the complete data set. Afterward, genes also responding to chitin were analyzed from that pool of CT-responding genes. The Venn diagrams show that the number of genes responding to either CT or chitin is lower in *cycam* roots (right) than in wild-type roots (left). After 4 h (top), the number of genes induced by CT and chitin is ~6 times higher in wild-type roots than in *cycam* roots, whereas after 8 h (bottom), the difference is only ~2-fold. Venn diagrams show genes that are up-regulated (blue) or down-regulated (pink) by CT and up-regulated (green) or down-regulated (red) by chitin. Only genes are considered that are regulated greater than 2.5-fold relative to the mock (water)-treated control ($\log_2 \geq 1.32$ or ≤ -1.32 in Supplemental Tables S2A and S2B). Data are based on three independent RNA samples per treatment. B, Pie chart of differentially regulated genes in wild-type plants 4 h after treatment with CT. Shown are the groups of genes of the associated pathways (in percentage) regulated by 10 μ M CT. A full list with numbers of genes and a comparison with genes also induced by chitin can be found in Table III. CHO, Carbohydrate.



(Fig. 4), it appears that CT induces a milder defense response in the roots than chitin (Fig. 8B; Table III; Supplemental Tables S2A and S2B).

CT- but not chitin-responsive genes can be divided further into those regulated in wild-type but not *cycam* roots. These genes respond to CT via a PARN- and/or Ca^{2+} -dependent pathway (Fig. 8A; Supplemental Tables S2A and S2B) and were found to encode Ca^{2+} -dependent proteins and proteins involved in Ca^{2+} -dependent signaling events, proteins involved in exocytosis, auxin and ethylene functions, defense, cell wall biosynthesis, cell and root growth, or metabolite and information transfer within the plant body (Supplemental Table S2B). The regulation of a few genes induced by CT in a PARN-dependent manner (Supplemental Table S2B) was analyzed further by real-time PCR and compared with their regulation by

chitin (not PARN-dependent genes) as well as the CWE of *A. brassicae* (PARN-dependent genes; Table II). Interestingly, the majority of the tested genes responded quite differently to the three stimuli, and many of them responded to CT but not or to a lesser extent to the CWE from *A. brassicae* or chitin (Table II). Among the genes that respond only to CT are those that encode proteins involved in cell and root growth, regulators of root development and elongation, exocytosis, cell division, transporters for metabolite distribution within the plant, and hormone effects (Supplemental Table S3). Among the genes responding to all three stimuli is *SWEET11* (At3g48740), which encodes a transporter involved in Suc phloem loading and carbon export from the leaves to the roots (Durand et al., 2016). Chen et al. (2010) showed that pathogens and symbionts promote the expression of several

Table II. Genes in *Arabidopsis* wild-type and *cycam* roots that are differentially regulated by CT (10 μ M, 50 μ L), a CWE from *A. brassicae* (50 μ L), or chitin (10 μ M, 50 μ L) 4 or 8 h after elicitor application

Data show fold induction values relative to values for roots treated with water. Data are based on three independent RT-qPCR experiments; errors are SE.

Arabidopsis Genome Initiative No.	Gene	Hours after Elicitor Application	CT		CWE from <i>A. brassicae</i>		Chitin	
			Wild Type	<i>cycam</i>	Wild Type	<i>cycam</i>	Wild Type	<i>cycam</i>
At3g09530	EXOCYST H3	4	4.5 \pm 0.3	0.1 \pm 0.1	0.1 \pm 0.1	0.2 \pm 0.1	0.1 \pm 0.2	0.1 \pm 0.1
At5g06510	NUCLEAR FACTOR Y, SUBUNIT A10	4	3.5 \pm 0.4	-0.2 \pm 0.1	0.2 \pm 0.1	0.2 \pm 0.1	0.4 \pm 0.2	-0.2 \pm 0.1
At1g66700	S-Adenosyl-Met methyltransferase	4	3.6 \pm 0.8	0.7 \pm 0.3	0.0 \pm 0.1	-0.4 \pm 0.2	1.1 \pm 0.3	1.6 \pm 0.4
At5g64890	PROPEP2 (ELICITOR PEPTIDE2 precursor)	4	2.2 \pm 0.4	0.1 \pm 0.0	0.3 \pm 0.1	0.0 \pm 0.0	0.3 \pm 0.2	0.8 \pm 0.3
At4g37710	VQ motif-containing protein, VQ29	4	5.1 \pm 1.0	0.2 \pm 0.1	-0.4 \pm 0.1	-0.2 \pm 0.1	-0.1 \pm 0.1	0.0 \pm 0.1
At4g37060	PATATIN-LIKE PROTEIN5	4	2.0 \pm 0.6	0.0 \pm 0.0	-1.1 \pm 0.3	0.0 \pm 0.0	-1.0 \pm 0.4	0.0 \pm 0.0
At5g65100	EIN3	4	1.5 \pm 0.3	-0.4 \pm 0.2	0.5 \pm 0.2	0.6 \pm 0.2	-0.1 \pm 0.2	-0.1 \pm 0.2
At1g79820	SUPPRESSOR OF G PROTEIN	4	1.9 \pm 0.5	0.0 \pm 0.2	0.1 \pm 0.2	0.0 \pm 0.1	0.0 \pm 0.2	0.0 \pm 0.2
At2g19030	RALF11	8	3.3 \pm 0.8	0.0 \pm 0.2	-0.2 \pm 0.2	-0.3 \pm 0.2	0.0 \pm 0.1	-0.2 \pm 0.2
At5g27495	Ion channel inhibitor	8	4.2 \pm 0.5	0.1 \pm 0.2	0.3 \pm 0.3	0.3 \pm 0.2	0.2 \pm 0.2	0.0 \pm 0.2
At5g06170	SUC-PROTON SYMPORTER9	8	4.0 \pm 0.6	0.0 \pm 0.2	-0.1 \pm 0.2	0.0 \pm 0.2	0.1 \pm 0.2	0.0 \pm 0.2
At2g29100	GLR2.9	8	4.4 \pm 0.6	0.4 \pm 0.2	0.1 \pm 0.0	0.3 \pm 0.2	0.8 \pm 0.4	0.6 \pm 0.3
At1g67770	TERMINAL EAR1-LIKE2	8	3.9 \pm 0.7	0.9 \pm 0.4	0.0 \pm 0.2	0.3 \pm 0.2	0.0 \pm 0.1	0.0 \pm 0.1
At3g04280	RESPONSE REGULATOR22	8	1.6 \pm 0.1	-1.0 \pm 0.4	0.0 \pm 0.2	-0.3 \pm 0.2	-0.2 \pm 0.2	-0.3 \pm 0.1
At1g26250	EXTENSIN18	8	1.9 \pm 0.5	0.2 \pm 0.2	0.2 \pm 0.1	0.0 \pm 0.1	0.3 \pm 0.3	0.0 \pm 0.2
At5g42800	DIHYDROFLAVONOL 4-REDUCTASE	8	1.5 \pm 0.4	-1.1 \pm 0.4	0.4 \pm 0.2	0.5 \pm 0.4	0.6 \pm 0.4	0.4 \pm 0.2
At4g37060	PHOSPHOLIPASE AIII β	8	1.8 \pm 0.3	0.0 \pm 0.2	0.0 \pm 0.2	0.0 \pm 0.2	-0.6 \pm 0.2	0.0 \pm 0.1
At3g48740	SWEET11	8	-3.3 \pm 0.6	-1.2 \pm 0.2	-3.1 \pm 1.0	-1.1 \pm 0.4	-2.8 \pm 1.0	-1.5 \pm 0.4
At2g42590	GENERAL REGULATORY FACTOR9	8	-2.4 \pm 0.7	0.3 \pm 0.2	0.2 \pm 0.2	0.3 \pm 0.2	0.4 \pm 0.3	0.2 \pm 0.3
At5g24920	GLN DUMPER5	8	-2.2 \pm 0.9	0.3 \pm 0.2	0.2 \pm 0.2	0.4 \pm 0.2	-0.1 \pm 0.2	0.3 \pm 0.2

SWEET genes for nutritional gain, including *SWEET11*.

DISCUSSION

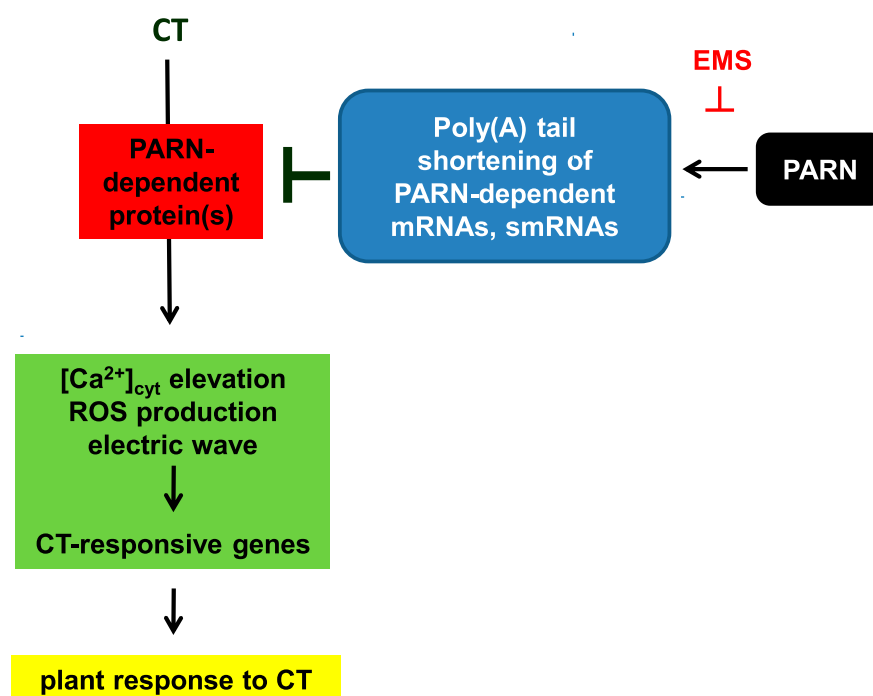
We demonstrate that CT from *P. indica* and a different low-molecular-mass compound from *A. brassicae* (Supplemental Fig. S6; Johnson et al., 2013) induce $[Ca^{2+}]_{cyt}$ elevation in *Arabidopsis* roots and that these responses require PARN. Furthermore, both elicitors activate different Ca^{2+} -dependent responses in *Arabidopsis* roots (Table II), suggesting that the specificity is established downstream of PARN (Fig. 9). Compared with chitin, CT induces a weak defense response (Fig. 4; Table II) and also stimulates the expression of genes, which do not respond to chitin. The isolated mutant with the weak *PARN* allele confirms that both *P. indica*-induced benefits and *A. brassicae*-activated defense responses are impaired (Table II; Johnson et al., 2013). PARN might control the efficient

translation of mRNAs for proteins that control $[Ca^{2+}]_{cyt}$ elevation and the proper responses of the plant to at least one beneficial and one pathogenic fungus.

CT and Early Signaling Events

β -Glucans are ubiquitous in plant and fungal cell walls. The β -1,4-glucan cellulose is one of the most abundant glucans in plants. Fungi can generate short-chain β -1,4-glucans by the degradation of cellulose or other glucan polymers (Karlsson et al., 2002; McCarthy et al., 2003; Liu et al., 2010; Chen et al., 2014). Since CT was isolated from *P. indica* growing without the host in a culture medium, cellulose from the plant cell wall as source can be excluded, and CT is most likely of fungal origin. The fungus forms a symbiotic interaction with *R. radiobacter* F4, an α -proteobacterium (Sharma et al., 2008; Glaeser et al., 2016; Guo et al., 2017), and a CWE from *A. tumefaciens*, a closely related species, also induces $[Ca^{2+}]_{cyt}$ elevation in *Arabidopsis* roots. This response occurs in the wild

Figure 9. Model describing the function of PARN in controlling $[Ca^{2+}]_{cyt}$ elevation in response to CT. Arrows indicate an induction of targets, while T-bars represent repression. EMS, Ethyl methanesulfonate.



type and the *cycam* mutant (Fig. 2J), suggesting that it functions genetically differently from the CT response. Apparently, a compound synthesized by the bacterium inducing $[Ca^{2+}]_{cyt}$ elevation is either not present in the cell wall preparation from *P. indica* (and its bacterial endophyte) or its concentration is too low for a detectable Ca^{2+} signal in the *cycam* mutant. Two scenarios are possible: *P. indica* might generate CT by a transglycosylation reaction using its own cellobiose as substrate, or the fungus degrades cellopolymers present in the fungus. Since the purification procedure results only in single Ca^{2+} -inducing peaks (Supplemental Fig. S1), the presence of other cellooligomers, such as cellobiose, as potential precursors for CT biosynthesis in the CWE is unlikely, since they also should induce $[Ca^{2+}]_{cyt}$ elevation (Fig. 2D). Thus, how CT is generated in the fungus remains unclear. Many fungal glucosidases possess efficient transglycosylation capacities for the synthesis of CT from cellobiose in the intracellular and extracellular spaces (Smaali et al., 2004; Suzuki et al., 2010; Zhao et al., 2015; Guo et al., 2016a; Mallek-Fakhfakh and Belghith, 2016; Boudabbous et al., 2017), and homologous enzymes can be found in the *P. indica* genome (J. Thürich and R. Oelmüller, unpublished data). The large number of genes encoding cellopolymer-degrading enzymes in the *P. indica* genome (Zuccaro et al., 2011) also might allow the fungus to generate CT by degrading cellooligomers or cellopolymers present in the fungus. Since $[Ca^{2+}]_{cyt}$ elevation is triggered by CT in nanomolar concentrations, the compound should be generated in low concentrations and not as an intermediate of an important biochemical pathway.

MAMPs are recognized by PRRs (Zipfel, 2008; Macho and Zipfel, 2014). PRRs for chitin and oligogalacturonides have been identified, but receptors of other oligosaccharides including β -glucans are unknown. BAK1, a coreceptor in many PRRs, is not required for CT-induced $[Ca^{2+}]_{cyt}$ elevation (Fig. 2K). How CT is recognized by the root cell is unknown at present; however, Glc shows no Ca^{2+} -inducing activity in Arabidopsis roots, and cellobiose as well as longer oligomers reduced activity compared with CT, suggesting specificity in the recognition. In general, the biological activity of oligosaccharides in eliciting plant responses is highly dependent on their degree of polymerization, and the responses are species specific (Trouvelot et al., 2014). The perception of oligogalacturonides, oligomers of α -1,4-linked galacturonosyl residues (Nothnagel et al., 1983) that induce resistance of Arabidopsis against *Botrytis cinerea* (Aziz et al., 2004; Ferrari et al., 2007), occurs by the WALL-ASSOCIATED KINASE1 (WAK1), a transmembrane receptor kinase (Kohorn and Kohorn, 2012). WAK1 binds oligogalacturonides (Brutus et al., 2010), which leads to the activation of the intramembrane kinase domain of WAK1 and the activation of plant immune responses (Trouvelot et al., 2014). A similar scenario with a so far unidentified receptor and early signaling compounds can be envisioned for CT.

Recently, Souza et al. (2017) demonstrated that oligomers derived from cellulose are perceived as signal molecules in Arabidopsis, thereby triggering a signaling cascade that shares similarities to responses to chitooligomers and oligogalacturonides. Cellobiose stimulates neither detectable ROS production nor callose deposition.

Cotreatments of cellobiose with flg22 or chitoooligomers led to synergistic increases in defense gene expression. The authors concluded that the perception of cellulose-derived oligomers may participate in cell wall integrity surveillance and represents an additional layer of signaling following plant cell wall breakdown during cell wall remodeling or pathogen attack. Many of their results and conclusions resemble those described here, and both studies demonstrate that plants perceive cellooligomers from different sources that interfere with well-studied defense signaling pathways. In our study using *Arabidopsis* roots, CT was more effective than cellobiose and other cellooligomers, but they share PARN for the induction of $[Ca^{2+}]_{cyt}$ elevation (Fig. 2I). Apparently, a so far uncharacterized perception system perceives cellopolymers from different sources to inform the plant about environmental changes and threats. Since the generation of Ca^{2+} , ROS, and electric signals in response to CT is impaired in the *cycam* mutant (Figs. 2–4), CT (and possibly cellooligomer) perception also may be used by the plant to inform distant cells or organs via systemic signal propagation (Gilroy et al., 2014, 2016, and refs. therein).

Previously, we demonstrated that the CWE from *P. indica* does not induce ROS production (Vadassery et al., 2009). Furthermore, cellobiose does not induce ROS production in leaves (Souza et al., 2017). However, CT induces ROS in *Arabidopsis* roots, although the overall level is low compared with chitin (Fig. 4). Direct comparison of the CT and CWE stimuli confirmed the differences in ROS accumulation, suggesting that the CWE contains an additional compound or compounds inhibiting CT-induced ROS production. Furthermore, Ca^{2+} -dependent NADPH oxidase D activation is required for rapid defense signal propagation (Dubiella et al., 2013). The strongly reduced ROS accumulation in the *rbhd* mutant after CT application supports the important role of this oxidase for the function of the elicitor.

Ultimately, receptor activation must lead to the opening of Ca^{2+} channels, and GLRs are potential candidate channels for CT-induced $[Ca^{2+}]_{cyt}$ elevation. GLR3.3 mediates leaf-to-leaf wound signaling (Li et al., 2013; Manzoor et al., 2013; Mousavi et al., 2013). However, CT-mediated $[Ca^{2+}]_{cyt}$ elevation is not impaired in the *glr3.3* mutant (Fig. 2L). In addition, GLR2.4 and GLR2.5 are not required for CT-mediated $[Ca^{2+}]_{cyt}$ elevation (Fig. 2L). Furthermore, wounding-induced systemic Ca^{2+} elevations are dependent on TPC1, a Ca^{2+} -activated vacuolar cation channel (Hedrich and Neher, 1987; Peiter et al., 2005; Peiter, 2011; Choi et al., 2014; Xiong et al., 2014; Kiep et al., 2015; Guo et al., 2016b); however, this channel also is not involved in CT-induced $[Ca^{2+}]_{cyt}$ elevation (Fig. 2K). Apparently, the initial steps between the perception and regulation of Ca^{2+} channel activities by CT differ from other known MAMP systems.

Response to CT

Microarray analyses identified CT-responsive genes in *Arabidopsis* roots. Approximately half of the genes also respond to chitin, suggesting overlapping

functions of both elicitors. These results are comparable to those from Güimil et al. (2005), who showed that more than 40% of the rice (*Oryza sativa*) genes responded to a beneficial and pathogenic root-colonizing fungus. Among the genes that are regulated only by CT (and not chitin) are candidates for proteins that participate in general root and cell growth, growth-related hormone functions, exocytosis, and transport processes. Compared with chitin, CT induces fewer defense-related genes, and their stimulation is lower and temporally retarded (Fig. 8; Tables II and III; Supplemental Tables S2A and S2B). CT-responsive genes can be classified further into those that require fully functional PARN and those that are regulated independently of PARN (Supplemental Tables S2A and S2B). At least one PARN-dependent pathway activated by CT operates via $[Ca^{2+}]_{cyt}$ elevation. Unlike chitin and the CWE from *A. brassicae*, several CT-induced and PARN-dependent genes code for proteins involved in growth and developmental processes (Table II; Supplemental Table S3).

PARN

In mammals, yeast, and insects, the adenosine-specific 3'-to-5' exonuclease PARN mediates the trimming of poly(A) tails of ~2% of all messenger RNAs. The enzyme plays an important role in mRNA stability, the quality control of gene expression, and the maturation of a class of small RNAs. PARN forms a dimer that recognizes the poly(A) tail and binds simultaneously to the 7-methyl-guanosine cap on the 5' end of mRNAs in mammals and insects (Godwin et al., 2013). Well-characterized PARN proteins contain three conserved domains; however, two of them, the R3H and RRM domains, are absent in the plant proteins, suggesting that they are not true homologs. Therefore, the exact function of AtPARN is not known.

AtPARN is essential for embryogenesis, and a complete knockout mutant is lethal (Chiba et al., 2004; Reverdatto et al., 2004). Weak mutants accumulate elevated ABA levels, and 12-d-old *cycam* seedlings contain ~2 times more ABA than the wild-type control (Fig. 7B; Johnson et al., 2013). They are sensitive to exogenously applied ABA in germination and growth assays (Nishimura et al., 2005, 2009; Johnson et al., 2013). Both features were confirmed for our *cycam* mutant (Fig. 7B; Johnson et al., 2013).

The *Arabidopsis* protein is located in the nucleus and cytoplasm, and the ectopically expressed protein showed poly(A) degradation activity in vitro (Chiba et al., 2004). Hirayama et al. (2013) demonstrated that AtPARN directly regulates the poly(A) tract of mRNA in conjunction with a bacteria-type poly(A) polymerase. Whether the protein has dual functions in the nucleus/cytoplasm and mitochondria is currently under study. The *PARN* mRNA is stress inducible, and a mutant with a weak *parn* allele is ABA sensitive and responds abnormally to salicylic acid (Nishimura et al.,

Table III. Number of genes differentially regulated by CT and chitin 4 h after elicitor application in wild-type plants

The number of CT-responding genes corresponding to the indicated AGI_LOCUS_TAIR10_Aug2012 pathways is shown. The third column shows the number of CT-responsive genes that also respond to chitin. Genes that respond to CT were analyzed from the complete data set. Afterward, genes also responding to chitin were analyzed from the pool of CT-responding genes.

Pathways (AGI_LOCUS_TAIR10_Aug2012)	No. of Genes Regulated in the Wild Type 4 h after CT Application	Subset of CT-Responsive Genes in the Wild Type Also Regulated 4 h after Chitin Application
Not assigned	472	131
Miscellaneous	123	30
Protein	110	36
RNA	105	34
Stress	94	20
DNA	71	27
Signaling	60	20
Cell wall	53	14
Transport	42	5
Development	37	3
Cell	24	8
Hormone metabolism	24	8
MicroRNA	22	9
Secondary metabolism	20	7
Lipid metabolism	15	1
Redox	15	6
Photosynthesis	6	2
Major carbohydrate metabolism	5	4
Metal handling	4	2
Amino acid metabolism	3	3
Nucleotide metabolism	3	1
Biodegradation of xenobiotics	2	0
Polyamine metabolism	2	1
Mitochondrial electron transport	2	0
Minor carbohydrate metabolism	2	0
Cofactor and vitamin metabolism	1	0
Glycolysis	1	0
TCA	1	1
Fermentation	1	0
Tetrapyrrole synthesis	1	0
N-metabolism	1	1

2005, 2009). In wild-type plants, the amount of *PARN* mRNA is not limiting for the Ca^{2+} response, since the *35S::PARN* plants do not show higher levels of $[\text{Ca}^{2+}]_{\text{cyt}}$ elevation in response to CT treatments. Our data suggest that the protein degrades the poly(A) tail of an mRNA that encodes one or more proteins required for $[\text{Ca}^{2+}]_{\text{cyt}}$ elevation in response to CT treatments and the CWE of *A. brassicae* in the cytoplasm of Arabidopsis roots. Candidates are proteins involved in all processes from elicitor perception to the syntheses or regulation of the corresponding Ca^{2+} channel activities, and they are likely negative regulators of CT-induced $[\text{Ca}^{2+}]_{\text{cyt}}$ elevation (Fig. 9). The genetic link between Ca^{2+} , ROS, and electric signals extends the list to additional candidates. The differences between the root responses to CT and those to the *A. brassicae* CWE suggest that specificity is achieved downstream of PARN (Table II). The absence of a functional PARN may result in the loss

of a number of proteins of which only a specific subset is involved in the realization of a particular elicitor program. Our data suggest that elicitor-triggered $[\text{Ca}^{2+}]_{\text{cyt}}$ elevation can be controlled at the level of mRNA stability via poly(A) tail shortening. In various eukaryotic organisms, the deadenylation reaction of specific mRNA species by PARNs is allosterically regulated, which may add an additional posttranscriptional control step to decoding of the CT information. In mammalian cells, PARN-mediated mRNA deadenylation is under the control of cis-acting regulatory elements, which include AU-rich elements and microRNA (miRNA) targeting sites within the 3' untranslated region of the mRNAs (Zhang et al., 2015, and refs. therein). Deadenylases promote miRNA-induced mRNA decay through their interaction with an miRNA-induced silencing complex (Zhang et al., 2015). Several miRNAs respond to CT treatment in the roots in a Ca^{2+} -/PARN-dependent

manner (Supplemental Table S2). These can be starting points to investigate the potential role of miRNAs in this scenario.

CONCLUSION

In conclusion, we identified CT as a novel elicitor that induces $[Ca^{2+}]_{cyt}$ elevation in Arabidopsis roots. CT is a simple chemical compound that can easily be synthesized or released from various abundantly available carbohydrate polymers in the rhizosphere. Almost all organisms contain an enzymatic repertoire with the capability to synthesize CT from cellobiose and Glc. Since it is active in the nanomole range, it may function as a sensor of environmental changes. The phenotype of the identified *cycam* mutant demonstrates that CT-induced $[Ca^{2+}]_{cyt}$ elevation is necessary for a proper plant response to environmental cues. We show that PARN is required for $[Ca^{2+}]_{cyt}$ elevation induced by at least two quite different elicitors: CT from a beneficial fungus and a low-molecular-mass compound from a pathogenic fungus (Fig. 2; Supplemental Fig. S6; Johnson et al., 2013). Thus, PARN appears to control different elicitor-induced signaling events. Posttranscriptional control of $[Ca^{2+}]_{cyt}$ elevation by selective shortening of poly(A) tails of specific mRNAs required for $[Ca^{2+}]_{cyt}$ elevation adds an additional novel feature to elicitor-induced signaling events in plants.

MATERIALS AND METHODS

Culturing and Growth Conditions of Fungi and Arabidopsis

Twelve-day-old Arabidopsis (*Arabidopsis thaliana*) seedlings were transferred from Murashige and Skoog plates to plates with solid plant nutrition medium and a nylon membrane (mesh size, 70 μ m) as described previously (Camehl et al., 2011). Seedlings were then grown for an additional 24 h under long-day conditions, with light applied from above (60–70 μ mol m⁻² s⁻¹, 16 h of light/8 h of dark), at 22°C. These seedlings were then used for the different experiments: transfer to fresh plates with fungi or incubation of the roots with elicitors.

For elicitor application, the roots were soaked in a solution containing either CT or other chemicals (see below), and autoclaved water was used as a control. The plates with the seedlings were then transferred back to long-day conditions, before the roots were harvested after the treatments described in the text.

Transgenic Arabidopsis expressing cytosolic apoaequorin in the Col-0 background (pMAQ2) was a gift from Marc Knight (Knight et al., 1991; Polisensky and Braam, 1996), *rbold* knockout seeds were a gift from Jonathan D.G. Jones, and *tpc1* in the aequorin background was a gift from Edgar Peiter. Knockout lines for *GRL2.4* (SALK_010571C), *GRL2.5* (SALK_078407C), and *GRL3.3* (SALK_099757C) were obtained from TAIR. After crossing with pMAQ2, homozygote knockout lines were generated using the primer pairs given by TAIR. Ethyl methanesulfonate mutants of pMAQ2 seeds, which were screened here, were generated in an earlier study (Johnson et al., 2014).

Piriformospora indica was cultured and maintained on Kaefar medium, pH 6.5, as described by Johnson et al. (2011b). The fungus also was grown on Kaefar medium broth for 18 d at 22°C to 24°C in complete darkness on a horizontal rotating shaker at 50 rpm for the preparation of the cell wall extracts (Vadassery and Oelmüller, 2009; Johnson et al., 2011b).

Alternaria brassicae (FSU-3951), *Mortierella hyalina* (FSU-509), and *Verticillium dahliae* (FSU-343) were obtained from the Jena Microbial Resource Centre, and *Periconia macrospinoso* was from Gabor Kovács. The fungi were grown on potato dextrose agar medium (pH 6.5–6.7) at 20°C \pm 1°C in a temperature-controlled

chamber under 12/12 h of light/dark and 75% relative humidity for 2 weeks. The fungi were inoculated to Arabidopsis seedlings and reisolated from the infected tissues every 6 months (Johnson et al., 2013). *Agrobacterium tumefaciens* was grown for 3 d in a medium containing 1% (w/v) yeast extract, 1% (w/v) tryptone peptone, and 0.5% (w/v) NaCl (pH 7) at 27°C, with shaking at about 200 rpm.

$[Ca^{2+}]_{cyt}$ Measurement and Mutant Screen

Aequorin-based luminescence measurements were performed using 16-d-old individual M2 plants grown on Hoagland medium (Vadassery and Oelmüller, 2009; Vadassery et al., 2009; Johnson et al., 2011b); pMAQ2 plants served as a control (Polisensky and Braam, 1996). For $[Ca^{2+}]_{cyt}$ measurements, approximately 70% of the roots per seedling were dissected and incubated overnight in 150 μ L of 7.5 μ M coelentrastine (P.J.K.) in the dark at 20°C on a 96-well plate (Thermo Fisher Scientific; catalog no. 9502887). Bioluminescence counts from roots were recorded as RLU with a microplate luminometer (Luminoskan Ascent, version 2.4; Thermo Electro). For the induction of the Ca^{2+} response, the CWE and purification fractions, CT (Sigma-Aldrich; C1167), other Glc oligomers (cellobiose, C7252; cellotriose, C1167; cellotetraose, C8286; cellopentaose, C8792 [Sigma-Aldrich]; cellohexaose, OCO6512; celloheptaose OCO5241 [Carbosynth]), monomeric sugars, flg22 (Biolab; up7201-m5) or chitin (chitohexaose, OH07433 [Carbosynth]), chitopentaose, chitoheptaose, and chitooctaose (P6967, H1271, and O6383 [Sigma-Aldrich]) were used as described in "Results." The mutant screen was performed with the CWE from *P. indica*; the putative M2 mutants were rescued and transferred to pots containing garden soil and vermiculite at 9:1 (v/v) for further screening and validation. The mutant seedlings were grown in a temperature-controlled growth chamber under short-day conditions (8-h/16-h light/dark cycle, temperature of 20°C \pm 1°C, light intensity of 80 μ mol m⁻² s⁻¹) for 4 weeks followed by long-day conditions in Aracon tubes. The seeds were harvested from individual M3 plants and again screened to confirm homozygosity.

Purification of the Ca^{2+} -Inducing Compound from *P. indica*

CWEs were prepared according to Anderson-Prouty and Albersheim (1975) with modifications (Johnson et al., 2011a, 2014; Lee et al., 2011). Mycelia from liquid cultures were harvested by filtration through four layers of nylon membrane (pore size, 70 μ m; Sefar) and washed five times with sterile water before homogenization in sterile water (1:5, w/v) with a Waring blender. The slurry was then filtered through four layers of nylon membrane. The residue was collected, washed again (three times) with sterile water, then twice with chloroform:methanol (1:1), and finally twice with acetone. The material representing a crude mycelial cell wall preparation was air dried for 2 h under sterile conditions. For the preparation of the CWE, the material was suspended in sterile water (1 g:100 mL, w/v) and autoclaved for 30 min according to Anderson-Prouty and Albersheim (1975). However, autoclaving is not necessary for the elicitor preparation. After cooling, the extract was filtered through four layers of nylon membrane and finally sterilized by passing it through a 0.22- μ m filter. The CWE was then purified by passing it through a reverse-phase Supelclean LC-18 SPE cartridge (10-g bed weight, 60-mL volume; Sigma-Aldrich; catalog no. 57136). The eluting fractions were collected, and the active fraction in the void volume was identified by $[Ca^{2+}]_{cyt}$ elevation measurements (Johnson et al., 2011a, 2014; Lee et al., 2011). This fraction from *P. indica* was used for the Arabidopsis mutant screen described below. The CWEs from *A. brassicae*, *V. dahliae*, *P. macrospinoso*, *M. hyalina*, and *A. tumefaciens* were prepared in the same way.

For purification of the active compound in the *P. indica* cell wall preparation, the proteins were removed by precipitation with 80% (v/v) methanol, and the supernatant was collected after centrifugation at 6,000g for 5 min. The supernatant was applied to a Roti-Spin Mini column with a molecular mass cutoff of 3 kD (Roth), and the flow through was concentrated in a Speed-Vac. Further purification was performed by HPLC with an LC-18-DB column, 25 cm \times 4.60 mm i.d. (Supelco), followed by an Asahipak NH2P-50 4E column, 25 cm \times 4.6 mm i.d. (Schodex). The active fractions were collected for measuring $[Ca^{2+}]_{cyt}$ elevation, pooled, and concentrated in a Speed-Vac. Finally, the active fractions were separated using two UPLC columns, first an Acclaim C18 column, 250 \times 2.1 mm, 2.2 μ m (Dionex), and then a C18 phenyl column, 150 \times 2.1 mm, 1.7 μ m (Phenomenex), fitted to an Ultimate 3000 series RSLC system (Dionex). For all HPLC and UPLC separations, an acetonitrile:water gradient (0–100%) was used as the mobile phase (30-min run) with flow rates of 1 mL min⁻¹ for HPLC and 0.3 mL min⁻¹ for UPLC.

Structure Elucidation of the Ca²⁺-Inducing Compound from *P. indica*

Prepurified active fractions from the above-mentioned separations were analyzed on an Ultimate 3000 series RSLC system (Dionex) coupled to an LTQ-Orbitrap XL Mass Spectrometer (Thermo Fisher Scientific) equipped with an electrospray ionization source. The Orbitrap mass analyzer was set to 60,000 m/Δm resolving power mass resolutions at *m/z* 200 and operated in positive or negative ion modes. The instrument was calibrated using commercial CalMix (Thermo) prior to each sequence. Continuum spectral data of *m/z* 70 to 2,000 mass span were collected and analyzed using Xcalibur version 2.0.7. software (Thermo Fisher Scientific). For collision-induced dissociation tandem mass spectrometry spectra, masses of interest were selected in a quadrupole using a 2D selection window, and normalized fragmentation energy was set from 10 to 35 V.

¹H-NMR spectra, ¹H,¹H-DQF-COSY spectra, seITOCOSY spectra, multiplicity-edited heteronuclear single quantum coherence spectra, and heteronuclear multiple-bond correlation spectra were measured at 300°K on a Bruker Avance III HD 700 NMR spectrometer (Bruker Biospin) using a cryogenically cooled 1.7-mm TCI ¹H-¹³C probe. The operating frequency was 700.45 MHz for ¹H and 176.13 MHz for ¹³C. D₂O was used as a solvent, and the spectra were referenced to sodium trimethylsilyl propionate as a standard. The residual HDO signal in the ¹H-NMR spectra was suppressed using the PURGE pulse program (Simpson and Brown, 2005).

The ¹H-NMR spectrum of the trisaccharide displayed four doublets characteristic for protons at the anomeric center of carbohydrates. The coupling constants of ³J_{H-H} = 8 Hz of the signals at δ 4.53, 4.55, and 4.68 indicated β-configuration of hexopyranoses, and ³J_{H-H} = 4.1 Hz of the doublet at δ 5.24 indicated α-configuration (Supplemental Fig. S2). The integral values of 0.4 for the signal at δ 5.24 and 0.6 for the signal at δ 4.68 add up to a common value of 1, indicating that the two signals represent α- and β-anomers of the terminal carbohydrate unit. The two signals at δ 4.55 (¹H) and δ 4.53 (¹H) each represent a nonreducing carbohydrate unit in the molecule. ¹H,¹H-DQF-COSY (Supplemental Fig. S3) and the seITOCOSY experiments (Supplemental Fig. S4) dissected the crowded region of the carbohydrate methine and methylene signals and enabled the assignment of all ¹H-NMR signals of the three sugar units. Large coupling constants of ³J_{H-H} = 8 to 9 Hz indicated transdiaxial configuration of H-1 to H-5 in each unit and, hence, identified them as three glucopyranoses, A, B, and C. Moreover, the H-4 signals of Glc-A and Glc-B shifted to the low field at δ 3.67 and 3.68, respectively, suggesting 1→4 linkage of the sugar units. According to these data, the structure of the trisaccharide was identified as CT.

For acid hydrolysis of the purified fraction from the *P. indica* and *A. brassicae* cell wall (Supplemental Fig. S6) and the commercially available CT (Fig. 2; Supplemental Fig. S6), the samples (50 μL) were treated with 1 N H₂SO₄ in a water bath at 80°C for 1 h and neutralized with 1 N NaOH after cooling, before use for [Ca²⁺]_{cyt} measurements.

Quantitative Intracellular H₂O₂ and ROS Measurements

Quantitative H₂O₂ measurement from leaves and roots were performed using the Amplex Red Hydrogen Peroxide/Peroxidase Assay Kit (Molecular Probes, Invitrogen) according to the manufacturer's instructions. Leaf sections of 0.5 to 1 mm width and root sections of 2 to 3 cm length were incubated in the reaction mixture for 10 min in darkness at room temperature. The fluorescence intensity was quantified with a fluorescence microplate reader (TECAN Infinite 200 plate reader) with excitation at 540 nm and emission at 610 nm. H₂O₂ was used to prepare the standard curve. The reaction mixture without the molecular probe or without the plant material served as a control.

Gene Expression Analyses by RT-qPCR

RNA was isolated from the tissues with TRIzol (Thermo Fisher Scientific) according to the manufacturer's protocol followed by DNase treatment. The RNA was reverse transcribed for RT-qPCR analyses using a CFX CONNECT real-time detection system (Bio-Rad). Total RNA was isolated from three independent biological experiments. cDNA was synthesized using the Omniscript cDNA synthesis kit (Qiagen) with 1 μg of RNA. For the amplification of the reverse transcription PCR products, iQ SYBR Green Supermix (Bio-Rad) was used according to the manufacturer's protocol in a final volume of 20 μL. The cycler was programmed to 95°C for 3 min; 40 cycles of 95°C for 30 s, 57°C for 15 s, and 72°C for 30 s; 72°C for 10 min; followed by a melting curve program from 55°C to 95°C in increasing steps of 0.5°C. All reactions were performed

with three biological and three technical replicates. The mRNA levels for each cDNA probe were normalized with respect to the plant *ACTIN2* mRNA level. Fold induction values of target genes were calculated with the ΔΔCP equation (Pfaffl, 2001) and related to the mRNA level of the target genes as indicated. Primer pairs used in this study are given in Supplemental Table S4. Primers were designed with the CLC Main Workbench program (<http://www.clcbio.com/products/clc-main-workbench>).

Identification of the *cycam* Mutation

The *cycam* mutant was crossed with the pMAQ2 line, and in the F2 generation, two pools of offspring plants were generated. The first pool contained 25 individual plants that displayed the *cycam* phenotype, and the second pool contained plants that displayed a wild-type-like phenotype (control pool). The DNA of both pools was analyzed by Illumina (100-bp paired-end) sequencing. The reads from the first and second pools were mapped separately against the TAIR10 reference genome (Lamesch et al., 2012) using CLC Genomics Workbench (version 5.1). Single-nucleotide polymorphisms (SNPs) with a frequency between 20% and 100% were detected using the variant detection tool in both mappings, and the resulting SNP tables were exported to Microsoft Excel. In Excel, SNPs were identified that had higher frequencies in the *cycam* pool than in the control pool using the custom sorting tool. For each of the five Arabidopsis chromosomes, the frequencies of these SNPs were plotted against their reference positions. The obtained scatterplots were inspected manually for areas of high linkage (SNP frequencies near 100%). A region of about 3.5 Mb on the lower arm of chromosome 1 was identified that contained five SNPs with a frequency of 100% in annotated genes (loci At1g53310, At1g54985, At1g55870, At1g56140, and At1g60110). Of these, two nonsynonymous SNPs were predicted to cause amino acid exchanges in the corresponding gene products of At1g53310, encoding PHOSPHOENOLPYRUVATE CARBOXYLASE1, and At1g55870, encoding AtPARN. At1g55870 was analyzed further (see below).

Generation of the Construct for the Complementation of *cycam* and Arabidopsis Transformation

The Gateway system with pDonor207 was used as an entry vector, and pEarlyGate 103 with a BASTA resistance and stop codon before the C-terminal GFP-Taq was used as a destination vector (Earley et al., 2006; Katzen, 2007). For the amplification of the cDNA of the wild-type version of *AtPARN* (At1g55870), Phusion High-Fidelity-Taq (Thermo Fisher) was used for amplification of the cDNA and, in a second PCR, fusion of the *AtB* sequence. The DNA was purified by the NucleoSpin Gel and PCR Clean-Up Kit (Macherey-Nagel). The sequences were confirmed by sequencing (Eurofinsgenomics). Parental *aequorin* and *cycam* plants were transformed with the wild-type version of *AtPARN* using the floral dip method with *A. tumefaciens* strain GV3101 (Zhang et al., 2006). Complemented plants were selected using a 0.1% (v/v) BASTA solution 14 and 18 d after sowing.

Microarray Analyses

Total RNA from roots of transgenic Arabidopsis (Col-0) expressing cytosolic apoaquorin (pMAQ2; Knight et al., 1991; Polisensky and Braam, 1996) and the *cycam* mutant (in the pMAQ2 background) from three independent biological experiments was exposed to CT or chitin or mock treated with water and harvested at 4 and 8 h after elicitor application. For each treatment, identical amounts of RNA from the three independent biological replicates were labeled and hybridized according to Agilent's One-Color Microarray-Based Gene Expression Analysis (OAK Lab). The quality of the RNA samples was checked by photometrical measurements with the Nanodrop 2000 spectrophotometer (Thermo Scientific) and then analyzed on agarose gels (2%, w/v) as well as by using the 2100 Bioanalyser (Agilent Technologies) to determine the RNA integrity. The Low Input Quick Amp Labeling Kit (Agilent Technologies) was used for the generation of fluorescent cRNA. Default cRNAs were amplified using oligo(dT) primers labeled with cyanine 3-CTP according to the manufacturer's protocol. Cyanine 3-CTP-labeled probes were hybridized to 8 × 60 k custom-designed Agilent microarray chips. For hybridization, the Agilent Gene Expression Hybridization Kit (Agilent Technologies) was used. The hybridized slides were washed and scanned using the SureScan Microarray Scanner (Agilent Technologies) at a resolution of 3 μm, generating a 20-bit TIFF file.

Data extractions from images were performed using Agilent's Feature Extraction software version 11. Feature-extracted data were analyzed using

DirectArray version 2.1 software from Agilent. Data were normalized with DirectArray using ranked median quantiles according to Bolstad et al. (2003). To identify significantly differentially expressed genes, \log_2 fold changes were calculated and Student's *t* test was performed. In summary, raw data were normalized by rank median quantiles, intensity values from replicate probes were averaged, \log_2 ratios between the treatments were calculated, and Student's *t* statistics were applied to test for significance. Genes with \log_2 -fold change < -1.33 or > 1.33 and $P < 0.05$ were considered to be significantly different. Data show genes that are regulated by CT or chitin in wild-type or *cycam* roots. Differentially expressed genes were then assigned using the Arabidopsis Gene Ontology software (TAIR's GO annotations; Berardini et al., 2004) and transcript abundance was classified based on their functional categories and pathways using MapMan software. Microarray data were submitted to the NCBI and are available under accession number GEO GSE9888.

Membrane Potential Recordings of Bulging Root Hair Cells and CT Application

Sterile germination and growth of Col-0 and *cycam* seedlings for root hair plasma membrane potential recordings took place as described by Wang et al. (2015). Col-0 and *cycam* seedlings were placed in a bath solution (0.1 mM KCl, 1 mM $CaCl_2$, and 5 mM MES/BTP, pH 5.5) at least 20 to 30 min before the start of the experiments. The response of the root hair plasma membrane potential to CT application was measured by sharp microelectrodes impaled through the tip of bulging root hair cells. Microelectrodes were prepared and plasma membrane potential recordings took place as described by Wang et al. (2015). CT was applied via back pressure-operated application pipettes produced from microelectrodes. The tips of the microelectrodes were manually broken off to yield openings of approximately 20 to 40 μ m in diameter. Pipettes, back filled with CT-containing bath solution, were mounted on a Triple Axis Micromanipulator (Sensapex Oy), and pressure pulses of 1 s were applied through a Picospritzer II microinjection dispense system (General Valve) operating at 30 p.s.i.

ABA and Stomatal Closure Measurements

A total of 100 mg of leaf material was frozen in liquid nitrogen and kept at $-80^\circ C$. The extraction procedure and determination of the ABA concentrations were performed as described by Matsuo et al. (2015). Stomatal closure was determined as described by Vahabi et al. (2016).

Performance of *cycam* in the Presence of *P. indica*

The fresh weights of wild-type and *cycam* seedlings in the presence or absence of *P. indica* were determined as described by Johnson et al. (2014) 6 d after cocultivation (19-d-old seedlings). Drought tolerance was tested as described by Sherameti et al. (2008). On day 13, the seedlings were transferred to fresh medium with *P. indica* mycelium and kept for an additional 6 d. Then, the lids were removed. After 72 h, differences in fresh weight were determined.

Accession Numbers

Sequence data from this article can be found in the GenBank/EMBL data libraries under accession numbers.

Supplemental Data

The following supplemental materials are available.

Supplemental Figure S1. Purification of the fungal compound inducing $[Ca^{2+}]_{cyt}$ elevation from the *P. indica* CWE.

Supplemental Figure S2. Full and expanded partial 1H -NMR spectra of the trisaccharide from *P. indica*.

Supplemental Figure S3. 1H - 1H -DQF-COSY spectrum of the trisaccharide from *P. indica*.

Supplemental Figure S4. Selective total correlation spectra of the trisaccharide from *P. indica*.

Supplemental Figure S5. The *cycam* mutant was backcrossed with the pMAQ2 line, and in the F2 generation, DNA from a pool of offspring

plants with the *cycam* phenotype and from a pool of plants with a wild-type-like phenotype (control pool) were Illumina sequenced.

Supplemental Figure S6. Acid hydrolysis products of CWEs from *A. brassicae*, *P. indica*, and cellooligomers were used to test for $[Ca^{2+}]_{cyt}$ elevation in Arabidopsis roots.

Supplemental Table S1. Refractory behavior of pathogen-associated molecular patterns and cellooligomers after CT application.

Supplemental Table S2A. Cycam-dependent response 4 and 8 h after elicitor application.

Supplemental Table S2B. Cycam-independent response 4 and 8 h after elicitor application.

Supplemental Table S3. Description of genes that are preferentially regulated by CT.

Supplemental Table S4. Primers used for this study.

ACKNOWLEDGMENTS

We thank Claudia Röppischer, Sarah Mußbach, and Elke Woker for technical assistance.

Received October 18, 2017; accepted January 12, 2018; published January 25, 2018.

LITERATURE CITED

- Achatz B, Kogel KH, Franken P, Waller F (2010) *Piriformospora indica* mycorrhization increases grain yield by accelerating early development of barley plants. *Plant Signal Behav* 5: 1685–1687
- Anderson-Prouty AJ, Albersheim P (1975) Host-pathogen interactions. VIII. Isolation of a pathogen-synthesized fraction rich in glucan that elicits a defense response in the pathogen's host. *Plant Physiol* 56: 286–291
- Aziz A, Heyraud A, Lambert B (2004) Oligogalacturonide signal transduction, induction of defense-related responses and protection of grapevine against *Botrytis cinerea*. *Planta* 218: 767–774
- Bakshi M, Vahabi K, Bhattacharya S, Sherameti I, Varma A, Yeh KW, Baldwin I, Johri AK, Oelmüller R (2015) WRKY6 restricts *Piriformospora indica*-stimulated and phosphate-induced root development in Arabidopsis. *BMC Plant Biol* 15: 305
- Baltruschat H, Fodor J, Harrach BD, Niemczyk E, Barna B, Gullner G, Janeczko A, Kogel KH, Schäfer P, Schwarczinger I, et al (2008) Salt tolerance of barley induced by the root endophyte *Piriformospora indica* is associated with a strong increase in antioxidants. *New Phytol* 180: 501–510
- Banhara A, Ding Y, Kühner R, Zuccaro A, Parniske M (2015) Colonization of root cells and plant growth promotion by *Piriformospora indica* occurs independently of plant common symbiosis genes. *Front Plant Sci* 6: 667
- Berardini TZ, Mundodi S, Reiser L, Huala E, Garcia-Hernandez M, Zhang P, Mueller LA, Yoon J, Doyle A, Lander G, et al (2004) Functional annotation of the Arabidopsis genome using controlled vocabularies. *Plant Physiol* 135: 745–755
- Bolstad BM, Irizarry RA, Astrand M, Speed TP (2003) A comparison of normalization methods for high density oligonucleotide array data based on variance and bias. *Bioinformatics* 19: 185–193
- Boudabbous M, Ben Hmad I, Saibi W, Mssawra M, Belghith H, Gargouri A (2017) Trans-glycosylation capacity of a highly glycosylated multi-specific β -glucosidase from *Fusarium solani*. *Bioprocess Biosyst Eng* 40: 559–571
- Brutus A, Sicilia F, Macone A, Cervone F, De Lorenzo G (2010) A domain swap approach reveals a role of the plant wall-associated kinase 1 (WAK1) as a receptor of oligogalacturonides. *Proc Natl Acad Sci USA* 107: 9452–9457
- Camehl I, Drzewiecki C, Vadassery J, Shahollari B, Sherameti I, Forzani C, Munnik T, Hirt H, Oelmüller R (2011) The OX11 kinase pathway mediates *Piriformospora indica*-induced growth promotion in Arabidopsis. *PLoS Pathog* 7: e1002051
- Capoen W, Sun J, Wysham D, Otegui MS, Venkateshwaran M, Hirsch S, Miwa H, Downie JA, Morris RJ, Ané JM, et al (2011) Nuclear

- membranes control symbiotic calcium signaling of legumes. *Proc Natl Acad Sci USA* **108**: 14348–14353
- Chabaud M, Genre A, Sieberer BJ, Faccio A, Fournier J, Novero M, Barker DG, Bonfante P (2011) Arbuscular mycorrhizal hyphopodia and germinated spore exudates trigger Ca^{2+} spiking in the legume and nonlegume root epidermis. *New Phytol* **189**: 347–355
- Charpentier M, Bredemeier R, Wanner G, Takeda N, Schleiff E, Parniske M (2008) *Lotus japonicus* CASTOR and POLLUX are ion channels essential for perinuclear calcium spiking in legume root endosymbiosis. *Plant Cell* **20**: 3467–3479
- Chen J, Gutjahr C, Bleckmann A, Dresselhaus T (2015) Calcium signaling during reproduction and biotrophic fungal interactions in plants. *Mol Plant* **8**: 595–611
- Chen LQ, Hou BH, Lalonde S, Takanaga H, Hartung ML, Qu XQ, Guo WJ, Kim JG, Underwood W, Chaudhuri B, et al (2010) Sugar transporters for intercellular exchange and nutrition of pathogens. *Nature* **468**: 527–532
- Chen YC, Chen WT, Liu JC, Tsai LC, Cheng HL (2014) A highly active beta-glucanase from a new strain of rumen fungus *Orpinomyces* sp. Y102 exhibits cellobiohydrolase and celotriohydrolase activities. *Bioresour Technol* **170**: 513–521
- Chiba Y, Johnson MA, Lidder P, Vogel JT, van Erp H, Green PJ (2004) AtPARN is an essential poly(A) ribonuclease in *Arabidopsis*. *Gene* **328**: 95–102
- Choi WG, Toyota M, Kim SH, Hilleary R, Gilroy S (2014) Salt stress-induced Ca^{2+} waves are associated with rapid, long-distance root-to-shoot signaling in plants. *Proc Natl Acad Sci USA* **111**: 6497–6502
- Daneshkhah R, Cabello S, Rozanska E, Sobczak M, Grundler FM, Wieczorek K, Hofmann J (2013) *Piriformospora indica* antagonizes cyst nematode infection and development in *Arabidopsis* roots. *J Exp Bot* **64**: 3763–3774
- Das A, Kamal S, Shakil NA, Sherameti I, Oelmüller R, Dua M, Tuteja N, Johri AK, Varma A (2012) The root endophyte fungus *Piriformospora indica* leads to early flowering, higher biomass and altered secondary metabolites of the medicinal plant, *Coleus forskohlii*. *Plant Signal Behav* **7**: 103–112
- Dubiella U, Seybold H, Durian G, Komander E, Lassig R, Witte CP, Schulze WX, Romeis T (2013) Calcium-dependent protein kinase/NADPH oxidase activation circuit is required for rapid defense signal propagation. *Proc Natl Acad Sci USA* **110**: 8744–8749
- Durand M, Porcheron B, Hennion N, Maurousset L, Lemoine R, Pourtau N (2016) Water deficit enhances C export to the roots in *Arabidopsis thaliana* plants with contribution of sucrose transporters in both shoot and roots. *Plant Physiol* **170**: 1460–1479
- Earley KW, Haag JR, Pontes O, Oppen K, Juehne T, Song K, Pikaard CS (2006) Gateway-compatible vectors for plant functional genomics and proteomics. *Plant J* **45**: 616–629
- Ferrari S, Galletti R, Denoux C, De Lorenzo G, Ausubel FM, Dewdney J (2007) Resistance to *Botrytis cinerea* induced in *Arabidopsis* by elicitors is independent of salicylic acid, ethylene, or jasmonate signaling but requires PHYTOALEXIN DEFICIENT3. *Plant Physiol* **144**: 367–379
- Franken P (2012) The plant strengthening root endophyte *Piriformospora indica*: potential application and the biology behind. *Appl Microbiol Biotechnol* **96**: 1455–1464
- Freymark G, Diehl T, Miklis M, Romeis T, Panstruga R (2007) Antagonistic control of powdery mildew host cell entry by barley calcium-dependent protein kinases (CDPKs). *Mol Plant Microbe Interact* **20**: 1213–1221
- Genre A, Chabaud M, Balzergue C, Puech-Pagès V, Novero M, Rey T, Fournier J, Rochange S, Bécarg D, Bonfante P, et al (2013) Short-chain chitin oligomers from arbuscular mycorrhizal fungi trigger nuclear Ca^{2+} spiking in *Medicago truncatula* roots and their production is enhanced by strigolactone. *New Phytol* **198**: 190–202
- Gilroy S, Bialasek M, Suzuki N, Górecka M, Devireddy AR, Karpinski S, Mittler R (2016) ROS, calcium, and electric signals: key mediators of rapid systemic signaling in plants. *Plant Physiol* **171**: 1606–1615
- Gilroy S, Suzuki N, Miller G, Choi WG, Toyota M, Devireddy AR, Mittler R (2014) A tidal wave of signals: calcium and ROS at the forefront of rapid systemic signaling. *Trends Plant Sci* **19**: 623–630
- Glaeser SP, Imani J, Alabid I, Guo H, Kumar N, Kämpfer P, Hardt M, Blom J, Goesmann A, Rothballer M, et al (2016) Non-pathogenic *Rhizobium radiobacter* F4 deploys plant beneficial activity independent of its host *Piriformospora indica*. *ISME J* **10**: 871–884
- Godwin AR, Kojima S, Green CB, Wilusz J (2013) Kiss your tail goodbye: the role of PARN, Nocturnin, and Angel deadenylases in mRNA biology. *Biochim Biophys Acta* **1829**: 571–579
- Güimil S, Chang HS, Zhu T, Sesma A, Osbourn A, Roux C, Ioannidis V, Oakeley EJ, Docquier M, Descombes P, et al (2005) Comparative transcriptomics of rice reveals an ancient pattern of response to microbial colonization. *Proc Natl Acad Sci USA* **102**: 8066–8070
- Guo B, Sato N, Biely P, Amano Y, Nozaki K (2016a) Comparison of catalytic properties of multiple β -glucosidases of *Trichoderma reesei*. *Appl Microbiol Biotechnol* **100**: 4959–4968
- Guo H, Glaeser SP, Alabid I, Imani J, Haghighi H, Kämpfer P, Kogel KH (2017) The abundance of endofungal bacterium *Rhizobium radiobacter* (syn. *Agrobacterium tumefaciens*) increases in its fungal host *Piriformospora indica* during the tripartite Sebacinalean symbiosis with higher plants. *Front Microbiol* **8**: 629
- Guo J, Zeng W, Chen Q, Lee C, Chen L, Yang Y, Cang C, Ren D, Jiang Y (2016b) Structure of the voltage-gated two-pore channel TPC1 from *Arabidopsis thaliana*. *Nature* **531**: 196–201
- Gutjahr C, Parniske M (2013) Cell and developmental biology of arbuscular mycorrhiza symbiosis. *Annu Rev Cell Dev Biol* **29**: 593–617
- Hedrich R, Neher E (1987) Cytoplasmic calcium regulates voltage-dependent ion channels in plant vacuoles. *Nature* **329**: 833–836
- Hirayama T, Matsuura T, Ushiyama S, Narusaka M, Kurihara Y, Yasuda M, Ohtani M, Seki M, Demura T, Nakashita H, et al (2013) A poly(A)-specific ribonuclease directly regulates the poly(A) status of mitochondrial mRNA in *Arabidopsis*. *Nat Commun* **4**: 2247
- Johnson JM, Nongbri PL, Sherameti I, Oelmüller R (2011a) Calcium signaling and cytosolic calcium measurements in plants. *Endocyt Cell Res* **21**: 64–76
- Johnson JM, Reichelt M, Vadassery J, Gershenzon J, Oelmüller R (2014) An *Arabidopsis* mutant impaired in intracellular calcium elevation is sensitive to biotic and abiotic stress. *BMC Plant Biol* **14**: 162
- Johnson JM, Sherameti I, Ludwig A, Nongbri PL, Sun C, Varma A, Oelmüller R (2011b) Protocols for *Arabidopsis thaliana* and *Piriformospora indica* co-cultivation: a model system to study plant beneficial traits. *Endocyt Cell Res* **21**: 101–113
- Johnson JM, Sherameti I, Nongbri PL, Oelmüller R (2013) Standardized conditions to study beneficial and nonbeneficial traits in the *Piriformospora indica* / *Arabidopsis thaliana* interaction. In A Varma, G Kost, R Oelmüller, eds, *Piriformospora indica*: Sebaciniales and Their Biotechnological Applications. Soil Biology, Vol 33. Springer, Berlin, pp 325–343
- Johri AK, Oelmüller R, Dua M, Yadav V, Kumar M, Tuteja N, Varma A, Bonfante P, Persson BL, Stroud RM (2015) Fungal association and utilization of phosphate by plants: success, limitations, and future prospects. *Front Microbiol* **6**: 984
- Kadota Y, Shirasu K, Zipfel C (2015) Regulation of the NADPH oxidase RBOHD during plant immunity. *Plant Cell Physiol* **56**: 1472–1480
- Karlsson J, Siika-aho M, Tenkanen M, Tjerneld F (2002) Enzymatic properties of the low molecular mass endoglucanases Cel12A (EG III) and Cel45A (EG V) of *Trichoderma reesei*. *J Biotechnol* **99**: 63–78
- Katzen F (2007) Gateway® recombinational cloning: a biological operating system. *Expert Opin Drug Discov* **2**: 571–589
- Kiep V, Vadassery J, Lattke J, Maaß JP, Boland W, Peiter E, Mithöfer A (2015) Systemic cytosolic Ca^{2+} elevation is activated upon wounding and herbivory in *Arabidopsis*. *New Phytol* **207**: 996–1004
- Knecht K, Seyffarth M, Desel C, Thureau T, Sherameti I, Lou B, Oelmüller R, Cai D (2010) Expression of *BvGLP-1* encoding a germin-like protein from sugar beet in *Arabidopsis thaliana* leads to resistance against phytopathogenic fungi. *Mol Plant Microbe Interact* **23**: 446–457
- Knight MR, Campbell AK, Smith SM, Trewavas AJ (1991) Transgenic plant aequorin reports the effects of touch and cold-shock and elicitors on cytoplasmic calcium. *Nature* **352**: 524–526
- Kohorn BD, Kohorn SL (2012) The cell wall-associated kinases, WAKs, as pectin receptors. *Front Plant Sci* **3**: 88
- Kosuta S, Hazledine S, Sun J, Miwa H, Morris RJ, Downie JA, Oldroyd GED (2008) Differential and chaotic calcium signatures in the symbiosis signaling pathway of legumes. *Proc Natl Acad Sci USA* **105**: 9823–9828
- Lahrmann U, Ding Y, Banhara A, Rath M, Hajirezaei MR, Döhlemann S, von Wirén N, Parniske M, Zuccaro A (2013) Host-related metabolic cues affect colonization strategies of a root endophyte. *Proc Natl Acad Sci USA* **110**: 13965–13970

- Lahrman U, Zuccaro A (2012) *Opprimo ergo sum*: evasion and suppression in the root endophytic fungus *Piriformospora indica*. *Mol Plant Microbe Interact* **25**: 727–737
- Lamesch P, Berardini TZ, Li D, Swarbreck D, Wilks C, Sasidharan R, Muller R, Dreher K, Alexander DL, Garcia-Hernandez M, et al (2012) The Arabidopsis Information Resource (TAIR): improved gene annotation and new tools. *Nucleic Acids Res* **40**: D1202–D1210
- Lee YC, Johnson JM, Chien CT, Sun C, Cai D, Lou B, Oelmüller R, Yeh KW (2011) Growth promotion of Chinese cabbage and Arabidopsis by *Piriformospora indica* is not stimulated by mycelium-synthesized auxin. *Mol Plant Microbe Interact* **24**: 421–431
- Li F, Wang J, Ma C, Zhao Y, Wang Y, Hasi A, Qi Z (2013) Glutamate receptor-like channel3.3 is involved in mediating glutathione-triggered cytosolic calcium transients, transcriptional changes, and innate immunity responses in Arabidopsis. *Plant Physiol* **162**: 1497–1509
- Li L, Li M, Yu L, Zhou Z, Liang X, Liu Z, Cai G, Gao L, Zhang X, Wang Y, et al (2014) The FLS2-associated kinase BIK1 directly phosphorylates the NADPH oxidase RbohD to control plant immunity. *Cell Host Microbe* **15**: 329–338
- Liu G, Wei X, Qin Y, Qu Y (2010) Characterization of the endoglucanase and glucomannanase activities of a glycoside hydrolase family 45 protein from *Penicillium decumbens* 114-2. *J Gen Appl Microbiol* **56**: 223–229
- Lu D, Wu S, Gao X, Zhang Y, Shan L, He P (2010) A receptor-like cytoplasmic kinase, BIK1, associates with a flagellin receptor complex to initiate plant innate immunity. *Proc Natl Acad Sci USA* **107**: 496–501
- Macho AP, Zipfel C (2014) Plant PRRs and the activation of innate immune signaling. *Mol Cell* **54**: 263–272
- Mallek-Fakhfakh H, Belghith H (2016) Physicochemical properties of thermotolerant extracellular β -glucosidase from *Talaromyces thermophilus* and enzymatic synthesis of cello-oligosaccharides. *Carbohydr Res* **419**: 41–50
- Manzoor H, Kelloniemi J, Chiltz A, Wendehenne D, Pugin A, Poinssot B, Garcia-Brugger A (2013) Involvement of the glutamate receptor AtGLR3.3 in plant defense signaling and resistance to *Hyaloperonospora arabidopsidis*. *Plant J* **76**: 466–480
- Matsuo M, Johnson JM, Hieno A, Tokizawa M, Nomoto M, Tada Y, Godfrey R, Obokata J, Sherameti I, Yamamoto YY, et al (2015) High redox responsive transcription factor1 levels result in accumulation of reactive oxygen species in *Arabidopsis thaliana* shoots and roots. *Mol Plant* **8**: 1253–1273
- McCarthy T, Hanniffy O, Savage AV, Tuohy MG (2003) Catalytic properties and mode of action of three endo-beta-glucanases from *Talaromyces emersonii* on soluble beta-1,4- and beta-1,3;1,4-linked glucans. *Int J Biol Macromol* **33**: 141–148
- Miwa H, Sun J, Oldroyd GE, Downie JA (2006) Analysis of calcium spiking using a cameleon calcium sensor reveals that nodulation gene expression is regulated by calcium spike number and the developmental status of the cell. *Plant J* **48**: 883–894
- Mousavi SA, Chauvin A, Pascaud F, Kellenberger S, Farmer EE (2013) GLUTAMATE RECEPTOR-LIKE genes mediate leaf-to-leaf wound signalling. *Nature* **500**: 422–426
- Nishimura N, Kitahata N, Seki M, Narusaka Y, Narusaka M, Kuromori T, Asami T, Shinozaki K, Hirayama T (2005) Analysis of ABA hypersensitive germination2 revealed the pivotal functions of PARN in stress response in Arabidopsis. *Plant J* **44**: 972–984
- Nishimura N, Okamoto M, Narusaka M, Yasuda M, Nakashita H, Shinozaki K, Narusaka Y, Hirayama T (2009) ABA hypersensitive germination2-1 causes the activation of both abscisic acid and salicylic acid responses in Arabidopsis. *Plant Cell Physiol* **50**: 2112–2122
- Nothnagel EA, McNeil M, Albersheim P, Dell A (1983) Host-pathogen interactions. XXII. A galacturonic acid oligosaccharide from plant cell walls elicits phytoalexins. *Plant Physiol* **71**: 916–926
- Oldroyd GE (2013) Speak, friend, and enter: signalling systems that promote beneficial symbiotic associations in plants. *Nat Rev Microbiol* **11**: 252–263
- Peiter E (2011) The plant vacuole: emitter and receiver of calcium signals. *Cell Calcium* **50**: 120–128
- Peiter E, Maathuis FJ, Mills LN, Knight H, Pelloux J, Hetherington AM, Sanders D (2005) The vacuolar Ca^{2+} -activated channel TPC1 regulates germination and stomatal movement. *Nature* **434**: 404–408
- Peiter E, Sun J, Heckmann AB, Venkateshwaran M, Riely BK, Otegui MS, Edwards A, Freshour G, Hahn MG, Cook DR, et al (2007) The *Medicago truncatula* DMI1 protein modulates cytosolic calcium signaling. *Plant Physiol* **145**: 192–203
- Peškan-Berghöfer T, Shahollari B, Giang PH, Hehl S, Markert C, Blanke V, Varma AK, Oelmüller R (2004) Association of *Piriformospora indica* with *Arabidopsis thaliana* roots represents a novel system to study beneficial plant-microbe interactions and involves early plant protein modifications in the endoplasmic reticulum and at the plasma membrane. *Physiol Plant* **122**: 465–477
- Pfaffl MW (2001) A new mathematical model for relative quantification in real-time RT-PCR. *Nucleic Acids Res* **29**: e45
- Polisensky DH, Braam J (1996) Cold-shock regulation of the *Arabidopsis* TCH genes and the effects of modulating intracellular calcium levels. *Plant Physiol* **111**: 1271–1279
- Reverdatto SV, Dutko JA, Chekanova JA, Hamilton DA, Belostotsky DA (2004) mRNA deadenylation by PARN is essential for embryogenesis in higher plants. *RNA* **10**: 1200–1214
- Schäfer P, Pfiffi S, Voll LM, Zajic D, Chandler PM, Waller F, Scholz U, Pons-Kühnemann J, Sonnewald S, Sonnewald U, et al (2009) Phytohormones in plant root-*Piriformospora indica* mutualism. *Plant Signal Behav* **4**: 669–671
- Schäffner AR (1998) Mapping mutations with ARMS. *Methods Mol Biol* **82**: 183–198
- Shahollari B, Vadassery J, Varma A, Oelmüller R (2007) A leucine-rich repeat protein is required for growth promotion and enhanced seed production mediated by the endophytic fungus *Piriformospora indica* in *Arabidopsis thaliana*. *Plant J* **50**: 1–13
- Sharma M, Schmid M, Rothballer M, Hause G, Zuccaro A, Imani J, Kämpfer P, Domann E, Schäfer P, Hartmann A, et al (2008) Detection and identification of bacteria intimately associated with fungi of the order Sebaciales. *Cell Microbiol* **10**: 2235–2246
- Sherameti I, Shahollari B, Venus Y, Altschmied L, Varma A, Oelmüller R (2005) The endophytic fungus *Piriformospora indica* stimulates the expression of nitrate reductase and the starch-degrading enzyme glucan-water dikinase in tobacco and Arabidopsis roots through a homeodomain transcription factor that binds to a conserved motif in their promoters. *J Biol Chem* **280**: 26241–26247
- Sherameti I, Tripathi S, Varma A, Oelmüller R (2008) The root-colonizing endophyte *Piriformospora indica* confers drought tolerance in Arabidopsis by stimulating the expression of drought stress-related genes in leaves. *Mol Plant Microbe Interact* **21**: 799–807
- Shi H, Shen Q, Qi Y, Yan H, Nie H, Chen Y, Zhao T, Katagiri F, Tang D (2013) BR-SIGNALING KINASE1 physically associates with FLAGELIN SENSING2 and regulates plant innate immunity in Arabidopsis. *Plant Cell* **25**: 1143–1157
- Sieberer BJ, Chabaud M, Fournier J, Timmers ACJ, Barker DG (2012) A switch in Ca^{2+} spiking signature is concomitant with endosymbiotic microbe entry into cortical root cells of *Medicago truncatula*. *Plant J* **69**: 822–830
- Sieberer BJ, Chabaud M, Timmers AC, Monin A, Fournier J, Barker DG (2009) A nuclear-targeted cameleon demonstrates intranuclear Ca^{2+} spiking in *Medicago truncatula* root hairs in response to rhizobial nodulation factors. *Plant Physiol* **151**: 1197–1206
- Simpson AJ, Brown SA (2005) Purge NMR: effective and easy solvent suppression. *J Magn Reson* **175**: 340–346
- Smaali MI, Michaud N, Marzouki N, Legoy MD, Maugard T (2004) Comparison of two beta-glucosidases for the enzymatic synthesis of beta-(1-6)-beta-(1-3)-gluco-oligosaccharides. *Biotechnol Lett* **26**: 675–679
- Souza CA, Li S, Lin AZ, Boutrot F, Grossmann G, Zipfel C, Somerville SC (2017) Cellulose-derived oligomers act as damage-associated molecular patterns and trigger defense-like responses. *Plant Physiol* **173**: 2383–2398
- Steinhorst L, Kudla J (2014) Signaling in cells and organisms: calcium holds the line. *Curr Opin Plant Biol* **22**: 14–21
- Sun C, Shao Y, Vahabi K, Lu J, Bhattacharya S, Dong S, Yeh KW, Sherameti I, Lou B, Baldwin IT, et al (2014) The beneficial fungus *Piriformospora indica* protects Arabidopsis from *Verticillium dahliae* infection by downregulation plant defense responses. *BMC Plant Biol* **14**: 268
- Suzuki H, Igarashi K, Samejima M (2010) Cellotriose and cellotetraose as inducers of the genes encoding cellobiohydrolases in the basidiomycete *Phanerochaete chrysosporium*. *Appl Environ Microbiol* **76**: 6164–6170
- Trouvelot S, Héloir MC, Poinssot B, Gauthier A, Paris F, Guillier C, Combier M, Trdál L, Daire X, Adrian M (2014) Carbohydrates in plant

- immunity and plant protection: roles and potential application as foliar sprays. *Front Plant Sci* **5**: 592
- Vadassery J, Oelmüller R (2009) Calcium signaling in pathogenic and beneficial plant microbe interactions: what can we learn from the interaction between *Piriformospora indica* and *Arabidopsis thaliana*. *Plant Signal Behav* **4**: 1024–1027
- Vadassery J, Ranf S, Drzewiecki C, Mithöfer A, Mazars C, Scheel D, Lee J, Oelmüller R (2009) A cell wall extract from the endophytic fungus *Piriformospora indica* promotes growth of *Arabidopsis* seedlings and induces intracellular calcium elevation in roots. *Plant J* **59**: 193–206
- Vahabi K, Dorcheh SK, Monajembashi S, Westermann M, Reichelt M, Falkenberg D, Hemmerich P, Sherameti I, Oelmüller R (2016) Stress promotes *Arabidopsis*-*Piriformospora indica* interaction. *Plant Signal Behav* **11**: e1136763
- Venkateshwaran M, Cosme A, Han L, Banba M, Satyshur KA, Schleiff E, Parniske M, Imaizumi-Anraku H, Ané JM (2012) The recent evolution of a symbiotic ion channel in the legume family altered ion conductance and improved functionality in calcium signaling. *Plant Cell* **24**: 2528–2545
- Verma SA, Varma A, Rexer KH, Hassel A, Kost G, Sarbhoy A, Bisen P, Bütehorn B, Franken P (1998) *Piriformospora indica*, gen. et sp. nov., a new root-colonizing fungus. *Mycologia* **90**: 898–905
- Virtanen A, Henriksson N, Nilsson P, Nissbeck M (2013) Poly(A)-specific ribonuclease (PARN): an allosterically regulated, processive and mRNA cap-interacting deadenylase. *Crit Rev Biochem Mol Biol* **48**: 192–209
- Waller F, Achatz B, Baltruschat H, Fodor J, Becker K, Fischer M, Heier T, Hückelhoven R, Neumann C, von Wettstein D, et al (2005) The endophytic fungus *Piriformospora indica* reprograms barley to salt-stress tolerance, disease resistance, and higher yield. *Proc Natl Acad Sci USA* **102**: 13386–13391
- Wang Y, Dindas J, Rienmüller F, Krebs M, Waadt R, Schumacher K, Wu WH, Hedrich R, Roelfsema MR (2015) Cytosolic Ca²⁺ signals enhance the vacuolar ion conductivity of bulging *Arabidopsis* root hair cells. *Mol Plant* **8**: 1665–1674
- Weiß M, Waller F, Zuccaro A, Selosse MA (2016) Sebaciniales: one thousand and one interactions with land plants. *New Phytol* **211**: 20–40
- Xiong TC, Ronzier E, Sanchez F, Corratgé-Faillie C, Mazars C, Thibaud JB (2014) Imaging long distance propagating calcium signals in intact plant leaves with the BRET-based GFP-aequorin reporter. *Front Plant Sci* **5**: 43
- Yadav V, Kumar M, Deep DK, Kumar H, Sharma R, Tripathi T, Tuteja N, Saxena AK, Johri AK (2010) A phosphate transporter from the root endophytic fungus *Piriformospora indica* plays a role in phosphate transport to the host plant. *J Biol Chem* **285**: 26532–26544
- Zhang J, Li W, Xiang T, Liu Z, Laluk K, Ding X, Zou Y, Gao M, Zhang X, Chen S, et al (2010) Receptor-like cytoplasmic kinases integrate signaling from multiple plant immune receptors and are targeted by a *Pseudomonas syringae* effector. *Cell Host Microbe* **7**: 290–301
- Zhang X, Devany E, Murphy MR, Glazman G, Persaud M, Kleiman FE (2015) PARN deadenylase is involved in miRNA-dependent degradation of TP53 mRNA in mammalian cells. *Nucleic Acids Res* **43**: 10925–10938
- Zhang X, Henriques R, Lin SS, Niu QW, Chua NH (2006) Agrobacterium-mediated transformation of *Arabidopsis thaliana* using the floral dip method. *Nat Protoc* **1**: 641–646
- Zhao J, Guo C, Tian C, Ma Y (2015) Heterologous expression and characterization of a GH3 β -glucosidase from thermophilic fungi *Myceliophthora thermophila* in *Pichia pastoris*. *Appl Biochem Biotechnol* **177**: 511–527
- Zipfel C (2008) Pattern-recognition receptors in plant innate immunity. *Curr Opin Immunol* **20**: 10–16
- Zuccaro A, Lahrman U, Güldener U, Langen G, Piffi S, Biedenkopf D, Wong P, Samans B, Grimm C, Basiewicz M, et al (2011) Endophytic life strategies decoded by genome and transcriptome analyses of the mutualistic root symbiont *Piriformospora indica*. *PLoS Pathog* **7**: e1002290

Manuscript 2

Arabidopsis thaliana responds to colonisation of *Piriformospora indica* by secretion of symbiosis-specific proteins

Johannes Thürich, Doreen Meichsner, Alexandra C. U. Furch, Jeannette Pfalz, Thomas Krüger, Olaf Kniemeyer, Axel Brakhage, Ralf Oelmüller

PLoS ONE 13(12): e0209658. <https://doi.org/10.1371/journal.pone.0209658>

Summary

In this publication the influence of *P. indica* on the secretome of *A. thaliana* and *vice versa* was studied. A shift in the proteins in the supernatant of the different treatments was found. The involvement of Polycystin, Lipoxygenase, Alpha-toxin and Triacylglycerol lipase 1 (PLAT1) and the role of the phenolic coumarins scopolin/ scopoletin, and ER-bodies on symbiosis were studied more in detail.

I designed the experiments with the help of Doreen Meichsner, Axel Brakhage, and Ralf Oelmüller. Together with Thomas Krüger, I performed the Solid-Phase-Extraction (SPE) experiments. Together with Doreen Meichsner, I performed the gene expression studies, High Performance Liquid Chromatography (HPLC), and growth experiments. Together with Alexandra Furch, I performed the microscopic studies. I performed the GO-term (Gene Ontology) analysis, statistical analysis, literature research of the secretome, and generated the graphs. I wrote the original draft of the article which was reviewed by Alexandra Furch, Jeannette Pfalz, and Ralf Oelmüller.

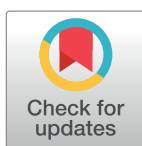
RESEARCH ARTICLE

Arabidopsis thaliana responds to colonisation of *Piriformospora indica* by secretion of symbiosis-specific proteins

Johannes Thürich¹, Doreen Meichsner¹, Alexandra C. U. Furch¹, Jeannette Pfalz¹, Thomas Krüger², Olaf Kniemeyer², Axel Brakhage^{2,3}, Ralf Oelmüller^{1*}

1 Plant Physiology, Matthias-Schleiden-Institute for Genetics, Bioinformatics and Molecular Botany, Faculty of Biological Science, Friedrich-Schiller-University Jena, Jena, Germany, **2** Molecular and Applied Microbiology, Leibniz Institute for Natural Product Research and Infection Biology Hans Knöll Institute, Jena, Germany, **3** Institute of Microbiology, Friedrich Schiller University Jena, Jena, Germany

* ralf.oelmueller@uni-jena.de



OPEN ACCESS

Citation: Thürich J, Meichsner D, Furch ACU, Pfalz J, Krüger T, Kniemeyer O, et al. (2018) *Arabidopsis thaliana* responds to colonisation of *Piriformospora indica* by secretion of symbiosis-specific proteins. PLoS ONE 13(12): e0209658. <https://doi.org/10.1371/journal.pone.0209658>

Editor: Ricardo Aroca, Estacion Experimental del Zaidin, SPAIN

Received: May 4, 2018

Accepted: December 10, 2018

Published: December 27, 2018

Copyright: © 2018 Thürich et al. This is an open access article distributed under the terms of the [Creative Commons Attribution License](https://creativecommons.org/licenses/by/4.0/), which permits unrestricted use, distribution, and reproduction in any medium, provided the original author and source are credited.

Data Availability Statement: All relevant data are within the paper and its Supporting Information files with the exception of the mass spectrometry proteomics data. They have been deposited to the ProteomeXchange Consortium via the PRIDE partner repository with the dataset identifier PXD009563 (Reviewer account details: Username: reviewer95832@ebi.ac.uk; Password: zHk3U002).

Funding: This research was funded by Deutsche Forschungsgemeinschaft (CRC1127 – ChemBioSys to JT, AB, and RO), (CRC/Transregio

Abstract

Plants interact with a wide variety of fungi in a mutualistic, parasitic or neutral way. The associations formed depend on the exchange of nutrients and signalling molecules between the partners. This includes a diverse set of protein classes involved in defence, nutrient uptake or establishing a symbiotic relationship. Here, we have analysed the secretomes of the mutualistic, root-endophytic fungus *Piriformospora indica* and *Arabidopsis thaliana* when cultivated alone or in a co-culture. More than one hundred proteins were identified as differentially secreted, including proteins associated with growth, development, abiotic and biotic stress response and mucilage. While some of the proteins have been associated before to be involved in plant-microbial interaction, other proteins are newly described in this context. One plant protein found in the co-culture is PLAT1 (Polycystin, Lipoxygenase, Alpha-toxin and Triacylglycerol lipase). PLAT1 has not been associated with plant-fungal-interaction and is known to play a role in abiotic stress responses. In colonised roots PLAT1 shows an altered gene expression in a stage specific manner and *plat1* knock-out plants are colonised stronger. It co-localises with Brassicaceae-specific endoplasmic reticulum bodies (ER-bodies) which are involved in the formation of the defence compound scopolin. We observed degraded ER-bodies in infected *Arabidopsis* roots and a change in the scopolin level in response to the presence of the fungus.

Introduction

The roots of more than 80% of all land plants form mycorrhizal interaction [1]. The interactions can shift from mutualism to parasitism depending on environmental conditions and the communication between the organisms [2]. The communication between the symbionts is driven by molecules released into the rhizosphere by both partners including diverse protein classes [3–6]. Based on genome analyses, it has been estimated that the proportion of released fungal proteins represent about 3% to 10% of the corresponding total proteome [6]. Furthermore, the

124 – FungiNet (project Z2) to TK and OK), and the Jena School of Microbial Communication. The funders had no role in study design, data collection and analysis, decision to publish, or preparation of the manuscript.

Competing interests: The authors have declared that no competing interests exist.

size of the predicted secretomes correlates with the lifestyle of a fungus. For example, pathogenic fungi appear to have more secretory proteins compared to saprophytic and mutualistic species [6, 7]. Proteomic-based technologies and bioinformatic tools identified multiple fungal proteins which determine the mode of interaction and reprogram the root cells [8–10]. Depending on the organism and strain colonising the plant, the number and amount of the secreted proteins from both partners can vary, as shown during the symbiotic interaction of different fungi with *Pisum sativum*, *Medicago truncatula* and *Nicotiana benthamiana* [11–14]. Mutualistic fungi secrete also various effector proteins that repress plant defence responses. After entering the plant cell, some effector proteins are transported to the plant nucleus, where they can interact with transcription factors and repress plant defence [15]. This is well studied for the small secreted protein 7 (SP7) from *Rhizophagus irregularis* and MISSP7 (mycorrhiza-induced small secreted protein-7) from *Laccaria bicolor* [16–18].

Similar to the fungal secretome, between 6% to 17% of plant proteins are estimated to be secreted [19, 20]. These proteins have multiple functions including growth regulation, communication, nutrient uptake and defence responses. However, most of them are uncharacterised [21, 22]. Among the better studied are germin-like proteins which can produce reactive oxygen species in response to stress and during plant growth. They have multiple roles outside the cell, particularly in defence and development [23, 24]. Furthermore, small peptides, such as members of the CLE (clavata3/embryo-surrounding region) family, have been implicated in development, inter-plant communication, defence and in the formation of new symbiosis related organs such as nodules [21, 25, 26].

Exudate proteins are often identified by bioinformatic tools based on the prediction of their N-terminal secretion sequence which directs them into the endoplasmic reticulum (ER) from where they are secreted via vesicle fusion with the plasma membrane [16, 27, 28]. However, only ~ 50% of the known secreted plant proteins possess such a signal [11, 22] whereas others utilise unconventional mechanisms of secretion, which resemble those of animal exosomes [29] or include exocyst-like structures [30]. For example, between 50% to 80% of proteins found in the secretome of *Arabidopsis* after treatment with salicylic acid or pathogens do not possess a N-terminal secretory sequence [11, 31, 32]. Although some of these proteins can also be contaminations, e.g. due to cell damage, untargeted secretome studies are valuable addition to bioinformatic-based studies. While *A. thaliana* does not form mycorrhizal associations, the plant can be colonised by endophytes, such as *Piriformospora indica*. This fungus of the order Sebaciales was isolated from roots of plants growing in the Indian Thar desert [33]. The fungus has a saprophytic lifestyle and colonises the roots of many plant species. Colonised plants produce more biomass, in particular under unfavourable conditions, and are more resistant to abiotic and biotic stresses [34–36]. Based on expression profiles during the colonisation of *Arabidopsis* [37] and barley roots [5], the interaction can roughly be split into three stages, which corresponds to the saprophytic and mutualistic traits of *P. indica* [38]. The initial contact is characterised by the down-regulation of plant defence mechanisms, followed by a phase in which the fungus reduces the expression of genes associated with saprophism [38]. During the last phase, a long-lasting beneficial interaction is established [5, 12, 37].

To balance beneficial and non-beneficial traits in a symbiosis, the propagation of microbes in the roots must be controlled by host defence compounds. One of them is the coumarin scopoletin, which accumulates in the ER-body [39]. The ER-bodies derive as subdomains from the ER network and have specialised functions in glucosinolate-based defence [39–41]. ER-bodies harbour high levels of β -glucosidases including PYK10, the most abundant enzyme of the organelle [42]. When ER-bodies are disrupted during pathogen attack or damage, PYK10 and other enzymes are released into the cytoplasm. PYK10 is involved in establishing the interaction between *P. indica* and *A. thaliana* roots [43]. The roots of mutant lines with reduced

PYK10 level are overcolonised by *P. indica*, although *PYK10* expression is unaffected by *P. indica* in wild type (WT) seedlings [43, 44]. PYK10 hydrolyses multiple indole glucosinolates and scopoletin to scopolin [44, 45]. Scopoletin, and its glycone scopolin, accumulates in roots and helps plants to fine tune their defence responses by scavenging of reactive oxygen species [46, 47]. Scopoletin acts as antifungal component against *Alternaria alternata* in tobacco and is strongly suppressed in the beneficial symbiosis of tomato with *R. irregularis* [48, 49]. A key enzyme for scopoletin biosynthesis is the feruloyl-CoA 6'-hydroxylase 1 (F6'H1), and the accumulation of this secondary metabolite is severely reduced in the corresponding knock-out line [46]. Interestingly, biosynthesis of scopoletin can also be stimulated by ectopic expression of the Arabidopsis PLAT1 and -2 (Polycystin, Lipoxxygenase, Alpha-toxin and Triacylglycerol lipases) proteins in tobacco [50]. It has been hypothesized that the PLAT domain provides a docking platform for proteins to regulate their catalytic activities [51–53]. AtPLAT1 and -2 proteins are functionally and physically associated with ER-bodies [51]. This suggests an interaction with PYK10, although the exact function of the PLAT domain is still enigmatic.

In this study, we identified proteins which are found in the growth medium of *A. thaliana*, *P. indica* or *P. indica* co-cultivated with *A. thaliana*. Proteins which are only found in the co-culture or disappear from it, are considered symbiosis-specific and are mainly involved in growth and defence-related processes. Many enzymes belonging to the latter category are implicated in the production or release of secondary metabolites. The role of one of these proteins, PLAT1, was investigated in more detail and its postulated function in the formation of the defence compound scopolin was related to the degradation of ER-bodies and root colonisation.

Results

Secretome analysis of *P. indica* and *A. thaliana* reveal distinct changes in the co-culture

To identify symbiosis-specific proteins that are secreted during the early phase of the interaction between *P. indica* and *A. thaliana*, we co-cultivated both organisms in liquid plant nutrition media (PNM) for three days and compared them with cultures of the plant and fungus grown separately (S1 Fig). The spent media were filtered and proteins were isolated by solid phase extraction followed by LC-MS/MS (liquid chromatography–tandem mass spectrometry) analysis. The resulting MS/MS spectra were searched against the UniProt database (<http://www.uniprot.org/>) [54] where a total of 590 different *A. thaliana* and 164 *P. indica* proteins were identified in three independent biological replicates (S1 Table). In the single cultures of Arabidopsis 199, 316 and 117 proteins were observed within three replicates, while the number of identified proteins in the single fungal cultures were 39, 76 and 76. In the co-culture 140, 311 and 85 plant proteins and 120, 108 and 84 fungal proteins were observed per replicate. The Venn diagram in S2A Fig shows the overlap of Arabidopsis proteins in the co-culture among all replicates. 57 plant proteins were common to all three replicates, which represent 16% of all identified proteins. In total, 33% of proteins were found in at least 2 replicates (S2A Fig). When comparing the replicates of the plant and fungal single cultures, similar percentages were found.

For further investigations, we took all identified plant proteins and classified them (S2 Table) according to their GO (Gene ontology) terms using AmiGO (<http://www.geneontology.org>, version 1.8) [55–57]. Due to the absence of a functional annotation for a high number of fungal proteins, no GO terms have been captured for *P. indica*. The GO terms annotated to plant proteins were sorted within the categories “molecular functions”, “biological processes” and “cellular components” (Fig 1A–1C). For each category, the 20 most abundant terms are shown in Fig 1A–1C. The functional categorisation revealed that secreted plant proteins in both cultures belong mainly

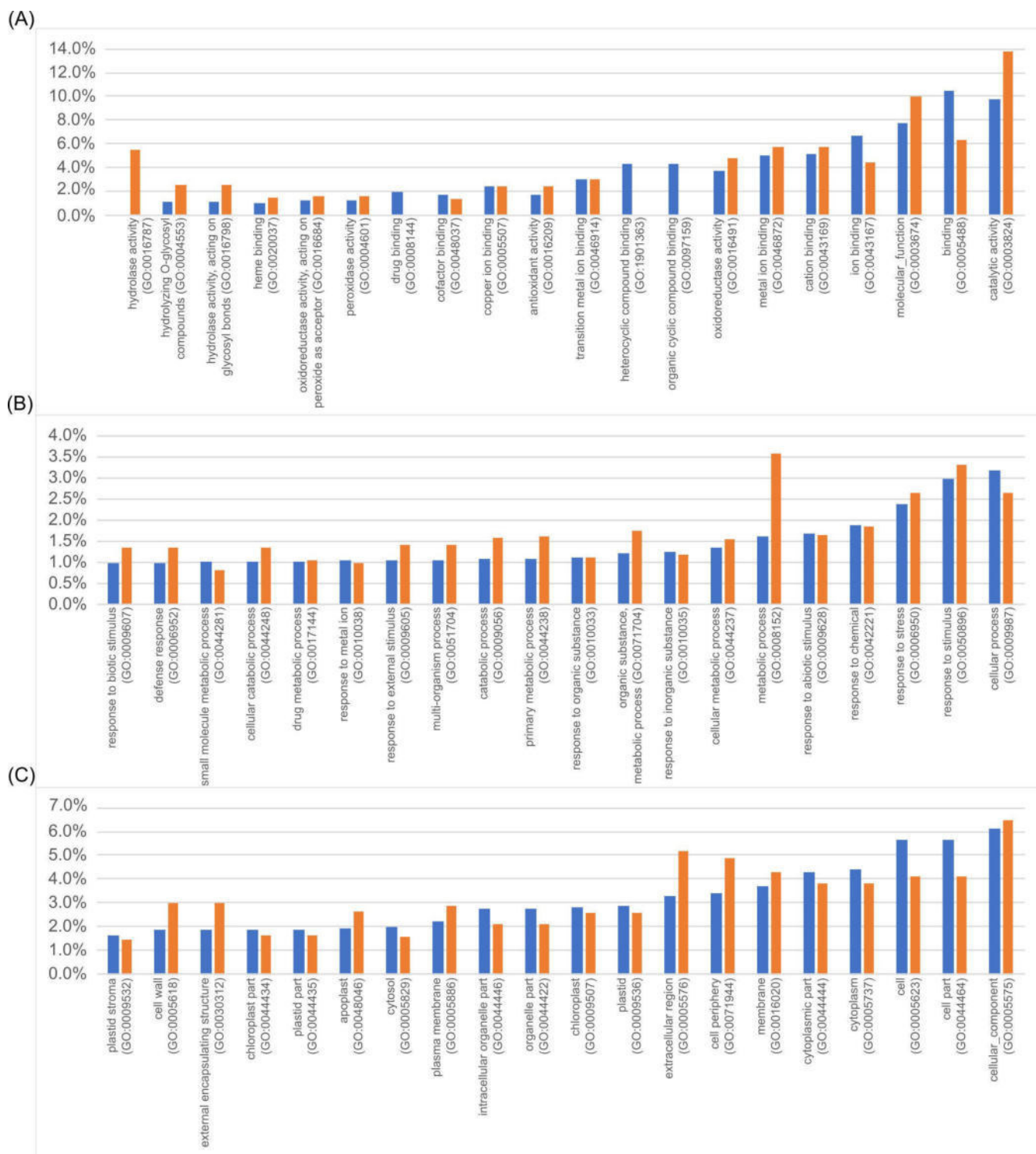


Fig 1. GO enrichment analysis of the secretomes. All identified plant proteins were analysed using the GO term analysis tool using AmiGO (<http://www.geneontology.org>, version 1.8) and sorted according to the categories of biological processes (A), molecular functions (B) and cellular components (C). The 20 most abundant GO terms are presented here (in percentage). Blue bars indicate the frequency of this GO term in single cultures, orange bars indicate the frequency of the respective GO term in co-cultures.

<https://doi.org/10.1371/journal.pone.0209658.g001>

to identical GO terms, however, the number of protein entries varies for each term. As shown in Fig 1A, the most frequent term (10%) related to proteins found in the single culture of *Arabidopsis* is “binding of different compounds” (GO:0005488), whereas the most abundant term related to proteins from the co-culture (12%) is “catalytic activity” (GO:0003824). As another example, about 5% of the proteins in the co-culture play a role in hydrolysis (GO:00016787), while proteins associated with this GO term were not found in the single culture. Among the terms of the category “biological processes” (Fig 1B), slight differences between the single and co-culture were observed. For instance, proteins with the GO term “metabolic process” (GO:0008152) were found twice as often in the co-culture. Furthermore, the terms “defence”, “external stimuli”, “response to biotic stimulus” and “catabolic process” were found more often for co-cultures. The category “cellular component” (Fig 1C) included notably more proteins associated with the GO terms “extracellular region” and “cell periphery” in the co-culture. Contrary, GO terms associated with “cellular processes” or “organelles” were more frequently found in the single culture.

***A. thaliana* responds to the presence of *P. indica* by an altered secretion of proteins associated with defence and growth.** To better understand changes in the composition of secreted proteins, we looked for specific differences between the co-culture and single culture (S2 Table). The analysis considered only proteins found in two or more root exudates and these proteins were classified based on their function. We observed 102 proteins to be differentially secreted (Fig 2). The most enriched proteins in the single culture are associated with the functions “primary metabolism”, “abiotic stress response”, “growth and development” and “biotic stress response” (~20% each). In the co-cultures, 55% of the proteins play a role in defence against biotic stresses, 20% have been described in the context of growth and development, 11% belong to the primary metabolism and 7% proteins are related to abiotic stress responses. Furthermore, 11% proteins are classified as miscellaneous. Interestingly, 7% of the differentially secreted proteins are associated with mucilage.

Among proteins, which were involved in development and growth and which were predominantly detected in the co-culture, are the ribonuclease T2 (At1G14220), the lipid recognition protein At5G23840 and the pectin methylesterase inhibitor At1G23205. Examples related to biotic stress responses include the pathogenesis-related protein 5 (At1G75040), which was

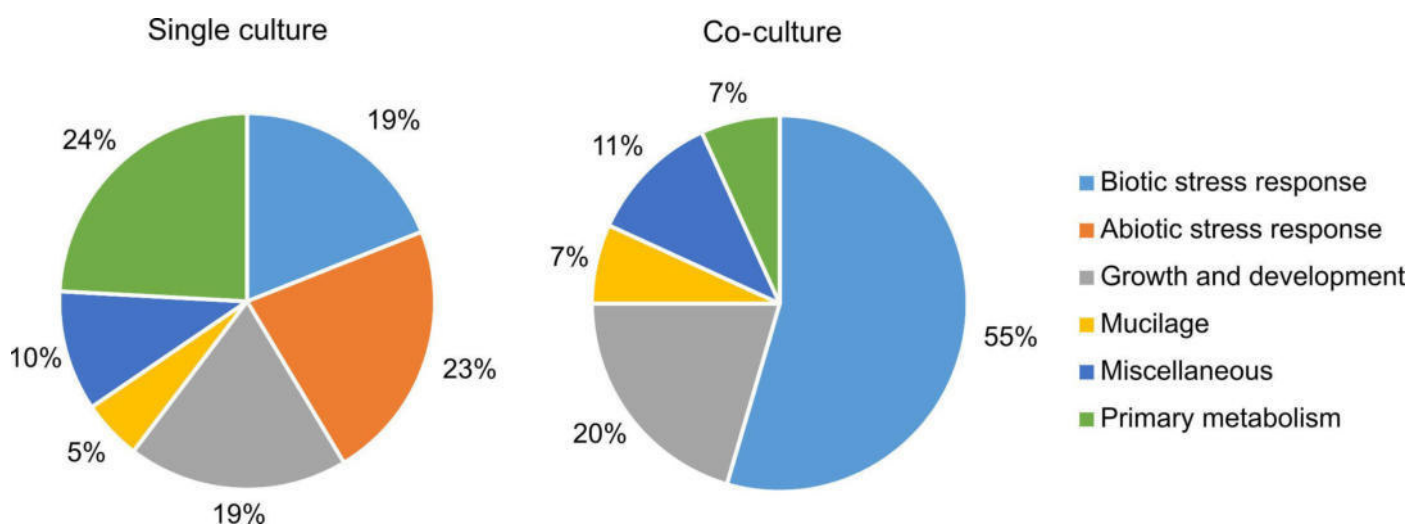


Fig 2. Differentially secreted proteins. *Arabidopsis* proteins that were found in at least two replicates and with different frequencies in the single and co-culture (S2 Table) were sorted according to their primary function. Numbers are given in %.

<https://doi.org/10.1371/journal.pone.0209658.g002>

strongly induced by the fungus. In Arabidopsis, it has been implicated in systemic acquired resistance [58]. Furthermore, the two functionally distinct germin like proteins (GLPs), GLP2 (At1G02335) and GLP4 (At1G18970) appear to be secreted into the co-culture upon interaction with the fungus. Additionally, PLAT1 (At4G39730) was found in the medium of the co-culture.

The single cultures contain a different set of proteins. The list includes several proteins associated with abiotic stress responses, particularly some proteins involved in cadmium stress such as At1G11860 (aminomethyl transferase), At1G48030 (dihydrolipoyl dehydrogenase 1) and At3G23990 (chaperonin CPN60) [59]. The single culture also contains ABA (abscisic acid)-inducible proteins such as At1G76180 (dehydrin ERD14), At1G20440 (dehydrin COR47), At5G15970 (stress-induced protein KIN2), the glycine-rich protein At1G04800 and the peroxidase 69 (At5G64100) [60–69]. Surprisingly, the well-known defence compound remorin 3 (At2G45820), which was shown to be associated with plasma membranes and to bind proteins derived from pathogens [70–72], was only detected in the single cultures. Interestingly, the analyses also detected six mucilage-related Arabidopsis proteins as potential targets for *P. indica* (S2 Table). In the co-culture, the mucilage-related proteins aspartic protease 1 (At3G18490), responsive to dehydration 21A (At1G47128) and its homologue 21B (At5G43060) were identified [73]. In contrast, the xyloglucan endotransglucosylase 6 (At5G65730) was only found in the single culture. A homologue of endotransglucosylase 6 was found in the mucilage of maize roots [74]. Also, the oxalate-CoA ligase At3G48990, which has a role in seed mucilage, and the subtilisin-like protease 1.8 (SBT1.8, At2G05920) were only found in the single culture [73, 75]. The latter is highly homologous to SBT1.7 (At5G67360), a key protein for mucilage formation, which is present in both the single and the co-culture (S1 Table). Other mucilage-associated proteins such as fasciclin-like arabinogalactan protein 10 (At3G60900), auxin-induced in root cultures protein 12 (At3G07390) and non-specific lipid-transfer protein 6 (At3G08770) were found in both fractions (S1 Table) [73].

All differentially enriched proteins were also examined individually to assess whether they possess an N-terminal secretion sequence using available bioinformatics tools TargetP 1.1 (<http://www.cbs.dtu.dk/services/TargetP/>), SignalP 4.1 (<http://www.cbs.dtu.dk/services/SignalP/>) and Predotar 1.3 (<https://urgi.versailles.inra.fr/Tools/Predotar>) [76, 77]. The results showed that 36 out of 44 proteins in the co-culture and 18 out of 58 proteins in the single culture possess a predicted N-terminal secretion sequence (S2 Table).

Symbiosis reprograms the *P. indica* secretome. A total of 164 *P. indica* proteins were found in all experiments (S1 Table): 36 of them were differentially enriched between the treatments (S2 Table). Among these proteins, two were found predominantly in the single fungal culture (S2 Table): PIIN_00867, an uncharacterised protein, -and PIIN_06517 related to glyoxal oxidase. 34 proteins were present only in the co-culture. Generally, many of the fungal proteins identified in this study are uncharacterised or possess homology to degrading enzymes. For instance, PIIN_01733, which was found in the co-cultures, is a putative beta-mannanase with homology to hydrolases from two saprophytic fungi [78]. Additionally, we analysed fungal proteins for subcellular localization using available bioinformatics tools: 21 contained an N-terminal secretory signal peptide (S2 Table). One of them is an indole-3-acetaldehyde dehydrogenase (PIIN_04899) which has been suggested to be involved in the formation of auxin [79].

***P. indica*-root colonisation influences PLAT1 and leads to changes in scopolin production.** As a case example to study the secretome, we further analysed the role of the Polycystin, Lipoygenase, Alpha-toxin and Triacylglycerol lipases 1 (PLAT1). This protein was found in the medium of the co-culture and has not been reported in context with *P. indica* before. We checked the expression level of *PLAT1* in colonised WT roots and observed a significant lower level of *plat1* mRNA at three and seven days of co-cultivation. After two weeks the level of

plat1 mRNA was comparable to uncolonised plants (Fig 3A). In shoots no regulation was observed (Fig 3B). A weak but not significant downregulation was observed for the homologous *plat2* mRNA, whereas for the putative pseudogene *plat3* no regulation was observed.

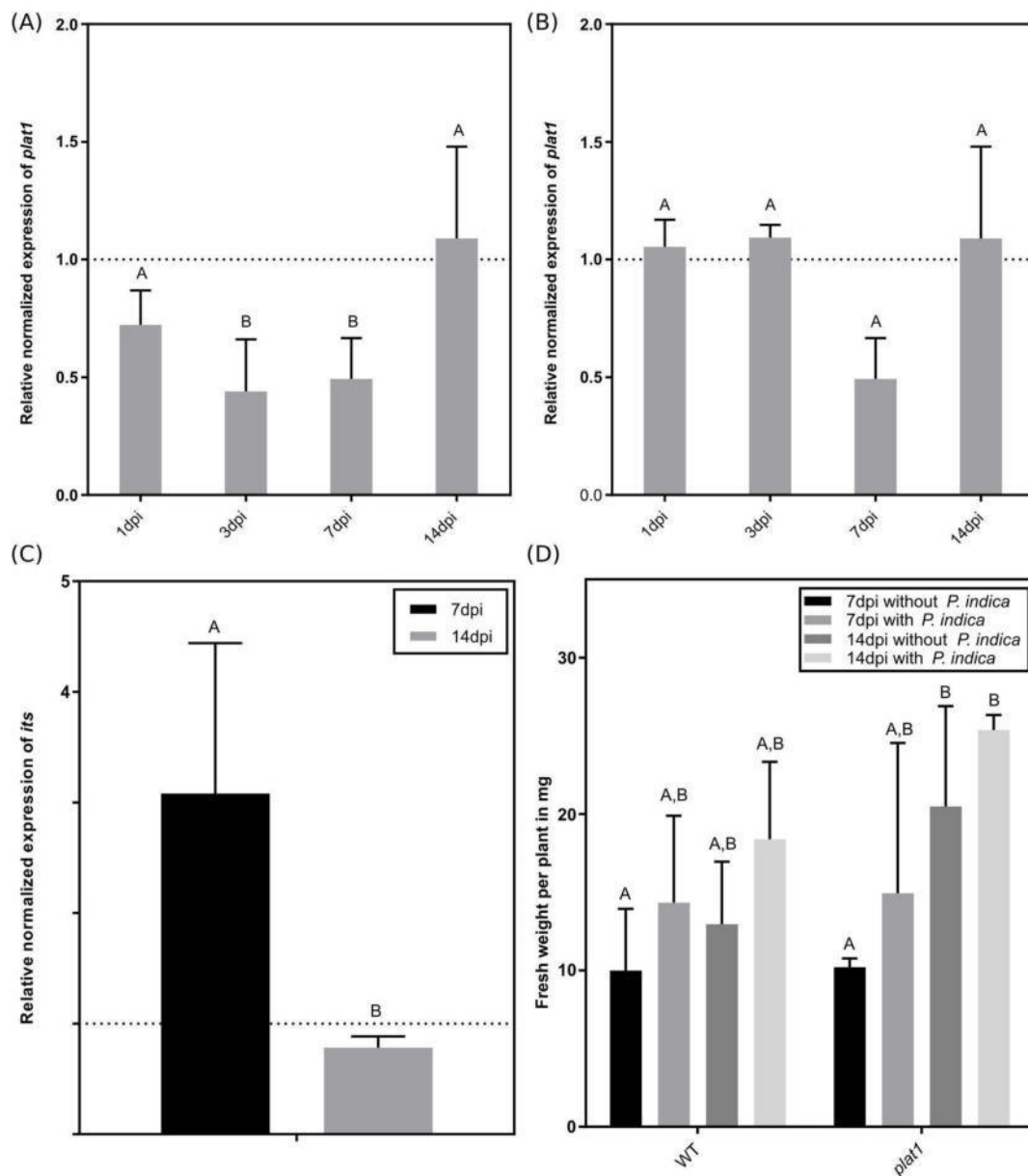


Fig 3. Characterisation of *plat1* mutant and *plat1* gene expression. Gene expression of *PLAT1* in WT roots (A) and leaves (B) was determined between one day and 14 days of colonisation. The dashed line represents levels of mRNA in uncolonised WT roots. (C) Colonisation of *P. indica* in WT and *plat1* roots determined by RT-qPCR. The dashed line represents the level of fungal internal transcribed spacer (*its*) mRNA in colonised WT roots after one and two weeks, respectively. At 7dpi (days post inoculation) the *plat1* mutant was significant stronger colonised compared to WT plants. (D) Effect of *P. indica* on fresh weight in WT and different mutant *A. thaliana* plants after one and two weeks of colonisation. All experiments were repeated three to six times with at least ten plants each. Error bars represent standard deviation. Different letters represent significant differences between treatments at $p < 0.05$ (Two-Way ANOVA, followed by a Bonferroni correction).

<https://doi.org/10.1371/journal.pone.0209658.g003>

Interestingly, a ten-time higher expression in leaves compared to roots was observed for *plat3*. Nevertheless, for all tested time points and plant parts the expression level of *plat3* was extremely low (S2B and S2C Fig). Since *P. indica* had the strongest effect on *PLAT1* expression, we took a closer look at the colonisation of *plat1* mutant seedlings by the fungus. After one week, we found a three times higher amount of fungal RNA in the *plat1* mutant compared to the WT seedlings, whereas after two weeks no differences in colonisation between *plat1* mutants and WT plants was observed (Fig 3C). This stronger colonisation did not have an impact on the total fresh weight of the *plat1* mutants (Fig 3D).

These results could be confirmed by microscopy (Fig 4): after seven days we observed a stronger colonisation in the *plat1* mutant (Fig 4A) compared to the WT (Fig 4B), where almost no fungus could be detected.

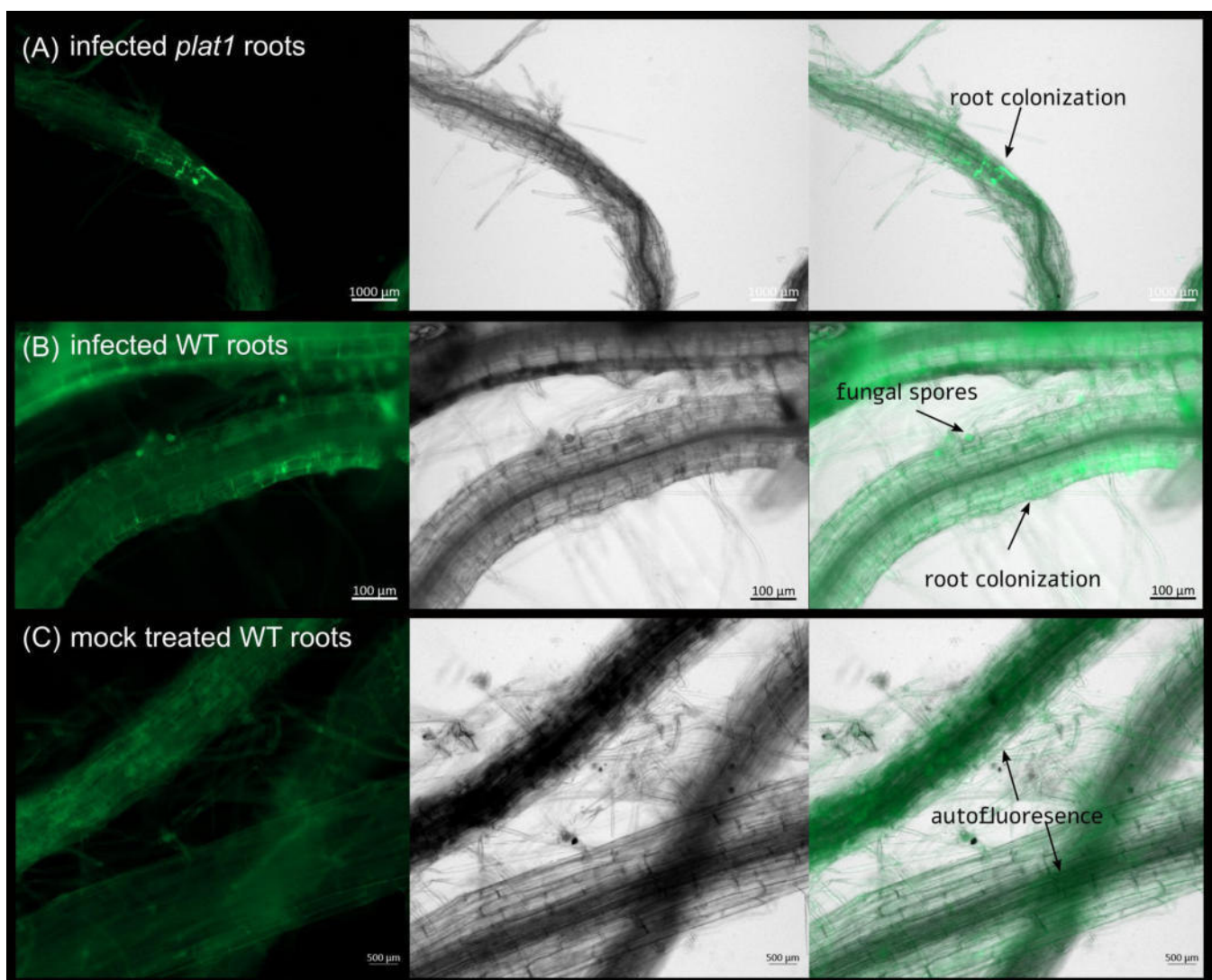


Fig 4. Root colonisation of Arabidopsis WT and *plat1* by *P. indica* at 7 dpi. Colonisation of Arabidopsis *plat1* (A) and WT roots (B) was imaged using fluorescence microscopy at 7 dpi. Uncolonised roots are shown at (C). The first pictures show the autofluorescence of the root and GFP (green fluorescent protein) fluorescence of *P. indica*. The second pictures show the bright field image. The last pictures show the overlay of all images for each row.

<https://doi.org/10.1371/journal.pone.0209658.g004>

Since AtPLAT1, which was identified in the co-culture, promotes scopoletin biosynthesis [50], and an upregulation of scopoletin in colonised *A. thaliana* roots has been described before [12], we analysed the connection between PLAT1, scopoletin and *P. indica* colonisation.

In a first step we examined the influence of scopolin and scopoletin on *P. indica* *in vitro* and found that both chemicals inhibit the growth of *P. indica* with a half maximal inhibitory concentrations (IC_{50}) of 0.34 mM and 0.45 mM, respectively (Fig 5).

Scopolin is much more abundant than scopoletin and can easily be measured in high quantities, in Arabidopsis roots [80]. Therefore, we studied the influence of *P. indica* on scopolin production in Arabidopsis roots *in vivo*. After two weeks, the mock treated WT roots showed a four-time upregulation of scopolin compared to the other time points, whereas in colonised roots the scopolin level was not altered. Instead, the same level of scopolin was observed for all time points and treatments in the *plat1* mutant (Fig 6).

To examine whether scopolin alone is responsible for the altered colonisation in the *plat1* mutant, we investigated the performance of the fungus in the *f6'h1* Arabidopsis mutant line where scopolin and scopoletin production is severely reduced (Fig 7A). When comparing the fresh weight between WT and *f6'h1* plants, we observed, similar to *plat1* (Fig 3D), that the

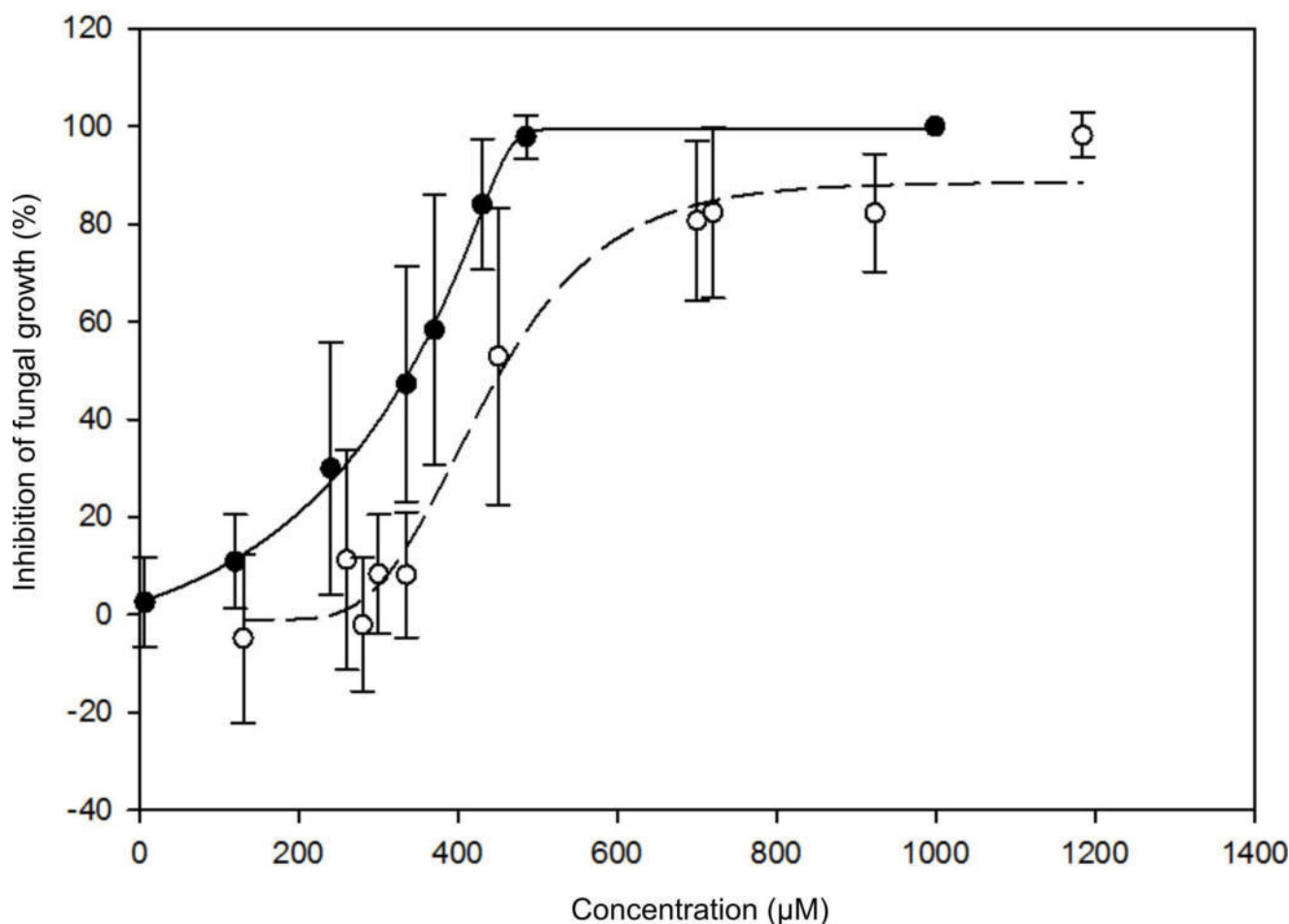


Fig 5. Growth inhibition of *P. indica* by scopoletin / scopolin. Sigmoidal regression line of the growth effect of scopoletin (full dots) and scopolin (hollow dots) on growth of *P. indica*. Error bars represent standard deviation. The experiment was repeated in three biological replicates with two technical replicates each.

<https://doi.org/10.1371/journal.pone.0209658.g005>

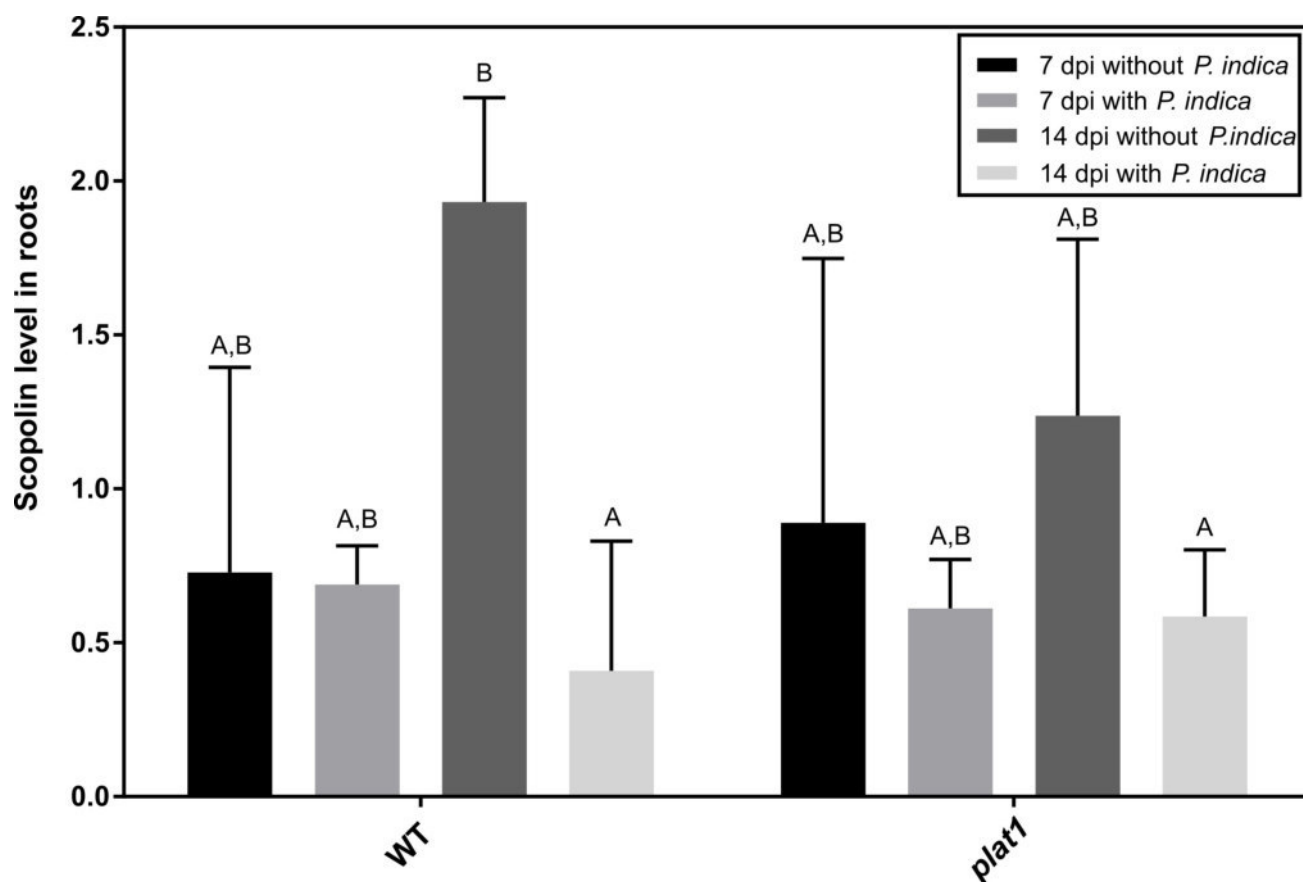


Fig 6. Characterisation of *plat1* mutant and *plat1* gene expression. First, we determined the scopolin levels in root of WT and *plat1*, and the peak areas of HPLC chromatograms were normalised by an internal standard. All experiments were repeated four to five times with at least ten plants each. Error bars represent standard deviation. Different letters represent significant differences between treatments at $p < 0.05$ (Two-Way ANOVA, followed by a Bonferroni correction).

<https://doi.org/10.1371/journal.pone.0209658.g006>

mutant lines are not influenced by the presence of the fungi. Furthermore, the mutant lines were smaller than WT plants (Fig 7B). Since PYK10 can be involved in scopolin formation, we checked its expression: *pyk10* is not influenced by the fungus neither in the WT plants nor in the *plat1* or the *f6'h1* mutant background (Fig 7C). Other genes, which are also associated with scopolin formation, are not influenced by the fungus in *f6'h1* or WT plants as well (S3 Fig).

We further analysed the colonisation of Arabidopsis roots by microscopy. Seven days after co-cultivation most of the hyphae associated with WT roots were detected on the root surface between the epidermal and subepidermal root cells and barely detectable within root cells, whereas in *f6'h1* mutant roots, hyphae could be detected around and within root cells. This effect was even stronger 14 and 19 days after co-cultivation (Fig 8).

***P. indica*-root colonisation causes degradation of ER-bodies.** The Arabidopsis lipases PLAT1 and -2 are functionally associated and co-localise with ER-bodies *in vivo* [51]. Thus, we analysed the fate of ER-bodies during the establishment of symbiosis (Fig 9). The size of ER-bodies in uncolonised roots is not altered during the development of the plant but decreases during the interaction with the fungus (Fig 9A). After three days, the ER-bodies in the WT have the normal rod-shaped structure (Fig 9B) but are slightly smaller in the colonised roots (Fig 9C). After seven days, the ER-bodies in the fungal treated roots have a significant reduced size and,

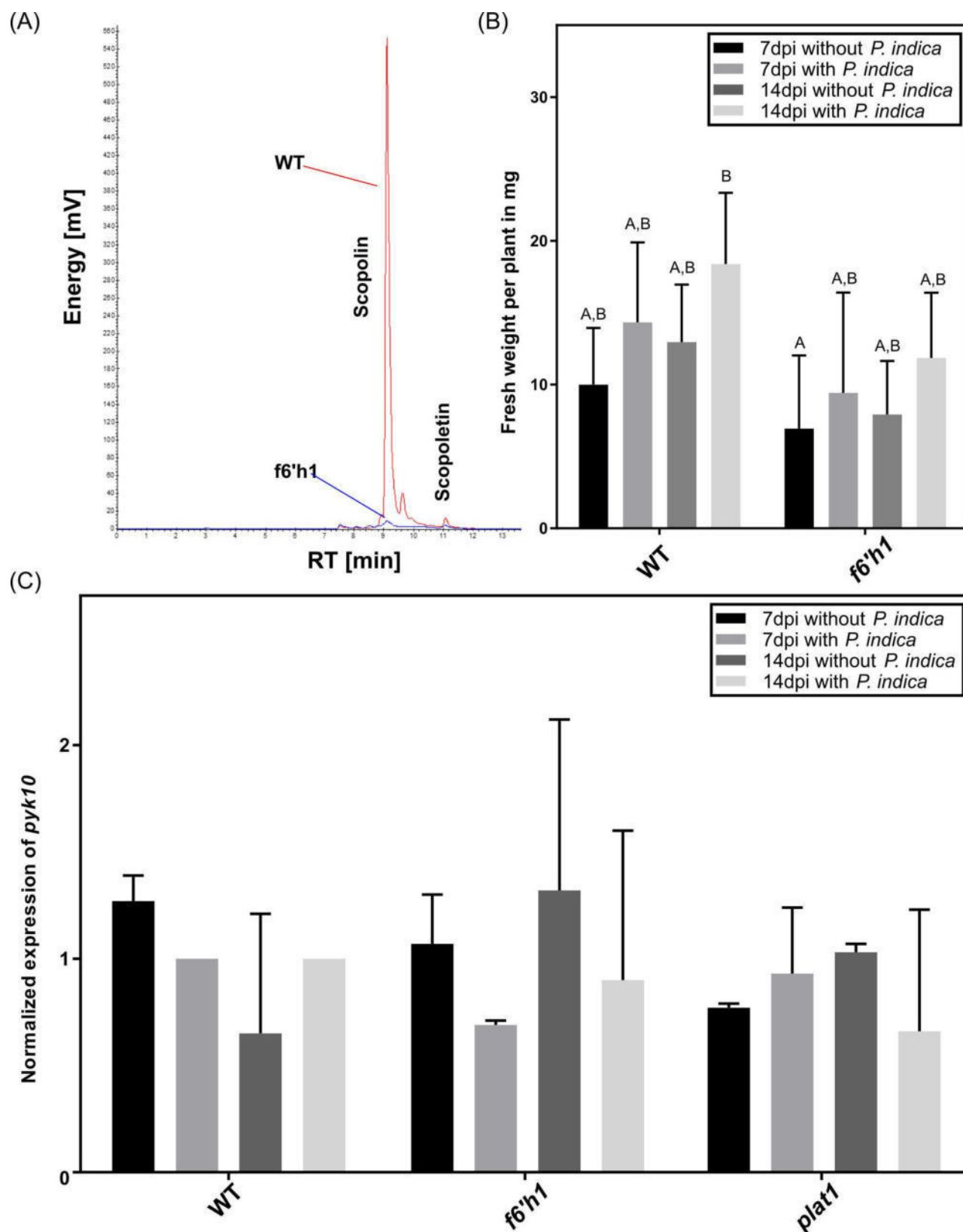


Fig 7. Characterisation of the *f6'h1* mutant. (A) Fluorescence (336/438 nm) HPLC chromatograms of root extracts from WT (red) and *f6'h1* (B) Growth promotion of WT and *f6'h1* by *P. indica* after 7 and 14 days of co-cultivation. At 14 dpi a slightly higher growth-stimulating effect was visible for *f6'h1* compared to the WT. (C) Expression of *PYK10* in the roots of WT and *f6'h1* mutants 14 days after co-cultivation with or without *P. indica*. All experiments were repeated three to four times with at least ten plants each. Error bars represent standard deviation. Different letters represent significant differences between treatments at $p < 0.05$ (Two-Way ANOVA, followed by a Bonferroni correction).

<https://doi.org/10.1371/journal.pone.0209658.g007>

moreover, a diffuse signal was observed (Fig 9D). This effect diminishes after two weeks and the size and structure of the ER-bodies was again comparable to the mock treated samples (Fig 9E).

We further determined the size of ER-bodies in the liquid culture at the time point of the secretome study. No difference in structure was observed between the mock treated and colonised roots (S4 Fig). But when comparing the liquid culture with the solid culture, a slight size-reduction was observed for the ER-bodies in untreated roots at 3 dpi (S5 Fig).

Discussion

P. indica alters the secretome of colonised plants

The availability of the complete genome sequence and a system of hydroponic cultivation makes *P. indica* an interesting model endophyte for studying the molecular basis of beneficial symbiotic interactions. In this study, *P. indica* and *A. thaliana* were cultivated alone and together in hydroponic media and the secreted proteins were compared after three days of co-cultivation. This approach allowed us to identify symbiosis-relevant proteins secreted during the early stage of interaction. At the time point of this study, the fungus and the plant have not established a mutualistic symbiosis and the fate of the interaction is still undetermined [12, 38, 81]. Our results demonstrate that 102 plant proteins were differentially enriched the presence of the fungus (S2 Table and Fig 2). The most severe alterations in the level of plant proteins affect biotic and abiotic stress responses, the primary metabolism and mucilage synthesis.

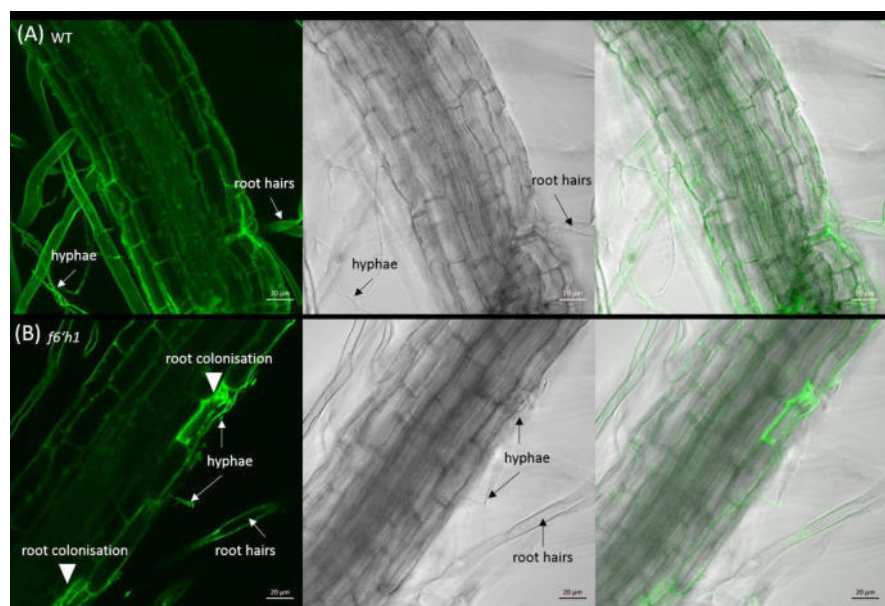


Fig 8. Root colonisation of Arabidopsis WT and *f6'h1* by *P. indica* at 14 dpi. Arabidopsis WT (A) and *f6'h1* (B) were imaged using confocal microscopy. The first pictures show the autofluorescence of the root and GFP fluorescence of *P. indica*. The second pictures show the bright field image. The last pictures show the overlay of all images for each row.

<https://doi.org/10.1371/journal.pone.0209658.g008>

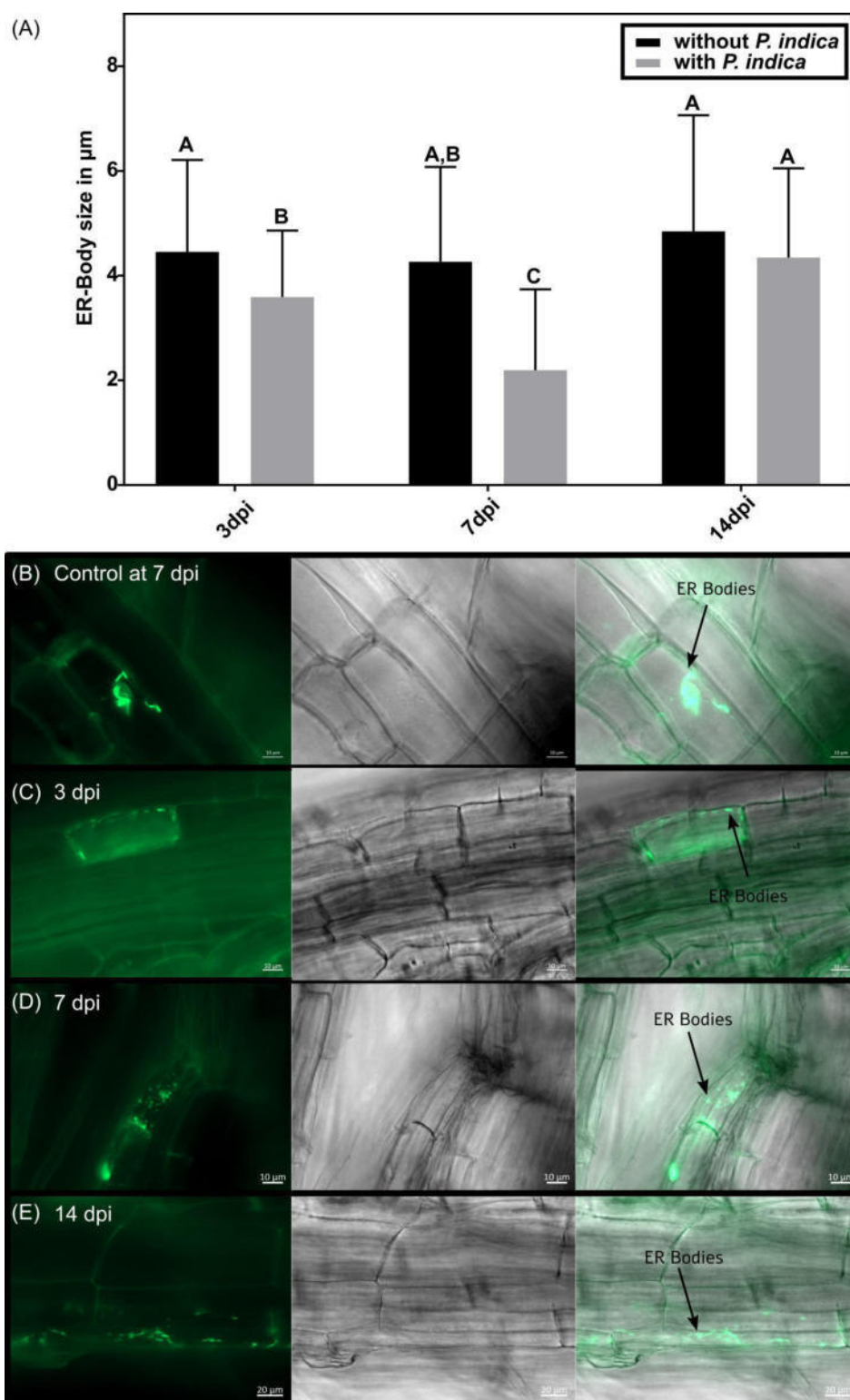


Fig 9. Effect of *P. indica* on ER-body size. (A) Comparison of the ER-body length in Arabidopsis root cells without and with *P. indica* at 3 dpi, 7 dpi and 14 dpi. Error bars represent standard deviation. Different letters represent significant differences between treatments at $p < 0.05$ (Two-Way ANOVA, followed by a Bonferroni correction). Per

time point and treatment four roots were used and the size of 20–100 ER-bodies per root was measured. (B) Fluorescence microscopy of ER-bodies in *A. thaliana* root without *P. indica* at 7 dpi and with *P. indica* at 3 dpi (C), 7 dpi (D) and 14 dpi (E).

<https://doi.org/10.1371/journal.pone.0209658.g009>

In the single culture, proteins belonging to the primary metabolism (24%), abiotic stress (23%), growth and development (19%) and biotic stress (19%) were present with a similar frequency. On the contrary, in the co-culture proteins involved in biotic stress responses (55%) as well as growth and development (20%) were more abundant. The high proportion of proteins associated with these GO terms is not surprising, as *P. indica* influences many aspects of plant growth and defence mechanisms [5, 34, 37, 81, 82].

Abiotic stress response was one of the most dominant categories in the single culture but not the co-culture. Interestingly, we identified several proteins associated with cadmium stress in the single culture. It is unclear whether these proteins play a direct role in cadmium stress responses or whether they have additional function, but intriguingly, for tobacco and sunflower it was reported that *P. indica* alleviate cadmium specific stress [83].

While abiotic stress, such as osmotic stress, can be expected in a liquid cultivation system, we were surprised to find almost no proteins which play a role in this category in the co-culture. As exception, the abiotic stress-related cysteine proteinase RD21A, the Aspartic Protease in Guard Cell 1 and PLAT1 were identified in the co-culture [73]. PLAT1 is induced by ABA and plays a role in abiotic stress response, but our and previous findings indicate an additional role of PLAT1 in plant-microbial interaction [50]. ABA plays a vital role in the interaction of plants with *P. indica*. It accumulates stage-specific in colonised roots, which is required for successful colonisation [81, 84]. Thus, an altered level of ABA induced by the fungus may be involved in or responsible for the observed differences in PLAT1 accumulation.

Besides PLAT1, we identified 34 differentially regulated proteins with a role in biotic stress. Some of the proteins have already been described in the context of *P. indica* colonisation before. For example, the polygalacturonase inhibitor 1, which restricts programmed cell death of the host [85], was found in the co-culture. A homologue of this protein was recently identified as a target of *P. indica* in Chinese cabbage [86]. Another protein from the co-culture, the pectin methylesterase inhibitor At1G23205 is induced by volatiles from a plant growth-promoting *Bacillus subtilis* strain [87].

In a recent proteome study, *Brassica napus* was co-cultivated with *P. indica*. Similar to our study, proteins associated with biotic stress as well as growth were identified. Another investigation showed that a GLP was downregulated in rape by the fungus after 28 days of co-cultivation [88]. In our short-time assay, homologues of this protein, GLP2 and GLP4, were found in the medium of the co-culture. While GLP4 has an important part in controlling *Blumeria graminis* infection in wheat and barley [89, 90], GLP2 plays a role in root development, possibly by controlling the distribution of carbohydrates between different root parts [91]. These findings are not surprising since the roots are in contact with different fungal cell wall components and the fungus might manipulate the carbohydrate metabolism in roots to stimulate plant growth [92]. Furthermore, the beginning of interaction is characterised by a stressful biotrophic-like phase [81]. At the early time point studied here, the fungus establishes the colonisation, which is accompanied by the balanced regulation of defence compounds. Interestingly, we found that the salicylic acid level is reduced while jasmonate, indolic glucosinolates and flavonoids are increased [12, 37]. Apparently, after 3 days of co-culture, jasmonate-dependent defence strategies dominate in the co-culture which further support the concept that a beneficial interaction phase has not yet been reached.

Another observation was that proteins of the primary metabolism were found predominantly in the single culture and not the co-culture (24% and 7%, respectively). Since secreted

proteins were analysed, this observation is difficult to explain. Based on the results discussed above, one would expect that the fungus represses the primary metabolism to shift metabolites towards defence during the early time point investigated in this study. Under this assumption the amount of both cellular and exudated proteins involved in the plant primary metabolism could be reduced when *P. indica* is present. The strong reduction of these proteins in the exudate preparations might be due to their easier accessibility for fungal proteases. The high number of putative degrading enzymes in the *P. indica* secretome supports this hypothesis. However, whether plant proteins involved in the primary metabolism are specifically degraded, is unclear. An interpretation of these results requires more information about the targets of the fungal proteases, which is still poor.

We also found proteins associated with mucilage in the media of the different cultures. Recent evidence points to mucilage function in seed germination, root tip growth and the formation of arbuscular mycorrhiza [93–95]. The importance of mucilage for arbuscular mycorrhiza has been shown for several plant symbioses including the interaction of maize roots with *Gigaspora gigantea* in which secreted plant components induce hyphal branching [96]. The function of mucilage during the interaction of Arabidopsis with microbes, such as *P. indica*, has not been studied before even though mucilage was investigated in Arabidopsis seeds [73]. Proteins associated with mucilage were identified in the single culture, in the co-culture or in both treatments (S2 Table). For example, the subtilisin-like protease 1.7 (SBT1.7) was present in both cultures (S1 Table), while its homologue SBT1.8 was only detected in the single culture. These quite specific effects suggest that the mucilage-related proteins have specific functions in the symbiosis and are differentially regulated by the fungus. Barely anything is known about the role of mucilage in controlling hyphae entry into root cells, the regulation of plant genes and proteins involved in their synthesis, although it is obvious that they might be an important barrier for fungal invasion, besides other functions which can be envisioned in symbiotic interactions cf. [93–96].

Secretome from *P. indica*

Even though the genome of *P. indica* is sequenced, the function of many proteins is still unknown. In our study, most of the differentially regulated proteins were found in the medium of the co-culture. For one of them (PIIN_04899, a putative indole-3-acetaldehyde dehydrogenase), Hilbert and colleagues (2012) showed an induction of this gene by arabinose, a cell wall component of *A. thaliana* [97, 98]. For another protein (PIIN_04899), a homologous protein from the *Pseudomonas syringae* strain DC3000 was described. This protein produces indole acetic acid (IAA) via indole-3-acetaldehyde dehydrogenase (ALDA) that catalyses the formation of IAA from indole-3-acetaldehyde. Disruption of *aldA* and a close homolog, *aldB*, leads to reduced IAA production and virulence of DC3000 on *A. thaliana*. McClerklin and colleagues (2017) further showed that the IAA produced by this pathway in DC3000 suppresses salicylic acid-mediated defences in Arabidopsis [99]. *P. indica* can produce IAA *in vitro* and its growth promoting effect in Arabidopsis can be imitated by this hormone [79]. In the interaction of *P. indica* with barley, IAA is required to establish a symbiotic interaction, but not for the growth promotion effect [97]. Hence, the identified fungal protein might trigger the IAA synthesis and, in turn, confer beneficial traits to Arabidopsis.

Role of PLAT1, ER-bodies and scopolin in the colonisation of *P. indica*

We found PLAT1 in the supernatant of the co-culture. PLAT1 functions as positive regulator of abiotic stress tolerance and promotes plant growth [51]. Furthermore, *PLAT1* expression is regulated by the ABA-dependent transcription factors 1–4 [51] which prompted us to have a

closer look at the function of the protein in the interaction. In the beginning of the colonisation the expression of this gene is reduced in colonised roots; in confirmation with this results *plat1* mutants are stronger colonised by the fungus after seven days. After two weeks, no difference to the wild-type can be detected. PLAT domains are found in different membrane- or lipid-associated proteins [52, 100–103] and exhibit similarity to the C2 domain involved in protein–protein and protein-membrane interactions [52, 104]. Therefore, it has been hypothesised that the PLAT domain provides a docking platform for proteins to regulate their catalytic activities and that the proteins *per se* do not have enzymatic activities [51–53]. Hyun and colleagues (2014) further observed a co-localisation of PLAT1 with ER-bodies [51]. Since PYK10, which is found in ER-bodies, is involved in the establishment of symbiosis between *P. indica* and *A. thaliana* [43], one could speculate that besides PYK10, also PLAT1 might play an important role, by regulating defence processes during early phases of the symbiotic interaction. This is supported by the stronger colonisation of *plat1* mutants seven days after colonisation and by the altered level of scopolin in *plat1* roots. Furthermore, the scopolin mutant *f6'h1* plants are stronger colonised by the fungus. This indicates that *F6'H1* or its product scopolin restricts the entry of *P. indica* hyphae into roots cells. In agreement with these results, scopolin inhibits growth of *P. indica* and other fungi *in vitro* [39]. Downregulation of the *plat1* mRNA in the infected roots seem to be associated with the observed degradation of the ER-bodies, whereas it is not clear whether the expression of *PLAT1* in the nucleus or the ER-bodies in the cytoplasm, or both are the primary target of the fungus in Arabidopsis roots, and whether both effects are directly connected to each other. The appearance of the PLAT1 protein in the exudate fraction might be caused by the disruption of cells, which occurs when the ER-bodies become gradually smaller due to the activation of defence processes against *P. indica*. Ultimately, smaller ER-bodies in colonised roots might restrict the liberation of defence compounds such as scopolin from its precursor scopoletin, allowing a more efficient colonisation of roots by the fungus.

Apparently, the early phase of interaction between *A. thaliana* and *P. indica* includes an arms-race in which *P. indica* tries to restrict the plant defence by reducing the amount and function of ER-bodies. At later time points, when a beneficial interaction starts and the fungus is recognized as a friend, the defence compounds PLAT1 and scopolin appear to be less important. These processes can be triggered by altered phytohormone levels. For example, Camehl and colleagues (2010) showed that ethylene can inhibit the fungus and is required for balancing the interaction between *P. indica* and *A. thaliana* [104]. Other defence-related phytohormones have been reported to be activated during different phases of the symbiotic interaction. Although they may explain alterations in the expression of genes involved in scopolin/scopoletin biosynthesis after exposure of the roots to *P. indica*, the role of PLAT1 and the coumarins in this scenario require more investigation.

Conclusion

In this study, we analysed the secretion of proteins during the early interaction between *A. thaliana* and *P. indica*. The identified fungal proteins demonstrate that root colonisation results in an almost complete alteration in the fungal exudation profile. Unfortunately, barely anything is known about the function of the secreted fungal proteins, making it difficult to draw meaningful conclusions.

Several of the identified Arabidopsis proteins are differentially regulated. They function in defence and might be required to restrict entry of the hyphae into the host cells. This includes remorin 3, germin like protein 4, osmotin like protein 34 or pathogenesis-related protein 5. For other defence-related proteins, a clear function has not yet been described. Our analysis

demonstrated that multiple peroxidases and proteins with a role in growth processes, such as patellin 1 and 2 as well as lipid transfer protein 8, were influenced by the fungus. Furthermore, proteins related to mucilage formation, such as RD21A, RD21B or aspartic protease 1, respond to the fungus. The quite unique regulation of the individual mucilage-related proteins in response to the fungus suggests that they play an important and so far, little investigated role, and that symbiosis-specific signals manipulate mucilage formation.

The establishment of symbiosis requires a reprogramming of fungal and plant proteins. Benefits for the host only become visible after successful root colonisation and the recognition of the microbe as mutualistic symbiont. Several identified proteins in the single and co-culture suggest that this phase has not yet been reached three days after infection, and that our analyses was performed at a time point when the arms-race between the two symbionts is ongoing.

ER-bodies are involved in defence and the degradation of ER-bodies in response to fungal colonisation might play a role in balancing defence and growth responses. The downregulation of *plat1* by the fungus seems to cause a downregulation of the defence compound scopolin and thus allowing a better colonisation. However, other enzymes and proteins with not well-defined functions are present in the ER-bodies and lower PLAT1 and scopolin levels after root colonisation may only be one aspect in the arms-race that involves ER-body functions.

Methods and material

Cultivation of *A. thaliana* and *P. indica*

Cultivation of *A. thaliana* and *P. indica* was performed as described before [105]. Briefly, *A. thaliana* wild type (Col-0) and mutant seeds (SALK_112728c for *plat1*, cs69080 for GFP-labelled ER-bodies and SALK_132418C for *f6'h1*) were surface-sterilised with a solution containing sterile distilled water (dH₂O), sodium lauroyl sarcosinate and Clorix (64%, 4%, 32%; v/v/v) for eight minutes under constant shaking, followed by six rinses with dH₂O. Surface-sterile seeds were sown on a 0.75% (w/v) agar plate. *P. indica* (*P. indica*-JE1) was cultured as described on solid Kaefer medium (KM) (1% (w/v) agar). *Arabidopsis* seeds were obtained from the Nottingham *Arabidopsis* Stock Centre [106].

Cultivation of *A. thaliana* with *P. indica* for secretome study. Seeds were planted on MS medium (Murashige and Skoog) [107] in Petri dishes closed with micropore band. After vernalisation at 4°C for two days the plates were kept under an 8 h light (60 μmol photons·m⁻²·s⁻¹)/ 16 h dark period with a constant temperature of 21°C for 12 days. For the experiment ten petri dishes were filled with 20 ml liquid PNM without sugar for each treatment. For the *P. indica* single culture and the co-culture, a fungal plaque with 1 cm diameter was added to the plates and cultivated at room temperature for three days, whereas for the single *A. thaliana* culture and the mock control (medium without fungus or plant) a KM plaque with the same diameter was added. After three days, four plants were added to the petri dishes of the *A. thaliana* single culture and the co-culture. To the *P. indica* single culture and the mock control, a plaque of MS media was added instead. The mock treatment was performed to check for contaminations. After three days, the supernatant was collected and used for the solid phase extraction.

Co-cultivation of *A. thaliana* with *P. indica* for expression and growth promotion studies. For the gene expression study, *A. thaliana* and *P. indica* were cultivated as described before [105]. A plaque with one cm diameter of *P. indica* and KM, respectively, was transferred to petri dishes with PNM covered by a sterilised nylon membrane. After seven days, four twelve-day old seedlings were transferred to the fungal plate and the control plate, respectively. For all experiments, WT and mutant plants were grown in parallel. Roots and leaves were harvested and snap frozen in liquid nitrogen prior further analysis.

Analysis of secreted proteins

Solid phase extraction. Supernatant of liquid spent culture medium was filtered (0.22 μ m PES (polyethersulfone) Corning bottle top filter Sigma-Aldrich, Munich, Germany) and treated with a protease inhibitor cocktail (1 tablet cOmplete Ultra, Mini, EDTA (ethylenediaminetetraacetic acid)-free, EasyPack (Roche, Basel, Switzerland) per 100 ml medium). Trifluoroacetic acid (TFA) was added to gain a final concentration of 0.1% TFA. Chromabond C4 SPE (solid phase extraction) cartridges (Macherey-Nagel, Dürren, Germany) were reconstituted with 3 ml acetonitrile (ACN) and 3 ml 0.1% TFA. Each 20 ml spent medium of 10 biological replicates of plant, fungus, co-culture or mock samples were aspirated (vacuum-driven) through the SPE cartridges. Subsequently, the cartridges were washed with 3 ml 5% MeOH (methanol), 0.1% TFA, and the enriched proteins were eluted from the C4 resin with 3 ml 0.1% TFA in ACN/H₂O (80%/ 20%, v/v). The eluates were freeze-dried in a Christ alpha 2–4 lyophilizer (Christ, Osterode am Harz, Germany). The lyophilised powder was resolubilised in 100 μ l denaturation buffer, i.e. 50 mM TEAB (triethylammonium bicarbonate) in 50/50 trifluoroethanol (TFE)/H₂O (v/v) by ultrasonification in the water bath for 15 min and heat treatment at 90°C for 10 min. For reduction of oxidised cysteine thiol residues 4 μ l 500 mM TCEP (tris(2-carboxyethyl) phosphine) in 100 mM TEAB was added for 1 h incubation at 55°C. Cysteine thiol alkylation was performed by addition of 4 μ l 625 mM iodoacetamide in 100 mM TEAB and incubation at room temperature in the dark for 30 min. Proteins were cleaned-up by MeOH/H₂O/chloroform precipitation using the protocol of Wessel and Flügge (1984) [108] and the precipitate was resolubilised in 100 μ l of 100 mM TEAB by 15 min ultrasonic bath treatment. Total protein concentration was determined by the Merck Millipore Direct Detect system (Merck, Darmstadt, Germany) according to the manufacturer's instructions. Trypsin and LysC protease mix (Promega Cat. # V5072) was added to the samples at a ratio of 1:25 protease mix to protein. Proteins were digested for 18 h at 37°C. Reactions were stopped by addition of 10 μ l 10% HCOOH, and the samples were dried in a SpeedVac (Thermo Fisher Scientific, Waltham, MA, USA). Tryptic peptides were resolubilised in 25 μ l 0.05% TFA, 2% ACN by 15 min ultrasonic bath treatment. Finally, samples were filtered through 10 kDa PES molecular weight cut-off centrifugal filters (VWR International, Radnor, PA, USA) for 15 min at 16000 g transferred into HPLC (high-performance liquid chromatography) vials and stored at -80°C until LC-MS/MS analysis.

LC-MS/MS analysis. LC-MS/MS analysis was carried out on an Ultimate 3000 RSLC Nano system coupled to a QExactive HF mass spectrometer (both Thermo Fisher Scientific). Peptides were enriched online using a nano trap column (Acclaim Pep Map 100, 2 cm x 75 μ m, 3 μ m, Thermo Fisher) at a flow rate of 5 μ l/min. Further peptide separation on an analytical column was performed on an Acclaim Pep Map RSLC nano column (50 cm x 75 μ m, 2 μ m) (Thermo Fisher Scientific). The mobile phase consisted of eluent (A) 0.1% (v/v) formic acid in H₂O and eluent (B) 0.1% (v/v) formic acid in ACN/H₂O (90%/ 10%, v/v). Gradient elution was performed as follows: 0 min at 4% B, 5 min at 6% B, 25 min at 8% B, 65 min at 20% B, 80 min at 30% B, 90 min at 50% B, 95–100 min at 96% B, 100.1–120 min at 4% B.

A stainless-steel emitter in the Nanospray Flex Ion Source (Thermo Fisher Scientific) was used to generate positively charged ions at a spray voltage of 2.2 kV. The quadrupole/orbitrap instrument was operated in Full MS / data-dependent MS2 (Top15) mode. Precursor ions were monitored at m/z 300–1500 at a resolution of 120k FWHM using a maximum injection time (IT_{max}) of 100 ms and an AGC (automatic gain control) target of 1e6. HCD fragmentation at 30% normalised collision energy (NCE) generated MS2 ions, which were scanned at 15k FWHM using a maximum IT_{max} of 100 ms and an AGC target of 2e5. Dynamic exclusion of precursor ions was set to 30 s. The LC-MS/MS instrument was controlled by Chromeleon 7.2, QExactive HF Tune 2.8 and Xcalibur 4.0 software (Thermo Fisher Scientific).

Protein database search. Tandem mass spectra were searched against the UniProt database of *A. thaliana* and *P. indica* (2017/02/05) using Proteome Discoverer (PD) 2.1 (Thermo Fisher Scientific) and the algorithms of Mascot 2.4 (Matrix Science, London, UK), Sequest HT (integral version of PD 2.1) and MS Amanda 1.0. Two missed cleavages were allowed for trypsin digestion. The precursor mass tolerance was set to 10 ppm and the fragment mass tolerance was set to 0.02 Da. Modifications were defined as dynamic methionine oxidation and static cysteine carbamidomethylation. At least 2 peptides per protein and a strict false discovery rate (FDR) < 1% were required for positive protein hits. The mass spectrometry proteomics data have been deposited to the ProteomeXchange Consortium via the PRIDE [109] partner repository with the dataset identifier PXD009563.

For the GO-Term analysis, all identified proteins were searched against the GO consortium database using AmiGO (<http://www.geneontology.org>, version 1.8) [55–57]. The frequency (in %) of a specific GO-Term was determined individually for each treatment and biological replicate. The mean frequency for the different treatments was calculated and the 20 most abundant terms were used for further analysis.

The algorithms TargetP 1.1 (<http://www.cbs.dtu.dk/services/TargetP/>), SignalP 4.1 (<http://www.cbs.dtu.dk/services/SignalP/>) and Predotar 1.3 (<https://urgi.versailles.inra.fr/Tools/Predotar>) were used for predicting subcellular localisation [76, 77].

Additional analysis

Gene expression studies

The co-culture of *P. indica* and *A. thaliana* was performed as described before [105]. Roots and leaves were collected for RNA extraction and cDNA (complementary Deoxyribonucleic acid) synthesis followed by RT-qPCR (reverse transcriptase quantitative polymerase chain reaction) as described in [81]. All experiments were repeated in three to four biological and three technical replicates. Primers are given in S3 Table. The efficiency of expression was manually determined by LinRegPCR 2014 [110] followed by the $\Delta\Delta$ Ct (threshold cycle) method [111]. Expression levels of genes were normalised by glyceraldehyde 3-phosphate dehydrogenase (*GAPDH*), whereas the relative normalised expression depends on the respective control as stated in the figures.

Microscopy

Three, seven and 14 days after infection of *A. thaliana* with GFP-labelled *P. indica* (gift from Prof. P. Schäfer, University Warwick) root colonisation was imaged using an LSM (laser scanning microscope) 880 (Zeiss Microscopy GmbH, Jena, Germany), with the 488 nm laser line of an argon multiline laser. Images were taken with a 40x objective (Plan-Apochromat 40x/0.8). Pictures for quantification of ER-bodies were taken with an AxioImager M2 microscope (Zeiss). Digital images were processed using ZEN (ZEISS Efficient Navigation) software.

Extraction of scopolin/ scopoletin from plant material for HPLC analysis

The procedure is based on Döll [112]. For 100 mg frozen plant material, 400 μ l methanol and 2mM trans-cinnamic acid (Sigma-Aldrich) per sample as internal standard was added and homogenized for 60 seconds at full speed by an electric homogenizer (RZR 2102 Control (Heidolph, Schwabach, Germany)). The samples were transferred to a centrifuge tube and centrifuged at 15.000 rpm and 4°C for 10 min. The supernatant was transferred to a new tube and the pellet resolved in 400 μ l methanol. After a second centrifugation step, the supernatants of

identical samples were mixed and centrifuged again for 10 min. Finally, the samples were filtered through a 20 µm filter into a glass vial.

HPLC measurement

For the measurement a JASCO HPLC 900 system (JASCO Germany GmbH, Gross-Umstadt, Germany) was used. It was equipped with a DG-2080-53 degaser, a LG-980-02 solvent mixer, a PU-980 vacuum pump, an AS-950-10 autosampler and a MD-910 multiwave length detector. We used C18 column (Kromasil C18 HPLC column 5µm particle size, pore size 100 Å, length 150 mm, inner diameter 4.6 mm, K08670356, Sigma-Aldrich) at 20°C with a flowrate of 0.6 ml/min. The device was coupled via a JASCO LC-Net II/ADC interface with the computer controlled by ChromPass/Galaxie 1.10.0.5590 from JASCO. Purging was performed for 1 min at a flow rate of 5 ml/min with 0.1% (v/v) formic acid in acetonitrile. This was followed by degassing with 0.1% (v/v) formic acid in water for 1 min at the same flowrate. The column was washed with 0.1% (v/v) formic acid in acetonitrile for ten minutes. For equilibration 2% (v/v) acetonitrile + 0.1% (v/v) formic acid in 98% (v/v) water + 0.1% formic acid (v/v) was used until constant pressure was reached. 10 µl of sample were injected and eluted over 27 min. In the beginning the acetonitrile content in the mobile phase was 2% (v/v) increasing to 100% over 15 min kept at 100% for 5 min, decreased to 2% over 1 min and kept for 6 min at 2%. As an authentic standard 10 µl of 0.1 mM scopolin and 10 µl of 0.625 mM scopoletin (Phytolab, Vestenbergsgreuth, Germany) were used. The amount of scopolin and scopoletin in the sample was determined by the peak area normalised with the peak for *trans*-cinnamic acid (Sigma-Aldrich).

Growth inhibition experiment of *P. indica* by scopoletin and scopolin

The procedure was performed as described by [113]. Scopolin and scopoletin was purchased from Sigma-Aldrich and diluted in methanol. Scopolin, scopoletin and methanol (for the control) were added to six-well plates. After evaporation of the solvent, the wells were filled with 1.5 ml liquid KM medium. 4.5×10^5 fungal spores were added per well. After 11 days of growth, *P. indica* was harvested and dried (60°C, overnight) to determine the dry weight for calculation of the inhibition of fungal growth in %. Bars represent standard deviation. The experiment was repeated in three biological replicates.

Statistics and data deposition

All statistic was performed by Sigma Plot 13.0.083 (Systat Software, Erkrath, Germany). Details are given in the figure legends.

The MS proteomics data in this paper have been deposited via ProteomeXchange with identifier PXD009563.

Supporting information

S1 Table. List of proteins identified in the secretomes from single and co-cultures. Selected proteins were identified by at least two unique peptides and a false discovery rate of <1%. The frequency of occurrence is given as Low (1 out of 3), Medium (2 out of 3) or High (3 out of 3 replicates) based on the frequency of detection in all replicates. (XLSX)

S2 Table. List of proteins enriched across all three secretomes. Identified proteins were considered differentially enriched, when they were found in at least two replicates in one treatment and not in the other treatment. Furthermore, proteins that were found with a high

frequency in one treatment and with a low frequency in the other treatment, were considered differentially secreted as well. Information about the function was obtained using the BLAST algorithm for homology searches against the UniProt database [54, 114]. The location was predicted using TargetP, SignalP and Predotar algorithms.

(XLSX)

S3 Table. List of primers used in this study.

(XLSX)

S1 Fig. Colonisation of *A. thaliana* by *P. indica* in liquid media at 3 dpi. Arabidopsis roots in liquid (A) and solid media (B) were imaged using fluorescence microscopy. In both cultures, only little fungus was found in and around the root. The first pictures show the autofluorescence of the root and GFP fluorescence of *P. indica*. The second pictures show the bright field image. The last pictures show the overlay of all images for each row. Liquid cultivation method from the secretome measurement was compared with the standard solid cultivation method.

(TIF)

S2 Fig. Overview of secretomes and Expression analyses of *plat* genes. (A) Venn diagram of *A. thaliana* proteins found in three replicates in the co-culture (generated with <http://bioinformatics.psb.ugent.be/webtools/Venn/>). (B) Profile for *plat2* expression in WT roots and leaves. (C) Profile for *plat3* expression in WT roots and leaves. For *plat3*, CT values were extremely low around 35–40 whereas for all other genes CT values were between 25 and 35. (D) Primer used in this study for RT-qPCR.

Dashed line represents the expression in the untreated WT plants. Error bars represent standard deviation calculated from four biological replicates. Different letters represent significant differences between treatments at $p < 0.05$ (Two-Way ANOVA, followed by a Bonferroni correction).

(TIF)

S3 Fig. Expression analyses of genes associated with the scopolin pathway. Expression of *PYK10* and other key genes of the scopolin pathway in roots of WT and *F6'H1* at 7 dpi (A) and 14 dpi (B). Error bars represent standard deviation calculated from four biological replicates. The asterisks shows the significant difference, as described in Fig 3A.

(TIF)

S4 Fig. Microscopy of ER-Bodies at 3 dpi in liquid media and in solid media. Fluorescence microscopy of ER-bodies in roots without and with *P. indica*. Liquid cultivation method from the secretome measurement was compared with the standard solid cultivation method. Mock treatment in liquid culture (A) and in solid culture (B) and colonised roots at 3 dpi in liquid culture (C) and in solid culture (D) are shown. The first pictures show the autofluorescence of the root ER-Bodies. The second pictures show the bright field image. The last pictures show the overlay of all images for each row. Liquid cultivation method from the secretome measurement was compared with the standard solid cultivation method.

(TIF)

S5 Fig. Measurement of ER-body size at 3 dpi in liquid media and in solid media. Comparison of the ER-body length in Arabidopsis root cells without and with *P. indica* at 3 dpi. Liquid cultivation method from the secretome measurement was compared with the standard solid cultivation method. Error bars represents standard deviation. Different letters represent significant differences between treatments at $p < 0.05$ (Two-Way ANOVA, followed by a Bonferroni correction). Per time point and treatment four roots were used and the size of 20–100

ER-Bodies per root was measured.
(TIF)

Acknowledgments

We would like to thank Anatoli Ludwig, Claudia Röppischer and Sarah Mußbach for their technical assistance during the cultivation of *A. thaliana* and *P. indica*

Author Contributions

Conceptualization: Johannes Thürich, Axel Brakhage, Ralf Oelmüller.

Formal analysis: Johannes Thürich, Doreen Meichsner, Thomas Krüger, Olaf Kniemeyer.

Funding acquisition: Axel Brakhage, Ralf Oelmüller.

Investigation: Johannes Thürich, Doreen Meichsner, Alexandra C. U. Furch, Thomas Krüger, Olaf Kniemeyer.

Methodology: Johannes Thürich, Doreen Meichsner, Alexandra C. U. Furch, Thomas Krüger.

Project administration: Jeannette Pfalz.

Resources: Axel Brakhage, Ralf Oelmüller.

Supervision: Alexandra C. U. Furch, Jeannette Pfalz, Ralf Oelmüller.

Validation: Johannes Thürich.

Visualization: Johannes Thürich, Alexandra C. U. Furch, Thomas Krüger.

Writing – original draft: Johannes Thürich, Alexandra C. U. Furch, Jeannette Pfalz, Ralf Oelmüller.

Writing – review & editing: Alexandra C. U. Furch, Jeannette Pfalz, Ralf Oelmüller.

References

1. Wang B, Qiu Y-L. Phylogenetic distribution and evolution of mycorrhizas in land plants. *Mycorrhiza*. 2006; 16: 299–363. <https://doi.org/10.1007/s00572-005-0033-6> PMID: 16845554
2. Johnson NC, Graham Jh, Smith Fa. Functioning of mycorrhizal associations along the mutualism-parasitism continuum. *New Phytol*. 1997; 135: 575–585. <https://doi.org/10.1046/j.1469-8137.1997.00729.x>
3. Bonfante P, Genre A. Arbuscular mycorrhizal dialogues: do you speak 'plantish' or 'fungish'. *Trends Plant Sci*. 2015; 20: 150–154. <https://doi.org/10.1016/j.tplants.2014.12.002> PMID: 25583176
4. Lanfranco L, Fiorilli V, Gutjahr C. Partner communication and role of nutrients in the arbuscular mycorrhizal symbiosis. *New Phytol*. 2018. <https://doi.org/10.1111/nph.15230> PMID: 29806959
5. Zuccaro A, Lahrmann U, Güldener U, Langen G, Pfiffi S, Biedenkopf D, et al. Endophytic life strategies decoded by genome and transcriptome analyses of the mutualistic root symbiont *Piriformospora indica*. *PLoS Pathog*. 2011; 7: e1002290. <https://doi.org/10.1371/journal.ppat.1002290> PMID: 22022265
6. Pellegrin C, Morin E, Martin FM, Veneault-Fourrey C. Comparative analysis of secretomes from ecto-mycorrhizal fungi with an emphasis on small-secreted proteins. *Front Microbiol*. 2015; 6: 1278. <https://doi.org/10.3389/fmicb.2015.01278> PMID: 26635749
7. Krijger J-J, Thon MR, Deising HB, Wiersel SGR. Compositions of fungal secretomes indicate a greater impact of phylogenetic history than lifestyle adaptation. *BMC Genomics*. 2014; 15: 722. <https://doi.org/10.1186/1471-2164-15-722> PMID: 25159997
8. De Wit, Pierre J G M, Mehrabi R, Van den Burg, Harrold A, Stergiopoulos I. Fungal effector proteins: past, present and future. *Mol Plant Pathol*. 2009; 10: 735–747. <https://doi.org/10.1111/j.1364-3703.2009.00591.x> PMID: 19849781
9. Gonzalez-Fernandez R, Jorin-Novo JV. Contribution of proteomics to the study of plant pathogenic fungi. *J Proteome Res*. 2012; 11: 3–16. <https://doi.org/10.1021/pr200873p> PMID: 22085090

10. Win J, Chaparro-Garcia A, Belhaj K, Saunders DGO, Yoshida K, Dong S, et al. Effector biology of plant-associated organisms: concepts and perspectives. *Cold Spring Harb Symp Quant Biol.* 2012; 77: 235–247. <https://doi.org/10.1101/sqb.2012.77.015933> PMID: 23223409
11. Kaffamik, Florian A R, Jones, Alexandra M E, Rathjen JP, Peck SC. Effector proteins of the bacterial pathogen *Pseudomonas syringae* alter the extracellular proteome of the host plant, *Arabidopsis thaliana*. *Mol. Cell Proteomics.* 2009; 8: 145–156. <https://doi.org/10.1074/mcp.M800043-MCP200> PMID: 18716313
12. Strehmel N, Mönchgesang S, Herklotz S, Krüger S, Ziegler J, Scheel D. *Piriformospora indica* stimulates root metabolism of *Arabidopsis thaliana*. *Int J Mol Sci.* 2016; 17. <https://doi.org/10.3390/ijms17071091> PMID: 27399695
13. Lippmann R, Kaspar S, Rutten T, Melzer M, Kumlehn J, Matros A, et al. Protein and metabolite analysis reveals permanent induction of stress defense and cell regeneration processes in a tobacco cell suspension culture. *Int J Mol Sci.* 2009; 10: 3012–3032. <https://doi.org/10.3390/ijms10073012> PMID: 19742122
14. Nogueira-Lopez G, Greenwood DR, Middleditch M, Winefield C, Eaton C, Steyaert JM, et al. The apoplastic secretome of *Trichoderma virens* during interaction with maize roots shows an inhibition of plant defence and scavenging oxidative stress secreted proteins. *Front Plant Sci.* 2018; 9: 409. <https://doi.org/10.3389/fpls.2018.00409> PMID: 29675028
15. Chiapello M, Perotto S, Balestrini R. Symbiotic Proteomics—State of the art in plant–mycorrhizal fungi interactions. In: Magdeldin S, editor. *Recent Advances in Proteomics Research.* 2015. <https://doi.org/10.5772/61331>
16. Kloppeholz S, Kuhn H, Requena N. A secreted fungal effector of *Glomus intraradices* promotes symbiotic biotrophy. *Curr. Biol.* 2011; 21: 1204–1209. <https://doi.org/10.1016/j.cub.2011.06.044> PMID: 21757354
17. Plett JM, Kemppainen M, Kale SD, Kohler A, Legué V, Brun A, et al. A secreted effector protein of *Laccaria bicolor* is required for symbiosis development. *Curr. Biol.* 2011; 21: 1197–1203. <https://doi.org/10.1016/j.cub.2011.05.033> PMID: 21757352
18. Plett JM, Daguerre Y, Wittulsky S, Vayssières A, Deveau A, Melton SJ, et al. Effector MISSP7 of the mutualistic fungus *Laccaria bicolor* stabilizes the *Populus* JAZ6 protein and represses jasmonic acid (JA) responsive genes. *Proc. Natl. Acad. Sci. U.S.A.* 2014; 111: 8299–8304. <https://doi.org/10.1073/pnas.1322671111> PMID: 24847068
19. Lum G, VanBuren R, Ming R, Min XJ. Secretome prediction and analysis in Sacred Lotus (*Nelumbo nucifera* Gaertn.). *Tropical Plant Biol.* 2013; 6: 131–137. <https://doi.org/10.1007/s12042-013-9121-5>
20. Analysis of the genome sequence of the flowering plant *Arabidopsis thaliana*. *Nature.* 2000; 408: 796–815. <https://doi.org/10.1038/35048692> PMID: 11130711
21. Krause C, Richter S, Knöll C, Jürgens G. Plant secretome—from cellular process to biological activity. *Biochim. Biophys. Acta.* 2013; 1834: 2429–2441. <https://doi.org/10.1016/j.bbapap.2013.03.024> PMID: 23557863
22. Agrawal GK, Jwa N-S, Lebrun M-H, Job D, Rakwal R. Plant secretome: unlocking secrets of the secreted proteins. *Proteomics.* 2010; 10: 799–827. <https://doi.org/10.1002/pmic.200900514> PMID: 19953550
23. Patnaik D, Khurana P. Germins and germin like proteins: an overview. *Indian J Exp Biol.* 2001; 39: 191–200. PMID: 11495276
24. El-Sharkawy I, Mila I, Bouzayen M, Jayasankar S. Regulation of two germin-like protein genes during plum fruit development. *J. Exp. Bot.* 2010; 61: 1761–1770. <https://doi.org/10.1093/jxb/erq043> PMID: 20202999
25. Miyawaki K, Tabata R, Sawa S. Evolutionarily conserved Cle peptide signaling in plant development, symbiosis, and parasitism. *Curr. Opin. Plant Biol.* 2013; 16: 598–606. <https://doi.org/10.1016/j.pbi.2013.08.008> PMID: 24035739
26. Mortier V, Den Herder G, Whitford R, van de Velde W, Rombauts S, D'Haeseleer K, et al. CLE peptides control *Medicago truncatula* nodulation locally and systemically. *Plant Physiol.* 2010; 153: 222–237. <https://doi.org/10.1104/pp.110.153718> PMID: 20348212
27. Assis RdAB, Polloni LC, Patané JSL, Thakur S, Felestrino ÉB, Diaz-Caballero J, et al. Identification and analysis of seven effector protein families with different adaptive and evolutionary histories in plant-associated members of the Xanthomonadaceae. *Sci. Rep.* 2017; 7: 16133. <https://doi.org/10.1038/s41598-017-16325-1> PMID: 29170530
28. Tawk C, Sharan M, Eulalio A, Vogel J. A systematic analysis of the RNA-targeting potential of secreted bacterial effector proteins. *Sci. Rep.* 2017; 7: 9328. <https://doi.org/10.1038/s41598-017-09527-0> PMID: 28839189

29. Tse YC, Mo B, Hillmer S, Zhao M, Lo SW, Robinson DG, et al. Identification of multivesicular bodies as prevacuolar compartments in *Nicotiana tabacum* BY-2 cells. *Plant Cell*. 2004; 16: 672–693. <https://doi.org/10.1105/tpc.019703> PMID: 14973159
30. Wang J, Ding Y, Wang J, Hillmer S, Miao Y, Lo SW, et al. Expo, an exocyst-positive organelle distinct from multivesicular endosomes and autophagosomes, mediates cytosol to cell wall exocytosis in *Arabidopsis* and tobacco cells. *Plant Cell*. 2010; 22: 4009–4030. <https://doi.org/10.1105/tpc.110.080697> PMID: 21193573
31. Floerl S, Majcherzyk A, Possienke M, Feussner K, Tappe H, Gatz C, et al. *Verticillium longisporum* infection affects the leaf apoplastic proteome, metabolome, and cell wall properties in *Arabidopsis thaliana*. *PLoS ONE*. 2012; 7: e31435. <https://doi.org/10.1371/journal.pone.0031435> PMID: 22363647
32. Cheng F-y, Blackburn K, Lin Y-m, Goshe MB, Williamson JD. Absolute protein quantification by LC/MS(E) for global analysis of salicylic acid-induced plant protein secretion responses. *J Proteome Res*. 2009; 8: 82–93. <https://doi.org/10.1021/pr800649s> PMID: 18998720
33. Verma S, Varma A, Rexer K-H, Hassel A, Kost G, Sarbhoy A, et al. *Piriformospora indica*, gen. et sp. nov., a new root-colonizing Fungus. *Mycologia*. 1998; 90: 896. <https://doi.org/10.2307/3761331>
34. Sun C, Shao Y, Vahabi K, Lu J, Bhattacharya S, Dong S, et al. The beneficial fungus *Piriformospora indica* protects *Arabidopsis* from *Verticillium dahliae* infection by downregulation plant defense responses. *BMC plant biology*. 2014; 14: 268. <https://doi.org/10.1186/s12870-014-0268-5> PMID: 25297988
35. Abdelaziz ME, Kim D, Ali S, Fedoroff NV, Al-Babili S. The endophytic fungus *Piriformospora indica* enhances *Arabidopsis thaliana* growth and modulates Na(+)/K(+) homeostasis under salt stress conditions. *Plant Sci*. 2017; 263: 107–115. <https://doi.org/10.1016/j.plantsci.2017.07.006> PMID: 28818365
36. Bakshi M, Sherameti I, Meichsner D, Thürich J, Varma A, Johri AK, et al. *Piriformospora indica* reprograms gene expression in *Arabidopsis* phosphate metabolism mutants but does not compensate for phosphate limitation. *Front Microbiol*. 2017; 8: 1262. <https://doi.org/10.3389/fmicb.2017.01262> PMID: 28747898
37. Lahrmann U, Strehmel N, Langen G, Frerigmann H, Leson L, Ding Y, et al. Mutualistic root endophytism is not associated with the reduction of saprotrophic traits and requires a noncompromised plant innate immunity. *New Phytol*. 2015. <https://doi.org/10.1111/nph.13411> PMID: 25919406
38. Lahrmann U, Zuccaro A. Opprimo ergo sum—evasion and suppression in the root endophytic fungus *Piriformospora indica*. *Molecular plant-microbe interactions: MPMI*. 2012; 25: 727–737. <https://doi.org/10.1094/MPMI-11-11-0291> PMID: 22352718
39. Nakano RT, Yamada K, Bednarek P, Nishimura M, Hara-Nishimura I. ER bodies in plants of the Brassicales order: biogenesis and association with innate immunity. *Front Plant Sci*. 2014; 5: 73. <https://doi.org/10.3389/fpls.2014.00073> PMID: 24653729
40. Gunning BES. The identity of mystery organelles in *Arabidopsis* plants expressing GFP. *Trends Plant Sci*. 1998; 3: 417. [https://doi.org/10.1016/S1360-1385\(98\)01336-3](https://doi.org/10.1016/S1360-1385(98)01336-3)
41. Hayashi Y. A Proteinase-storing body that prepares for cell death or stresses in the epidermal cells of *Arabidopsis*. *Plant and Cell Physiology*. 2001; 42: 894–899. <https://doi.org/10.1093/pcp/pce144> PMID: 11577182
42. Nagano AJ, Matsushima R, Hara-Nishimura I. Activation of an ER-body-localized beta-glucosidase via a cytosolic binding partner in damaged tissues of *Arabidopsis thaliana*. *Plant Cell Physiol*. 2005; 46: 1140–1148. <https://doi.org/10.1093/pcp/pci126> PMID: 15919674
43. Sherameti I, Venus Y, Drzewiecki C, Tripathi S, Dan VM, Nitz I, et al. PYK10, a beta-glucosidase located in the endoplasmic reticulum, is crucial for the beneficial interaction between *Arabidopsis thaliana* and the endophytic fungus *Piriformospora indica*. *The Plant journal: for cell and molecular biology*. 2008; 54: 428–439. <https://doi.org/10.1111/j.1365-313X.2008.03424.x> PMID: 18248598
44. Nakano RT, Piślewska-Bednarek M, Yamada K, Edger PP, Miyahara M, Kondo M, et al. PYK10 myrosinase reveals a functional coordination between endoplasmic reticulum bodies and glucosinolates in *Arabidopsis thaliana*. *Plant J*. 2017; 89: 204–220. <https://doi.org/10.1111/tj.13377> PMID: 27612205
45. Ahn YO, Shimizu B-i, Sakata K, Gantulga D, Zhou C, Zhou Z, et al. Scopolin-hydrolyzing beta-glucosidases in roots of *Arabidopsis*. *Plant Cell Physiol*. 2010; 51: 132–143. <https://doi.org/10.1093/pcp/pcp174> PMID: 19965874
46. Kai K, Mizutani M, Kawamura N, Yamamoto R, Tamai M, Yamaguchi H, et al. Scopoletin is biosynthesized via ortho-hydroxylation of feruloyl CoA by a 2-oxoglutarate-dependent dioxygenase in *Arabidopsis thaliana*. *Plant J*. 2008; 55: 989–999. <https://doi.org/10.1111/j.1365-313X.2008.03568.x> PMID: 18547395
47. Filipský T, Říha M, Macáková K, Anzenbacherová E, Karličková J, Mladěnka P. Antioxidant effects of coumarins include direct radical scavenging, metal chelation and inhibition of ROS-producing enzymes. *Curr Top Med Chem*. 2015; 15: 415–431. PMID: 25658804

48. Maier W, Schmidt J, Nimtz M, Wray V, Strack D. Secondary products in mycorrhizal roots of tobacco and tomato. *Phytochemistry*. 2000; 54: 473–479. [https://doi.org/10.1016/S0031-9422\(00\)00047-9](https://doi.org/10.1016/S0031-9422(00)00047-9) PMID: 10939350
49. Sun H, Wang L, Zhang B, Ma J, Hettenhausen C, Cao G, et al. Scopoletin is a phytoalexin against *Alternaria alternata* in wild tobacco dependent on jasmonate signalling. *J. Exp. Bot.* 2014; 65: 4305–4315. <https://doi.org/10.1093/jxb/eru203> PMID: 24821958
50. Hyun TK, Albacete A, van der Graaff E, Eom SH, Grosskinsky DK, Bohm H, et al. The Arabidopsis PLAT domain protein1 promotes abiotic stress tolerance and growth in tobacco. *Transgenic Res.* 2015; 24: 651–663. <https://doi.org/10.1007/s11248-015-9868-6> PMID: 25757741
51. Hyun TK, van der Graaff E, Albacete A, Eom SH, Grosskinsky DK, Bohm H, et al. The Arabidopsis PLAT domain protein1 is critically involved in abiotic stress tolerance. *PLoS ONE*. 2014; 9: e112946. <https://doi.org/10.1371/journal.pone.0112946> PMID: 25396746
52. Bateman A, Sandford R. The PLAT domain. A new piece in the PKD1 puzzle. *Current Biology*. 1999; 9: R588–S2. [https://doi.org/10.1016/S0960-9822\(99\)80380-7](https://doi.org/10.1016/S0960-9822(99)80380-7) PMID: 10469604
53. Allard JB, Brock TG. Structural organization of the regulatory domain of human 5-lipoxygenase. *Curr Protein Pept Sci.* 2005; 6: 125–131. PMID: 15853649
54. UniProt. The universal protein knowledgebase. *Nucleic Acids Res.* 2017; 45: D158–D169. <https://doi.org/10.1093/nar/gkw1099> PMID: 27899622
55. Carbon S, Ireland A, Mungall CJ, Shu S, Marshall B, Lewis S. AmiGO: online access to ontology and annotation data. *Bioinformatics*. 2009; 25: 288–289. <https://doi.org/10.1093/bioinformatics/btn615> PMID: 19033274
56. Ashburner M, Ball CA, Blake JA, Botstein D, Butler H, Cherry JM, et al. Gene ontology: tool for the unification of biology. The Gene Ontology Consortium. *Nat Genet.* 2000; 25: 25–29. <https://doi.org/10.1038/75556> PMID: 10802651
57. Gene Ontology Consortium. Going forward. *Nucleic Acids Res.* 2015; 43: D1049–56. <https://doi.org/10.1093/nar/gku1179> PMID: 25428369
58. Cao H, Glazebrook J, Clarke JD, Volko S, Dong X. The Arabidopsis *npr1* gene that controls systemic acquired resistance encodes a novel protein containing ankyrin repeats. *Cell*. 1997; 88: 57–63. [https://doi.org/10.1016/S0092-8674\(00\)81858-9](https://doi.org/10.1016/S0092-8674(00)81858-9) PMID: 9019406
59. Sarry J-E, Kuhn L, Ducruix C, Lafaye A, Junot C, Hugouvieux V, et al. The early responses of *Arabidopsis thaliana* cells to cadmium exposure explored by protein and metabolite profiling analyses. *Proteomics*. 2006; 6: 2180–2198. <https://doi.org/10.1002/pmic.200500543> PMID: 16502469
60. Huang D, Wu W, Abrams SR, Cutler AJ. The relationship of drought-related gene expression in *Arabidopsis thaliana* to hormonal and environmental factors. *J. Exp. Bot.* 2008; 59: 2991–3007. <https://doi.org/10.1093/jxb/ern155> PMID: 18552355
61. Prasad TK, Stewart CR. cDNA clones encoding *Arabidopsis thaliana* and *Zea mays* mitochondrial chaperonin HSP60 and gene expression during seed germination and heat shock. *Plant Mol Biol.* 1992; 18: 873–885. <https://doi.org/10.1007/BF00019202> PMID: 1349837
62. Virk N, Li D, Tian L, Huang L, Hong Y, Li X, et al. Arabidopsis Raf-like mitogen-activated protein kinase kinase gene RAF43 is required for tolerance to multiple abiotic stresses. *PLoS ONE*. 2015; 10: e0133975. <https://doi.org/10.1371/journal.pone.0133975> PMID: 26222830
63. Kuo W-Y, Huang C-H, Jinn T-L. Chaperonin 20 might be an iron chaperone for superoxide dismutase in activating iron superoxide dismutase (FESOD). *Plant Signal Behav.* 2013; 8: e23074. <https://doi.org/10.4161/psb.23074> PMID: 23299425
64. Zhang X-F, Jiang T, Wu Z, Du S-Y, Yu Y-T, Jiang S-C, et al. Cochaperonin CPN20 negatively regulates abscisic acid signaling in Arabidopsis. *Plant Mol Biol.* 2013; 83: 205–218. <https://doi.org/10.1007/s11103-013-0082-8> PMID: 23783410
65. Boyce JM, Knight H, Deyholos M, Openshaw MR, Galbraith DW, Warren G, et al. The *sfr6* mutant of Arabidopsis is defective in transcriptional activation via CBF/DREB1 and DREB2 and shows sensitivity to osmotic stress. *Plant J.* 2003; 34: 395–406. <https://doi.org/10.1046/j.1365-313X.2003.01734.x> PMID: 12753580
66. Xu J, Tran T, Padilla Marcia CS, Braun DM, Goggin FL. Superoxide-responsive gene expression in *Arabidopsis thaliana* and *Zea mays*. *Plant Physiol. Biochem.* 2017; 117: 51–60. <https://doi.org/10.1016/j.plaphy.2017.05.018> PMID: 28587993
67. Kovacs D, Kalmar E, Torok Z, Tompa P. Chaperone activity of ERD10 and ERD14, two disordered stress-related plant proteins. *Plant Physiol.* 2008; 147: 381–390. <https://doi.org/10.1104/pp.108.118208> PMID: 18359842
68. Gorsuch PA, Sargeant AW, Penfield SD, Quick WP, Atkin OK. Systemic low temperature signaling in Arabidopsis. *Plant Cell Physiol.* 2010; 51: 1488–1498. <https://doi.org/10.1093/pcp/pcq112> PMID: 20813832

69. Kim BH, Kim SY, Nam KH. Genes encoding plant-specific class III peroxidases are responsible for increased cold tolerance of the brassinosteroid-insensitive 1 mutant. *Molecules and Cells*. 2012; 34: 539–548. <https://doi.org/10.1007/s10059-012-0230-z> PMID: 23180292
70. Marmagne A, Rouet M-A, Ferro M, Rolland N, Alcon C, Joyard J, et al. Identification of new intrinsic proteins in *Arabidopsis* plasma membrane proteome. *Mol. Cell Proteomics*. 2004; 3: 675–691. <https://doi.org/10.1074/mcp.M400001-MCP200> PMID: 15060130
71. Marín M, Thallmair V, Ott T. The intrinsically disordered N-terminal region of AtREM1.3 remorin protein mediates protein-protein interactions. *J Biol Chem*. 2012; 287: 39982–39991. <https://doi.org/10.1074/jbc.M112.414292> PMID: 23027878
72. Jarsch IK, Ott T. Perspectives on remorin proteins, membrane rafts, and their role during plant-microbe interactions. *Mol Plant Microbe Interact*. 2011; 24: 7–12. <https://doi.org/10.1094/MPMI-07-10-0166> PMID: 21138374
73. Tsai AY-L, Kunieda T, Rogalski J, Foster LJ, Ellis BE, Haughn GW. Identification and characterization of *Arabidopsis* seed coat mucilage proteins. *Plant Physiol*. 2017; 173: 1059–1074. <https://doi.org/10.1104/pp.16.01600> PMID: 28003327
74. Ma W, Muthreich N, Liao C, Franz-Wachtel M, Schütz W, Zhang F, et al. The mucilage proteome of maize (*Zea mays* L.) primary roots. *J Proteome Res*. 2010; 9: 2968–2976. <https://doi.org/10.1021/pr901168v> PMID: 20408568
75. Foster J, Luo B, Nakata PA. An Oxalyl-CoA dependent pathway of oxalate catabolism plays a role in regulating calcium oxalate crystal accumulation and defending against oxalate-secreting phytopathogens in *Medicago truncatula*. *PLoS ONE*. 2016; 11: e0149850. <https://doi.org/10.1371/journal.pone.0149850> PMID: 26900946
76. Emanuelsson O, Brunak S, Heijne G von, Nielsen H. Locating proteins in the cell using TargetP, SignalP and related tools. *Nat. Protocols*. 2007; 2: 953–971. <https://doi.org/10.1038/nprot.2007.131> PMID: 17446895
77. Small I, Peeters N, Legeai F, Lurin C. Predotar. A tool for rapidly screening proteomes for N-terminal targeting sequences. *Proteomics*. 2004; 4: 1581–1590. <https://doi.org/10.1002/pmic.200300776> PMID: 15174128
78. Keymer A, Pimprikar P, Wewer V, Huber C, Brands M, Bucerius SL, et al. Lipid transfer from plants to arbuscular mycorrhiza fungi. *Elife*. 2017; 6. <https://doi.org/10.7554/eLife.29107> PMID: 28726631
79. Sirrenberg A, Gobel C, Grond S, Czempinski N, Ratzinger A, Karlovsky P, et al. *Piriformospora indica* affects plant growth by auxin production. *Physiologia plantarum*. 2007; 131: 581–589. <https://doi.org/10.1111/j.1399-3054.2007.00983.x> PMID: 18251849
80. Kai K, Shimizu B-i, Mizutani M, Watanabe K, Sakata K. Accumulation of coumarins in *Arabidopsis thaliana*. *Phytochemistry*. 2006; 67: 379–386. <https://doi.org/10.1016/j.phytochem.2005.11.006> PMID: 16405932
81. Vahabi K, Sherameti I, Bakshi M, Mrozinska A, Ludwig A, Reichelt M, et al. The interaction of *Arabidopsis* with *Piriformospora indica* shifts from initial transient stress induced by fungus-released chemical mediators to a mutualistic interaction after physical contact of the two symbionts. *BMC Plant Biol*. 2015; 15: 58. <https://doi.org/10.1186/s12870-015-0419-3> PMID: 25849363
82. Nongbri PL, Vahabi K, Mrozinska A, Seebald E, Sun C, Sherameti I, et al. Balancing defense and growth—Analyses of the beneficial symbiosis between *Piriformospora indica* and *Arabidopsis thaliana*. *Symbiosis*. 2012; 58: 17–28. <https://doi.org/10.1007/s13199-012-0209-8>
83. Hui F, Liu J, Gao Q, Lou B. *Piriformospora indica* confers cadmium tolerance in *Nicotiana tabacum*. *J Environ Sci (China)*. 2015; 37: 184–191. <https://doi.org/10.1016/j.jes.2015.06.005> PMID: 26574103
84. Peskan-Berghöfer T, Vilches-Barro A, Müller TM, Glawischmig E, Reichelt M, Gershenzon J, et al. Sustained exposure to abscisic acid enhances the colonization potential of the mutualist fungus *Piriformospora indica* on *Arabidopsis thaliana* roots. *New Phytol*. 2015. <https://doi.org/10.1111/nph.13504> PMID: 26075497
85. Zhang L, Kars I, Essenstam B, Liebrand TWH, Wagemakers L, Elberse J, et al. Fungal endopolygalacturonases are recognized as microbe-associated molecular patterns by the *Arabidopsis* receptor-like protein Responsiveness to Botrytis polygalacturonases1. *Plant Physiol*. 2014; 164: 352–364. <https://doi.org/10.1104/pp.113.230698> PMID: 24259685
86. Dong S, Tian Z, Chen PJ, Senthil Kumar R, Shen CH, Cai D, et al. The maturation zone is an important target of *Piriformospora indica* in Chinese cabbage roots. *J. Exp. Bot*. 2013; 64: 4529–4540. <https://doi.org/10.1093/jxb/ert265> PMID: 24006423
87. Zhang H, Kim M-S, Krishnamachari V, Payton P, Sun Y, Grimson M, et al. Rhizobacterial volatile emissions regulate auxin homeostasis and cell expansion in *Arabidopsis*. *Planta*. 2007; 226: 839–851. <https://doi.org/10.1007/s00425-007-0530-2> PMID: 17497164

88. Shrivastava N, Jiang L, Li P, Sharma AK, Luo X, Wu S, et al. Proteomic approach to understand the molecular physiology of symbiotic interaction between *Piriformospora indica* and *Brassica napus*. *Sci Rep*. 2018; 8: 5773. <https://doi.org/10.1038/s41598-018-23994-z> PMID: 29636503
89. Christensen AB, Thordal-Christensen H, Zimmermann G, Gjetting T, Lyngkjaer MF, Dudler R, et al. The germinlike protein GLP4 exhibits superoxide dismutase activity and is an important component of quantitative resistance in wheat and barley. *Mol Plant Microbe Interact*. 2004; 17: 109–117. <https://doi.org/10.1094/MPMI.2004.17.1.109> PMID: 14714874
90. Yin K, Han X, Xu Z, Xue H. Arabidopsis GLP4 is localized to the Golgi and binds auxin in vitro. *Acta Biochim Biophys Sin (Shanghai)*. 2009; 41: 478–487. <https://doi.org/10.1093/abbs/gmp036>
91. Ham B-K, Li G, Kang B-H, Zeng F, Lucas WJ. Overexpression of Arabidopsis plasmodesmata germinlike proteins disrupts root growth and development. *Plant Cell*. 2012; 24: 3630–3648. <https://doi.org/10.1105/tpc.112.101063> PMID: 22960910
92. Johnson JM, Thürich J, Petutschnig EK, Altschmied L, Meichsner D, Sherameti I, et al. A poly(A) ribonuclease controls the cellotriose-based interaction between *Piriformospora indica* and its host Arabidopsis. *Plant physiology*. 2018. <https://doi.org/10.1104/pp.17.01423> PMID: 29371249
93. Carminati A, Vetterlein D. Plasticity of rhizosphere hydraulic properties as a key for efficient utilization of scarce resources. *Ann Bot*. 2013; 112: 277–290. <https://doi.org/10.1093/aob/mcs262> PMID: 23235697
94. Kaiser C, Kilburn MR, Clode PL, Fuchslueger L, Koranda M, Cliff JB, et al. Exploring the transfer of recent plant photosynthates to soil microbes: mycorrhizal pathway vs direct root exudation. *New Phytol*. 2015; 205: 1537–1551. <https://doi.org/10.1111/nph.13138> PMID: 25382456
95. Francoz E, Ranocha P, Burlat V, Dunand C. Arabidopsis seed mucilage secretory cells: regulation and dynamics. *Trends Plant Sci*. 2015; 20: 515–524. <https://doi.org/10.1016/j.tplants.2015.04.008> PMID: 25998090
96. Nagahashi G, Douds DD. Isolated root caps, border cells, and mucilage from host roots stimulate hyphal branching of the arbuscular mycorrhizal fungus, *Gigaspora gigantea*. *Mycological Research*. 2004; 108: 1079–1088. PMID: 15506019
97. Hilbert M, Voll LM, Ding Y, Hofmann J, Sharma M, Zuccaro A. Indole derivative production by the root endophyte *Piriformospora indica* is not required for growth promotion but for biotrophic colonization of barley roots. *New Phytol*. 2012; 196: 520–534. <https://doi.org/10.1111/j.1469-8137.2012.04275.x> PMID: 22924530
98. Burget EG, Verma R, Møhlhøj M, Reiter W-D. The biosynthesis of l-Arabinose in plants: molecular cloning and characterization of a Golgi-localized UDP-d-Xylose 4-epimerase encoded by the *mur4* gene of Arabidopsis. *Plant Cell*. 2003; 15: 523–531. <https://doi.org/10.1105/tpc.008425> PMID: 12566589
99. McClerkin SA, Lee SG, Nwumeh R, Jez JM, Kunkel BN. Indole-3-Acetaldehyde dehydrogenase-dependent Auxin synthesis contributes to virulence of *Pseudomonas syringae* Strain DC3000; 2017.
100. Hong Y, Wang TW, Hudak KA, Schade F, Froese CD, Thompson JE. An ethylene-induced cDNA encoding a lipase expressed at the onset of senescence. *Proc. Natl. Acad. Sci. U.S.A.* 2000; 97: 8717–8722. <https://doi.org/10.1073/pnas.140213697> PMID: 10890894
101. Minor W, Steczko J, Stec B, Otwinowski Z, Bolin JT, Walter R, et al. Crystal structure of soybean lipoxxygenase L-1 at 1.4 Å resolution. *Biochemistry*. 1996; 35: 10687–10701. <https://doi.org/10.1021/bi960576u> PMID: 8718858
102. Shin R, An J-M, Park C-J, Kim YJ, Joo S, Kim WT, et al. *Capsicum annuum* tobacco mosaic virus-induced clone 1 expression perturbation alters the plant's response to ethylene and interferes with the redox homeostasis. *Plant Physiol*. 2004; 135: 561–573. <https://doi.org/10.1104/pp.103.035436> PMID: 15107506
103. Tomchick DR, Phan P, Cymborowski M, Minor W, Holman TR. Structural and functional characterization of second-coordination sphere mutants of soybean lipoxxygenase-1. *Biochemistry*. 2001; 40: 7509–7517. PMID: 11412104.
104. Camehl I, Sherameti I, Venus Y, Bethke G, Varma A, Lee J, et al. Ethylene signalling and ethylene-targeted transcription factors are required to balance beneficial and nonbeneficial traits in the symbiosis between the endophytic fungus *Piriformospora indica* and *Arabidopsis thaliana*. *The New phytologist*. 2010; 185: 1062–1073. <https://doi.org/10.1111/j.1469-8137.2009.03149.x> PMID: 20085621
105. Johnson JM, Sherameti I, Ludwig A, Nongbri PL, Sun C, Lou B, et al. Protocols for *Arabidopsis thaliana* and *Piriformospora indica* co-cultivation—A model system to study plant beneficial traits. *Journal of Endocytobiosis and Cell Research*. 2011; 101–113.
106. Scholl RL, May ST, Ware DH. Seed and molecular resources for Arabidopsis. *Plant Physiol*. 2000; 124: 1477–1480. <https://doi.org/10.1104/pp.124.4.1477> PMID: 11115863
107. Murashige T, Skoog F. A revised medium for rapid growth and bio assays with tobacco tissue cultures. *Physiol Plant*. 1962; 15: 473–497. <https://doi.org/10.1111/j.1399-3054.1962.tb08052.x>

108. Wessel D, Flügge UI. A method for the quantitative recovery of protein in dilute solution in the presence of detergents and lipids. *Anal. Biochem.* 1984; 138: 141–143. [https://doi.org/10.1016/0003-2697\(84\)90782-6](https://doi.org/10.1016/0003-2697(84)90782-6) PMID: 6731838
109. Vizcaíno JA, Csordas A, del-Toro N, Dianas JA, Griss J, Lavidas I, et al. 2016 update of the PRIDE database and its related tools. *Nucleic Acids Res.* 2016; 44: D447–56. <https://doi.org/10.1093/nar/gkv1145> PMID: 26527722
110. Ruijter JM, Ramakers C, Hoogaars WMH, Karlen Y, Bakker O, van den Hoff MJB, et al. Amplification efficiency: linking baseline and bias in the analysis of quantitative PCR data. *Nucleic Acids Res.* 2009; 37: e45. <https://doi.org/10.1093/nar/gkp045> PMID: 19237396
111. Pfaffl MW. A new mathematical model for relative quantification in real-time RT-PCR. *Nucleic Acids Res.* 2001; 29: e45. PMID: 11328886
112. Döll K. Analysis of toxigenic fungi and their mycotoxins in biotic interactions; 2014. (dissertation) Georg-August-Universität Göttingen; 2013. Available from: <http://hdl.handle.net/11858/00-1735-0000-0022-5E25-E>
113. Peterson JK, Harrison HF, Jackson DM, Snook ME. Biological activities and contents of scopolin and scopoletin in Sweetpotato clones. *HortScience.* 2003; 38: 1129–1133.
114. Johnson M, Zaretskaya I, Raytselis Y, Merezukh Y, McGinnis S, Madden TL. NCBI BLAST: a better web interface. *Nucleic Acids Res.* 2008; 36: W5–9. <https://doi.org/10.1093/nar/gkn201> PMID: 18440982

Manuscript 3

How does AtPARN connect RNA metabolism with Calcium signalling?

Johannes Thürich and Ralf Oelmüller

Review, in preparation

Summary

In this publication the link between AtPARN and calcium signalling was discussed.

I wrote the manuscript which was reviewed by Ralf Oelmüller.

How does AtPARN connect RNA metabolism with Calcium signalling?

<In preparation>

Johannes Thürich, Ralf Oelmüller

Plant Physiology, Matthias-Schleiden-Institute for Genetics, Bioinformatics and Molecular Botany, Faculty of Biological Science, Friedrich-Schiller-University Jena, Dornburger Str. 159, 07743 Jena, Germany

To whom correspondence should be addressed. E-mail: ralf.oelmueller@uni-jena.de

Abstract

The amount, activity and stability of proteins and other gene products can be controlled by RNA on a pre-translational and post-translational level. In our research we identified an Arabidopsis mutant (*cycam*) which is impaired in calcium signalling and is susceptible against exogenous level of abscisic acid. The causative mutation of the *cycam* mutation is located inside the active domain of a poly (A) specific ribonuclease (PARN). In this review we describe possible connections between RNA metabolism and the phenotype of *cycam*.

RNA metabolism

Many mRNA contain poly(A) tails at their 3' -ends which are involved in stability, nuclear export, quality control, localization, formation of the initiation complex at the ribosomes, as well as stalling and termination of translation (Barreau et al., 2005; Schuller and Green, 2018). The adenine rich region of 20 to 250 nucleotides, is added during RNA processing at the 3' UTR of mRNA (Nicholson and Pasquinelli, 2018). Occasionally, additional poly(A) sites can be found inside of genes, however, it is not clear whether they have the same functions (Xing and Li, 2011; Tian and Manley, 2017). The importance of poly(A) tails becomes apparent when considering that half of the human genes and between 50% to 70% of plant genes have alternative sites for polyadenylation of their mRNA (Tian et al., 2005; Hunt, 2008; Xing and Li, 2011). The exact function and mode of action of Poly (A) sequences is still poorly understood (Tian and Manley, 2017), and their involvement in multiple processes makes it difficult to generalize. However, mutations in poly(A) tail processing in almost all organisms have often severe phenotypical consequences, often associated with lethality. This has been reported for animals, plants, and yeast (Körner et al., 1998; Reverdatto et al., 2004; Goldstrohm and Wickens, 2008). Interestingly, in early embryonic stages, the size of the poly(A) tail strongly correlates with translation of mRNAs ribosomes and the stability of an mRNA. In contrast, at later embryonic stages and in mature cells no strong connection between the poly(A) tail and gene expression exist (Subtelny et al., 2014). For example, it was reported that mRNA of highly expressed genes in adult *Caenorhabditis elegans* have a very short poly(A) tail (Lima et al., 2017). These mRNA are strongly translated, have a long half-life and are found with a high abundancy (Lima et al., 2017). This indicates that additional regulatory mechanisms, independent of the poly(A) tail, must exist and that the poly(A) tail is involved in different processes in adults (Jalkanen et al., 2014; Subtelny et al., 2014; Nicholson and Pasquinelli, 2018).

The poly(A) tail is tightly coated by multiple copies of cytoplasmic poly(A)-binding protein (PABCs). PABCs are involved in termination of translation and induce as well as inhibit deadenylation. In the absence of PABC, RNA binding proteins with a CAF1 domain can deadenylate the poly(A) tail. This often occurs in low translated RNA and RNA with a low codon optimality (Nicholson and Pasquinelli, 2018).

In addition some micro RNA (miRNA), small non coding RNA which play an important role in gene expression, can be poly adenylated as well (Cai et al., 2004) They can bind to the 3'UTR of specific mRNAs where they terminate translation or recruit the RNA-induced silencing complex (RISC) which degrades the target mRNA (Morozova et al., 2012).

Interestingly, this regulatory circuit depends on the size of the poly(A) tail of the target mRNA, which influences its binding ability to their corresponding miRNA (Nam et al., 2014). Furthermore, miRNAs play an additional role in dissociation of mRNA from ribosomes and the dissociation of PABC from the poly(A) tail (Fabian et al., 2009; Ender and Meister, 2010).

In plants, an alteration of the poly (A) tail is associated with plant morphogenesis, embryonal development (Reverdatto et al., 2004), development of reproductive organs and organelle development (Simpson et al., 2003; Xing et al., 2008). While many components of the (de-) polyadenylation apparatus are conserved in plants (Hunt, 2008), the poly(A) sites of plants have a different structure (Xing und Li 2011). In contrast to the majority of animal genes, which have a specific poly(A) signal (AAUAAA) in the 3'UTR, only 10% of *Arabidopsis thaliana* genes possess this signal (Hunt, 2008; Xing and Li, 2011). Instead plants and yeast genes have additional flanking regions upstream and downstream of the poly(A) site at the 3' UTR (Hunt, 2008; Xing and Li, 2011).

A mutation in AtPARN causes the cycam phenotype

We identified an *Arabidopsis* mutant (cytoplasmic calcium mutant, *cycam*) which has a point mutation in the poly(A) specific ribonuclease AtPARN (At1G55870) (Johnson et al., 2018).

While wild-type plants (WT) show a strong calcium spike after treatment with cellotriose (Figure 1A), a compound derived from the endophytic mycorrhiza-fungi *Piriformospora indica* (Michal Johnson et al., 2014), *cycam* lacks this response. Interestingly, the calcium response induced by other chemical mediators, such as the pathogen- or microbe-associated patterns chitin or flagellin, is not affected by the mutation in the *cycam* mutant (Johnson et al., 2018). Furthermore, *cycam* plants have higher level of endogenous abscisic acid (ABA), show an inhomogeneous growth and an altered expression of several hundred genes including seven miRNAs (Table 1) (Johnson et al., 2018). This phenotype is caused by a point mutation resulting in a substitution of leucine to phenylalanine at position 135 inside the CAF1 domain of AtPARN. Phylogenetic analyses of PARN protein sequences showed that most plant proteins have either a leucine or an isoleucine at position 135 (Figure 2) indicating that this position is crucial in PARN.

Mutants with a complete knockout of *AtPARN* are embryo-lethal (Chiba et al., 2004; Reverdatto et al., 2004), however, another deletion mutant described by Nishimura et al. (2005) is viable and shows very similar phenotypes as the point mutation identified in our screen. This abscisic acid (ABA)-hypersensitive mutant (*ahg2-1*) has a 5-bp deletion in the fourth exon of *AtPARN*. It was identified because of its ABA-hypersensitive phenotype not only during germination, but also at later developmental stages, and displayed pleiotropic phenotypes. The mutated loci in *cycam* and *ahg2-1* are both located in the CAF1 domain of AtPARN, indicating an important role of this domain (Figure 1D). Overall, plants with a weak mutation in *AtPARN* have higher level of endogenous ABA, germinate with a lower efficiency (Figure 1C) (Nishimura et al., 2005), and share some functions in the RNA metabolism with PARNs from other kingdoms.

The biological function and mechanistic of the conserved protein PARN was studied extensively in different organisms such as yeast, xenopus, and humans (Körner et al., 1998;

93 Copeland and Wormington, 2001; Virtanen et al., 2013). PARNs belong to the DnaQ-like
94 superfamily of exonuclease, and play a role in RNA metabolisms and miRNA induced
95 silencing (miRISC) (Fabian et al., 2009; Tang et al., 2016). At the moment, PARN is the only
96 known deadenylases which can interact both with the 5' cap and the 3' poly(A) tail of mRNA
97 and is involved in the circulization of mRNA (Skeparnias et al., 2017). PARN itself is
98 regulated by interaction with the nuclear cap binding complex, directly the 5' CAP mRNA
99 structure, the eukaryotic translation ignition factor 4e, and poly(A) tail binding proteins such
100 as PABC (Gao et al., 2000; Martinez et al., 2000; Balatsos et al., 2006).

101 PARNs interact with a specific subset of mRNA, miRNA, small nucleolar RNA (snoRNA)
102 and small Cajal body RNAs (scaRNA) (Reverdatto et al., 2004; Berndt et al., 2012; Virtanen
103 et al., 2013; Zhang et al., 2015). Besides their involvement in embryonic development,
104 PARNs participate in telomere formation and in DNA damage repair after stress (Mittal et al.,
105 2011; Lee et al., 2012; Virtanen et al., 2013; Moon et al., 2015). It was shown in *C. elegans*,
106 that PARN interacts with small non coding RNAs (piwi-interacting RNAs), which are
107 essential in germ line development and fertility, probably by epigenetic regulation (Tang et
108 al., 2016).

109 The Arabidopsis PARN is structural and phylogenetic different from animal PARNs (Figure
110 3). AtPARN has a CAF1 domain (Virtanen et al., 2013) but in contrast to other PARNs,
111 AtPARN do not possess a RRM or a R3H domain. RRM is required for m7'G-cap binding
112 (Nagata et al., 2008) and R3H domain can bind poly nucleotide such as single stranded RNA
113 (Wu et al., 2005). Beside these differences, AtPARN shares high similarities with other
114 PARNs. For example, the catalytic CAF1 domain is to 2/3 identical with the human version
115 (Chiba et al., 2004). The impact of AtPARN on the poly(A) tail of selected embryonical
116 mRNAs has been addressed before (Reverdatto et al., 2004). The non-viable double-knock-
117 out mutants, showed altered adenylation in only one embryonic specific gene (Reverdatto et

al., 2004). This gene, PROLIFERA, which is a DNA helicase, is critically involved in early seed development, and had an increased poly(A) tail in the *Atparn* mutant (Reverdatto et al., 2004; Herridge et al., 2014). In contrast, other tested mRNAs did not have an altered poly(A) tail in the *parn* mutant, which emphasizes the target specificity of AtPARN.

We also compared the poly(A) tails of total mRNA of adult WT and *cycam* plants without any visible difference. Furthermore, for selected genes we did not observe any differences. One reason could be that the number of targeted mRNA species in plants is quite low. However, besides the classical function in the poly(A) tail shortening of mRNAs for proteins, the role of AtPARN in miRNA processing could play a crucial role in plants. The impact of PARN on human miRNA has been shown before (Zhang et al., 2015). Although this has not been shown yet for plants, the involvement of miRNAs in plant development and response to external signals becomes increasingly recognized (Blein and Laufs, 2016). Thus, it is not surprising, that we have found seven miRNAs upregulated in *cycam* plants (Table 1).

RNA and mitochondria

Hirayama et al (2013) showed that AtPARN can be located in mitochondria and proposed that it regulates the symbiotic activity of mitochondria, and degrades putative harmful mitochondrial RNAs (Hirayama et al., 2013; Hirayama, 2014). Angiosperms have the biggest mitochondrial genome described so far (Kubo and Newton, 2008). While most of the genes are conserved, a huge proportion of the genome are non-coding sequences (90% in *Arabidopsis*) (Hammani and Giegé, 2014). These insertions are from the nucleus, plastids, viruses, and unknown origin (Unseld et al., 1997; Holec et al., 2006; Kubo and Newton, 2008). For proper transcription, translation, and regulation, mitochondria constantly crosstalk with the nucleus (Hammani and Giegé, 2014; Planchard et al., 2018). One way for plants to crosstalk, are pentatricopeptide repeat proteins (PPR), one of the largest family of plant proteins (Barkan and Small, 2014). They are involved in most plant development and growth

steps including ABA signalling (Barkan and Small, 2014). They influence the expression of mitochondrial proteins by altering of RNA sequences, stability and translation rate (Barkan und Small 2014). This might be due to binding to the poly(A) tail of mitochondrial RNA similar to PABCs (Hammani and Giegé, 2014). An interplay of PARN with PPRs was proposed before (Hirayama, 2014). In addition, RNAses such as Polynucleotide Phosphorylase, were found in mitochondria where they are involved in the degradation of mRNA and rRNA but also poly (A) tailed non coding RNA (Holec et al., 2006). Whether AtPARN acts directly in the mitochondria by degrading the poly(A) tail or of a specific subset of mRNA or indirectly by degrading of miRNA is unclear. Nevertheless, one specific target inside mitochondria could be the UNIPLEX complex. This mitochondrial calcium uniporter (MCU) complex contains of calcium pore forming proteins MCU und MCUB, the regulator essential mitochondrial Ca^{2+} uniporter regulator (EMRE) and several mitochondrial Ca^{2+} uptake (MICU) proteins (Pallafacchina et al., 2018). In muscles, miRNA targets MCU specifically and regulates the translation of these calcium transporters (Zaglia et al., 2017). Recently the plant version of this complex was identified and characterized (Teardo et al., 2017). There it was show that AtMCU1 is highly expressed in roots and *atmcu1* mutants have shorter roots (Teardo et al., 2017).

Interestingly we found four mitochondrial genes upregulated in *cycam* and three genes with a predicted location in mitochondria, which are downregulated in *cycam* (Table 1). Whether one of these genes is the primary cause for the *cycam* phenotype will be addressed in future research.

Since *cycam* mutants are defective in embryonic development and calcium signalling, AtPARN seems to be involved in both aspects. This brings up the following questions:

- A) Are mRNAs, miRNAs, or other small RNAs the targets of AtPARN? Is the protein active in the nucleus, the cytosol or in the mitochondria?

- 168 B) Is the observed *cycam* phenotype caused by AtPARNs primary functions or due to
169 secondary effects (e.g. due to altered regulation of hormones such as ABA)
- 170 C) Does AtPARN has a different function / mode of action in embryos and adult plants?
- 171 D) How does the point-mutation in the CAF1 domain affects the function of PARN?

172 **References**

- 173 Balatsos, N.A.A., Nilsson, P., Mazza, C., Cusack, S., Virtanen, A., 2006. **Inhibition of**
174 **mRNA deadenylation by the nuclear cap binding complex (CBC).** The Journal of
175 biological chemistry 281 (7), 4517–4522. 10.1074/jbc.M508590200.
- 176 Barkan, A., Small, I., 2014. **Pentatricopeptide repeat proteins in plants.** Annual review of
177 plant biology 65, 415–442. 10.1146/annurev-arplant-050213-040159.
- 178 Barreau, C., Paillard, L., Osborne, H.B., 2005. **AU-rich elements and associated factors:**
179 **are there unifying principles?** Nucleic acids research 33 (22), 7138–7150.
180 10.1093/nar/gki1012.
- 181 Berndt, H., Harnisch, C., Rammelt, C., Stöhr, N., Zirkel, A., Dohm, J.C., Himmelbauer, H.,
182 Tavanez, J.-P., Hüttelmaier, S., Wahle, E., 2012. **Maturation of mammalian H/ACA box**
183 **snoRNAs: PAPD5-dependent adenylation and PARN-dependent trimming.** RNA (New
184 York, N.Y.) 18 (5), 958–972. 10.1261/rna.032292.112.
- 185 Blein, T., Laufs, P., 2016. **MicroRNAs (miRNAs) and plant development.** eLS. John Wiley
186 & Sons, Ltd: Chichester, 15, 1–11. 10.1002/9780470015902.a0020106.pub2.
- 187 Cai, X., Hagedorn, C.H., Cullen, B.R., 2004. **Human microRNAs are processed from**
188 **capped, polyadenylated transcripts that can also function as mRNAs.** RNA (New York,
189 N.Y.) 10 (12), 1957–1966. 10.1261/rna.7135204.
- 190 Chiba, Y., Johnson, M.A., Lidder, P., Vogel, J.T., van Erp, H., Green, P.J., 2004. **AtPARN is**
191 **an essential poly(A) ribonuclease in Arabidopsis.** Gene 328, 95–102.
192 10.1016/j.gene.2003.11.028.
- 193 Copeland, P.R., Wormington, M., 2001. **The mechanism and regulation of deadenylation:**
194 **identification and characterization of Xenopus PARN.** RNA (New York, N.Y.) 7 (6), 875–
195 886.
- 196 Ender, C., Meister, G., 2010. **Argonaute proteins at a glance.** Journal of cell science 123 (Pt
197 11), 1819–1823. 10.1242/jcs.055210.
- 198 Fabian, M.R., Mathonnet, G., Sundermeier, T., Mathys, H., Zipprich, J.T., Svitkin, Y.V.,
199 Rivas, F., Jinek, M., Wohlschlegel, J., Doudna, J.A., Chen, C.-Y.A., Shyu, A.-B., Yates, J.R.,
200 Hannon, G.J., Filipowicz, W., Duchaine, T.F., Sonenberg, N., 2009. **Mammalian miRNA**
201 **RISC recruits CAF1 and PABP to affect PABP-dependent deadenylation.** Molecular cell
202 35 (6), 868–880. 10.1016/j.molcel.2009.08.004.
- 203 Gao, M., Fritz, D.T., Ford, L.P., Wilusz, J., 2000. **Interaction between a poly(A)-Specific**
204 **ribonuclease and the 5' cap influences mRNA deadenylation rates *in vitro*.** Molecular cell
205 5 (3), 479–488.
- 206 Goldstrohm, A.C., Wickens, M., 2008. **Multifunctional deadenylase complexes diversify**
207 **mRNA control.** Nature reviews. Molecular cell biology 9 (4), 337–344. 10.1038/nrm2370.
- 208 Hammani, K., Giegé, P., 2014. **RNA metabolism in plant mitochondria.** Trends in plant
209 science 19 (6), 380–389. 10.1016/j.tplants.2013.12.008.

210 Herridge, R.P., Day, R.C., Macknight, R.C., 2014. **The role of the MCM2-7 helicase**
 211 **complex during Arabidopsis seed development.** Plant molecular biology 86 (1-2), 69–84.
 212 10.1007/s11103-014-0213-x.

213 Hirayama, T., 2014. **A unique system for regulating mitochondrial mRNA poly(A) status**
 214 **and stability in plants.** Plant signaling & behavior 9 (10), e973809.
 215 10.4161/15592324.2014.973809.

216 Hirayama, T., Matsuura, T., Ushiyama, S., Narusaka, M., Kurihara, Y., Yasuda, M., Ohtani,
 217 M., Seki, M., Demura, T., Nakashita, H., Narusaka, Y., Hayashi, S., 2013. **A poly(A)-specific**
 218 **ribonuclease directly regulates the poly(A) status of mitochondrial mRNA in**
 219 **Arabidopsis.** Nature communications 4, 2247. 10.1038/ncomms3247.

220 Holec, S., Lange, H., Kühn, K., Alioua, M., Börner, T., Gagliardi, D., 2006. **Relaxed**
 221 **transcription in Arabidopsis mitochondria is counterbalanced by RNA stability control**
 222 **mediated by polyadenylation and polynucleotide phosphorylase.** Molecular and cellular
 223 biology 26 (7), 2869–2876. 10.1128/MCB.26.7.2869-2876.2006.

224 Hunt, A.G., 2008. Messenger RNA 3' End Formation in Plants, in: Compan, R.W., Cooper,
 225 M.D., Honjo, T., Koprowski, H., Melchers, F., Oldstone, M.B.A., Olsnes, S., Vogt, P.K.,
 226 Reddy, A.S.N., Golovkin, M. (Eds.), **Nuclear pre-mRNA Processing in Plants**, vol. 326.
 227 Springer Berlin Heidelberg, Berlin, Heidelberg, pp. 151–177.

228 Jalkanen, A.L., Coleman, S.J., Wilusz, J., 2014. **Determinants and implications of mRNA**
 229 **poly(A) tail size--does this protein make my tail look big?** Seminars in cell &
 230 developmental biology 34, 24–32. 10.1016/j.semcd.2014.05.018.

231 Johnson, J.M., Thürich, J., Petutschnig, E.K., Altschmied, L., Meichsner, D., Sherameti, I.,
 232 Dindas, J., Mrozinska, A., Paetz, C., Scholz, S.S., Furch, A.C., Lipka, V., Hedrich, R.,
 233 Schneider, B., Svatoš, A., Oelmüller, R., 2018. **A poly(A) ribonuclease controls the**
 234 **cellotriose-based interaction between *Piriformospora indica* and its host Arabidopsis.**
 235 Plant physiology. 10.1104/pp.17.01423.

236 Körner, C.G., Wormington, M., Muckenthaler, M., Schneider, S., Dehlin, E., Wahle, E., 1998.
 237 **The deadenylating nuclease (DAN) is involved in poly(A) tail removal during the meiotic**
 238 **maturation of *Xenopus* oocytes.** The EMBO Journal 17 (18), 5427–5437.
 239 10.1093/emboj/17.18.5427.

240 Kubo, T., Newton, K.J., 2008. **Angiosperm mitochondrial genomes and mutations.**
 241 Mitochondrion 8 (1), 5–14. 10.1016/j.mito.2007.10.006.

242 Lee, J.E., Lee, J.Y., Trembly, J., Wilusz, J., Tian, B., Wilusz, C.J., 2012. **The PARN**
 243 **deadenylase targets a discrete set of mRNAs for decay and regulates cell motility in**
 244 **mouse myoblasts.** PLoS genetics 8 (8), e1002901. 10.1371/journal.pgen.1002901.

245 Lima, S.A., Chipman, L.B., Nicholson, A.L., Chen, Y.-H., Yee, B.A., Yeo, G.W., Collier, J.,
 246 Pasquinelli, A.E., 2017. **Short poly(A) tails are a conserved feature of highly expressed**
 247 **genes.** Nature Structural & Molecular Biology 24, 1057 EP -. 10.1038/nsmb.3499.

248 Martinez, J., Ren, Y.G., Thuresson, A.C., Hellman, U., Astrom, J., Virtanen, A., 2000. **A 54-**
 249 **kDa fragment of the poly(A)-specific ribonuclease is an oligomeric, processive, and cap-**
 250 **interacting poly(A)-specific 3' exonuclease.** The Journal of biological chemistry 275 (31),
 251 24222–24230. 10.1074/jbc.M001705200.

252 Michal Johnson, J., Reichelt, M., Vadassery, J., Gershenzon, J., Oelmuller, R., 2014. **An**
253 **Arabidopsis mutant impaired in intracellular calcium elevation is sensitive to biotic and**
254 **abiotic stress.** BMC plant biology 14, 162. 10.1186/1471-2229-14-162.

255 Mittal, S., Aslam, A., Doidge, R., Medica, R., Winkler, G.S., 2011. **The Ccr4a (CNOT6)**
256 **and Ccr4b (CNOT6L) deadenylase subunits of the human Ccr4-Not complex contribute**
257 **to the prevention of cell death and senescence.** Molecular biology of the cell 22 (6), 748–
258 758. 10.1091/mbc.E10-11-0898.

259 Moon, D.H., Segal, M., Boyraz, B., Guinan, E., Hofmann, I., Cahan, P., Tai, A.K., Agarwal,
260 S., 2015. **Poly(A)-specific ribonuclease (PARN) mediates 3'-end maturation of the**
261 **telomerase RNA component.** Nature genetics 47 (12), 1482–1488. 10.1038/ng.3423.

262 Morozova, N., Zinovyev, A., Nonne, N., Pritchard, L.-L., Gorban, A.N., Harel-Bellan, A.,
263 2012. **Kinetic signatures of microRNA modes of action.** RNA (New York, N.Y.) 18 (9),
264 1635–1655. 10.1261/rna.032284.112.

265 Nagata, T., Suzuki, S., Endo, R., Shirouzu, M., Terada, T., Inoue, M., Kigawa, T., Kobayashi,
266 N., Güntert, P., Tanaka, A., Hayashizaki, Y., Muto, Y., Yokoyama, S., 2008. **The RRM**
267 **domain of poly(A)-specific ribonuclease has a noncanonical binding site for mRNA cap**
268 **analog recognition.** Nucleic acids research 36 (14), 4754–4767. 10.1093/nar/gkn458.

269 Nam, J.-W., Rissland, O.S., Koppstein, D., Abreu-Goodger, C., Jan, C.H., Agarwal, V.,
270 Yildirim, M.A., Rodriguez, A., Bartel, D.P., 2014. **Global analyses of the effect of different**
271 **cellular contexts on microRNA targeting.** Molecular cell 53 (6), 1031–1043.
272 10.1016/j.molcel.2014.02.013.

273 Nicholson, A.L., Pasquinelli, A.E., 2018. **Tales of detailed poly(A) tails.** Trends in cell
274 biology. 10.1016/j.tcb.2018.11.002.

275 Nishimura, N., Kitahata, N., Seki, M., Narusaka, Y., Narusaka, M., Kuromori, T., Asami, T.,
276 Shinozaki, K., Hirayama, T., 2005. **Analysis of ABA hypersensitive germination2 revealed**
277 **the pivotal functions of PARN in stress response in Arabidopsis.** The Plant journal : for
278 cell and molecular biology 44 (6), 972–984. 10.1111/j.1365-313X.2005.02589.x.

279 Pallafacchina, G., Zanin, S., Rizzuto, R., 2018. **Recent advances in the molecular**
280 **mechanism of mitochondrial calcium uptake.** F1000Research 7.
281 10.12688/f1000research.15723.1.

282 Planchard, N., Bertin, P., Quadrado, M., Dargel-Graffin, C., Hatin, I., Namy, O., Mireau, H.,
283 2018. **The translational landscape of Arabidopsis mitochondria.** Nucleic acids research 46
284 (12), 6218–6228. 10.1093/nar/gky489.

285 Reverdatto, S.V., Dutko, J.A., Chekanova, J.A., Hamilton, D.A., Belostotsky, D.A., 2004.
286 **mRNA deadenylation by PARN is essential for embryogenesis in higher plants.** RNA
287 (New York, N.Y.) 10 (8), 1200–1214. 10.1261/rna.7540204.

288 Schuller, A.P., Green, R., 2018. **Roadblocks and resolutions in eukaryotic translation.**
289 Nature reviews. Molecular cell biology 19 (8), 526–541. 10.1038/s41580-018-0011-4.

290 Simpson, G.G., Dijkwel, P.P., Quesada, V., Henderson, I., Dean, C., 2003. **FY is an RNA 3'**
291 **end-processing factor that interacts with FCA to control the Arabidopsis floral**
292 **transition.** Cell 113 (6), 777–787.

293 Skeparnias, I., Anastasakis, D., Shaukat, A.-N., Grafanaki, K., Stathopoulos, C., 2017.
 294 **Expanding the repertoire of deadenylases.** RNA Biology 14 (10), 1320–1325.
 295 10.1080/15476286.2017.1300222.

296 Subtelny, A.O., Eichhorn, S.W., Chen, G.R., Sive, H., Bartel, D.P., 2014. **Poly(A)-tail**
 297 **profiling reveals an embryonic switch in translational control.** Nature 508, 66 EP -.
 298 10.1038/nature13007.

299 Tang, W., Tu, S., Lee, H.-C., Weng, Z., Mello, C.C., 2016. **The RNase PARN-1 trims**
 300 **piRNA 3' ends to promote transcriptome surveillance in *C. elegans*.** Cell 164 (5), 974–
 301 984. 10.1016/j.cell.2016.02.008.

302 Teardo, E., Carraretto, L., Wagner, S., Formentin, E., Behera, S., Bortoli, S. de, Larosa, V.,
 303 Fuchs, P., Lo Schiavo, F., Raffaello, A., Rizzuto, R., Costa, A., Schwarzländer, M., Szabò, I.,
 304 2017. **Physiological characterization of a plant mitochondrial calcium uniporter *in vitro***
 305 **and *in vivo*.** Plant physiology 173 (2), 1355–1370. 10.1104/pp.16.01359.

306 Tian, B., Hu, J., Zhang, H., Lutz, C.S., 2005. **A large-scale analysis of mRNA**
 307 **polyadenylation of human and mouse genes.** Nucleic acids research 33 (1), 201–212.
 308 10.1093/nar/gki158.

309 Tian, B., Manley, J.L., 2017. **Alternative polyadenylation of mRNA precursors.** Nature
 310 reviews. Molecular cell biology 18 (1), 18–30. 10.1038/nrm.2016.116.

311 Unseld, M., Marienfeld, J.R., Brandt, P., Brennicke, A., 1997. **The mitochondrial genome of**
 312 ***Arabidopsis thaliana* contains 57 genes in 366,924 nucleotides.** Nature genetics 15 (1), 57–
 313 61. 10.1038/ng0197-57.

314 Virtanen, A., Henriksson, N., Nilsson, P., Nissbeck, M., 2013. **Poly(A)-specific ribonuclease**
 315 **(PARN): an allosterically regulated, processive and mRNA cap-interacting deadenylase.**
 316 Critical reviews in biochemistry and molecular biology 48 (2), 192–209.
 317 10.3109/10409238.2013.771132.

318 Wu, M., Reuter, M., Lilie, H., Liu, Y., Wahle, E., Song, H., 2005. **Structural insight into**
 319 **poly(A) binding and catalytic mechanism of human PARN.** The EMBO Journal 24 (23),
 320 4082–4093. 10.1038/sj.emboj.7600869.

321 Xing, D., Li, Q.Q., 2011. **Alternative polyadenylation and gene expression regulation in**
 322 **plants.** Wiley interdisciplinary reviews. RNA 2 (3), 445–458. 10.1002/wrna.59.

323 Xing, D., Zhao, H., Li, Q.Q., 2008. **Arabidopsis CLP1-SIMILAR PROTEIN3, an ortholog**
 324 **of human polyadenylation factor CLP1, functions in gametophyte, embryo, and**
 325 **postembryonic development.** Plant Physiol. 148 (4), 2059–2069. 10.1104/pp.108.129817.

326 Zaglia, T., Ceriotti, P., Campo, A., Borile, G., Armani, A., Carullo, P., Prando, V., Coppini,
 327 R., Vida, V., Stølen, T.O., Ulrik, W., Cerbai, E., Stellin, G., Faggian, G., Stefani, D. de,
 328 Sandri, M., Rizzuto, R., Di Lisa, F., Pozzan, T., Catalucci, D., Mongillo, M., 2017. **Content**
 329 **of mitochondrial calcium uniporter (MCU) in cardiomyocytes is regulated by**
 330 **microRNA-1 in physiologic and pathologic hypertrophy.** Proceedings of the National
 331 Academy of Sciences of the United States of America 114 (43), E9006-E9015.
 332 10.1073/pnas.1708772114.

333 Zhang, X., Devany, E., Murphy, M.R., Glazman, G., Persaud, M., Kleiman, F.E., 2015.
334 **PARN deadenylase is involved in miRNA-dependent degradation of TP53 mRNA in**
335 **mammalian cells.** Nucleic acids research 43 (22), 10925–10938. 10.1093/nar/gkv959.

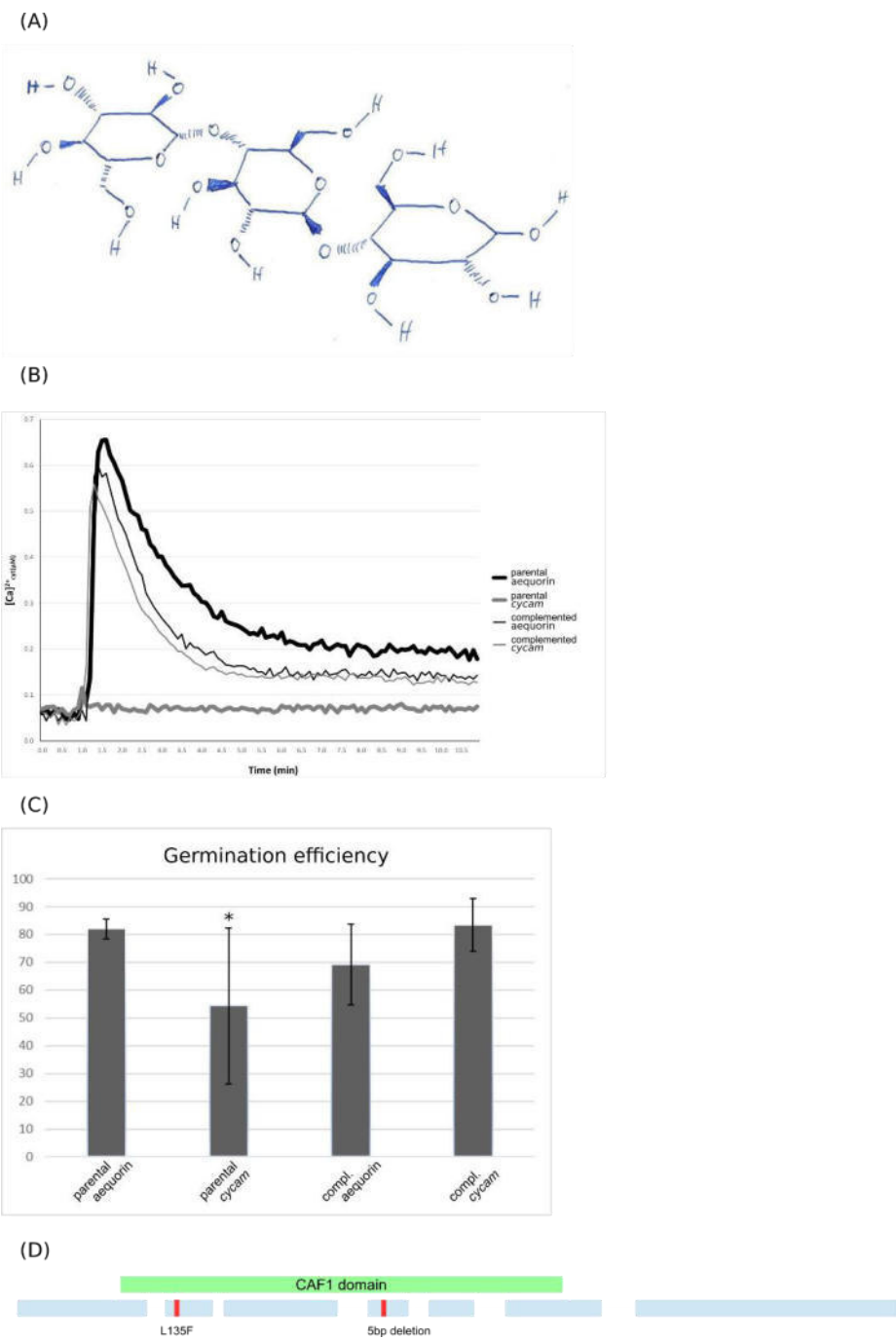


Figure 1 Characterization of the *cycam* phenotype

Figure 1 Characterization of the *cycam* phenotype

(A) Cellotriose is a trisaccharide consisting of three glucose molecules connected by an β -1,4 linkage. (B) While a specific calcium signal is induced in Arabidopsis reporter plants (parental aequorin) after application of cellotriose, this is not the case in *cycam* mutants. After

344 reintroduction of the wild-type version of PARN, complemented *cycam* mutant plants show a
345 normal response against celotriose. The insertion of the construct into parental aequorin plants
346 (complemented aequorin) does not have any impact on the calcium signal. (C) In addition to
347 the calcium response, *cycam* mutants react to the application of ABA. Exemplary, *cycam* seeds
348 germinate more irregular and with a lower frequency (7dpi, 0.3µm ABA, n=13, three biological
349 replicates, Two-Way-Anova). In contrast complemented plants show a similar germination
350 frequency compared to the wild-type. (D) Schematic representation of *AtPARN* and the
351 respective mutations in *cycam* (L135F) and in the *ahg2-1* mutant (deletion of 5 base pairs).

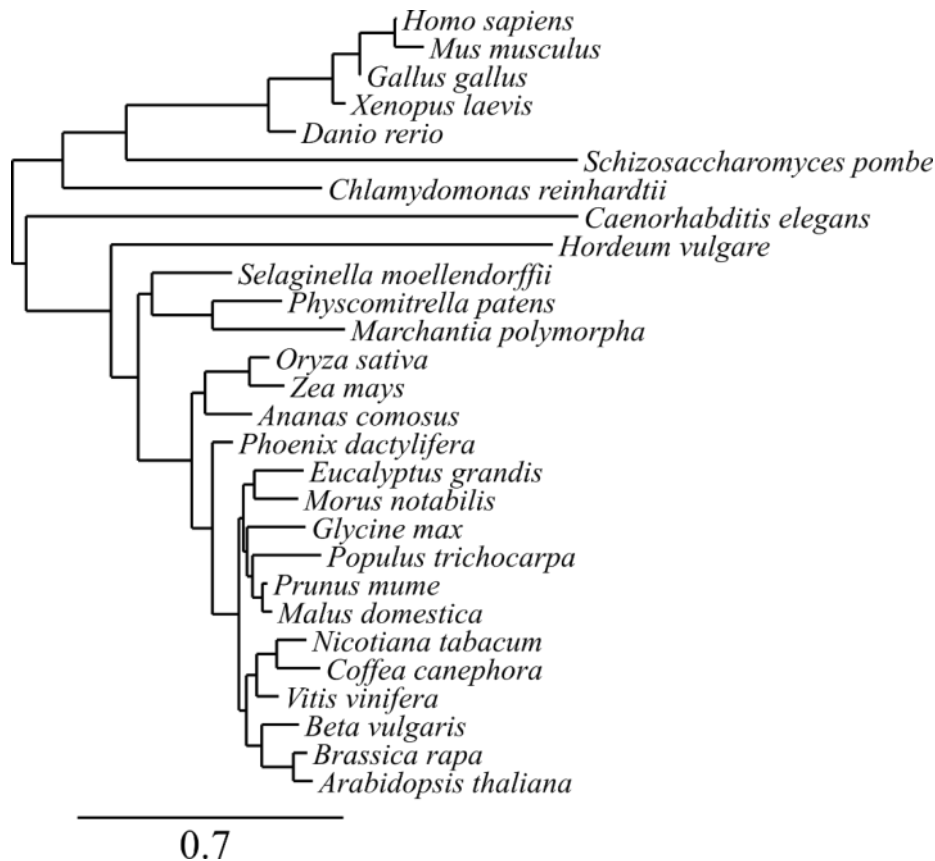


Figure 3 Phylogenetic tree of the PARN protein in different organisms

Figure 3 Phylogenetic tree of the PARN Protein in different organisms

The PARN gene clusters in two distinct groups with animals in one and plants (with the notable exception of barley) in the other group. Sequences were extracted from the NCBI database using BLASTP (version 2.7) algorithm. The sequences were used for constructing a phylogenetic tree using CLC Workbench (version 7.7.3).

Accession number	Name	Function (according to UniProt and TAIR)	Regulation in <i>cycam</i>
miRNA			
AT4G03455.1	MIR447B	targets several 2-phosphoglycerate kinase-related family members	8-fold up
AT3G26818.1	MIR169M	targets several HAP2 family members.	8-fold up
AT5G62848.1	MIR420	n.a.	12.9-fold up
AT1G14071.1	MIR830A	n.a.	6.3-fold up
AT5G39693.1	MIR869A	n.a.	3.7-fold up
AT2G25011.1	MIR836A	n.a.	2.5-fold up
AT3G44444.1	MIR849A	n.a.	3.2-fold up
Located in Mitochondria			
AT1G02700.1	GATA transcription factor-like protein	n.a.	7.9-fold up
AT2G22241.1	hypothetical protein	n.a.	3-fold up
AT2G29263.1	hypothetical protein	n.a.	7.8-fold up
Mitochondrial			
ATMG00290.1	Mitochondrial Ribosomal Protein S4	S4 is a constituent of the small subunit of the ribosomal complex	2.5-fold down
ATMG00030.1	hypothetical protein	n.a.	3.3-fold down
ATMG01010.1	Unknown conserved protein	n.a.	2.5-fold down
ATMG01000.1	hypothetical protein	n.a.	2.8-fold down
Poly(a) binding proteins			
AT1G22760.1	Poly(a) binding protein 3	Putative poly(A) binding protein	3.1-fold up
RNA binding protein			
AT2G18830.1	RNA-binding (RRM/RBD/RNP motif) family protein	n.a.	12.2-fold up
AT5G08695.1	RNA-binding (RRM/RBD/RNP motifs) family protein	n.a.	5.2-fold up
Connection to Calcium			
AT1G48590.2	Calcium-dependent lipid-binding (CaLB domain) family protein CAR5	Involved in abscisic acid-activated signalling pathway	4.6-fold down
AT2G36180.1	Probable calcium-binding protein CML31	Potential calcium sensor	12-fold up
AT4G00467.1	Calcium-dependent lipid-binding (CaLB domain) family protein	n.a.	3.5-fold up
AT2G36180.1	Probable calcium-binding protein CML31	Potential calcium sensor	12-fold up

370

371 **Table1 Regulation of selected genes in *cycam* plants**372 Two weeks old Arabidopsis seedlings (Col-0) and *cycam* plants. Microarrays experiments

373 were designed and performed by Doreen Meichsner and Ralf Oelmüller (personal

374 communication).

Chapter 3:

General Discussion And Conclusion

I. General Discussion

Mycorrhiza is an ancient form of plant-fungal interaction. Even though the ecological and economical importance of this symbiosis is known the exact mode of recognition and interaction is still subject of ongoing research. The emergence of the endophyte *P. indica* as an alternative model organism can give significant input for the research field.

In the following the two main topics of this thesis: the early interspecies crosstalk and the establishment and maintenance of symbiotic interactions, are discussed in detail.

II. Cellotriose And PARN

The generation of the cytosolic calcium mutant (*cycam*) gave invaluable insights into the communication between *A. thaliana* and *P. indica* (Johnson et al., 2014). After treatment with a cell wall extract (CWE) of axenically grown *P. indicia*, *A. thaliana* plants show a strong influx of cytosolic calcium into the roots. The calcium signal has a specific signature which shows a peak after approximately 90 seconds followed by a gradual decline. In contrast, *cycam* plants do not react to the CWE of *P. indica* but show normal responses to treatment with MAMPs such as chitin or flagellin. In the first manuscript of this thesis the active component of the fungal CWE was identified as cellotriose (CT) and the molecular mechanism of the *cycam* phenotype were analysed in depth.

The active compound of the CWE was isolated prior by Dr. Johnson (Johnson, 2009). It was identified as CT by mass spectrometry and nuclear magnetic resonance spectroscopy (Johnson et al., 2018). CT, which induces a calcium signal at low concentration (10 nm), is a trisaccharide consisting of three glucose molecules connected by an β -1,4 linkage.

CT bares structural resemblance to chitooligosaccharides (COs), such as chitotetraose or chitopentose. These fungal polysaccharides are found in germinating spore extracts of *R. irregularis* after treatment with strigolactones and activate common symbiosis genes in the host (Genre et al., 2013). COs have similar structures as LCOs but are active in lower concentration (Genre et al., 2013). COs employ an additional calcium signalling pathway as NOD factors. For example, NFP (NOD factor perception), a LysM-RLK, is essential for the perception of NOD factors but is not required for COs induced calcium signalling (Genre et al., 2013). COs also induce a calcium signal in *cycam* plants (Johnson et al., 2018). This indicates that a different pathway for both forms of oligosaccharides must exist. It is unclear whether

other LysM-RLK are involved in CT recognition, but it has been shown that one LysM-RLK, CERK1 (Chitin Elicitor Receptor Kinase 1) plays a role in *P. indica* colonisation.

CERK1 recognises long chitin-oligosaccharides and is involved in immune responses (Liu et al., 2012). CERK1 has a specific affinity to chitotetraose and chitoheptaose, whereas no activities for chitopentose can be observed (Liu et al., 2012). *A. thaliana cerk1* mutant plants are overcolonised by *P. indica* probably due to a lack of proper defence response of the host plant (Nongbri et al., 2012).

The origin and localisation of CT within the cell are still unclear. While it is likely that CT is derived from the cell wall of *P. indica*, this has not been proven. An alternative hypothesis for the origin of CT is the endofungal bacteria *Rhizobium radiobacter* which forms a symbiosis with *P. indica* (Glaeser et al., 2016). Since the CWE of *R. radiobacter* induces the same calcium response both in *A. thaliana* wild-type calcium reporter lines (pMAQ2) and *cycam* plants (Johnson et al., 2018), it is unlikely that CT is a NOD factor produced by the endofungal bacteria. Interestingly, after application of a germinating AMF spore extract, a calcium signature similar to that induced by CT was observed (Navazio et al., 2007). Since this effect was only observed in soybean but not *A. thaliana*, it could be speculated that for both plant species a similar signal reception mechanism exists but that the exact nature of the respective compound is different. The identification of fungal genes responsible for CT production can help to understand the evolutionary connections between saprophytic and mutualistic traits. The genome of *P. indica* is in large portions unannotated but the fungus possesses 230 putative glucosidases and 66 cellulases. One of these proteins, PIIN_04111, was found in the supernatant of *P. indica* liquid culture (Thürich et al., 2018). This probable β -glucosidases has high similarity (approximately 50% identity) with Glycoside hydrolase family 3 (XP_006964076) from *Trichoderma reesei* (Figure 2).

This transglycosidase has been shown to degrade cellulose with CT as intermediate product (Guo et al., 2016). Under high glucose condition (>100 mM) this process is reversed and CT is produced from cellobiose (Guo et al., 2016).

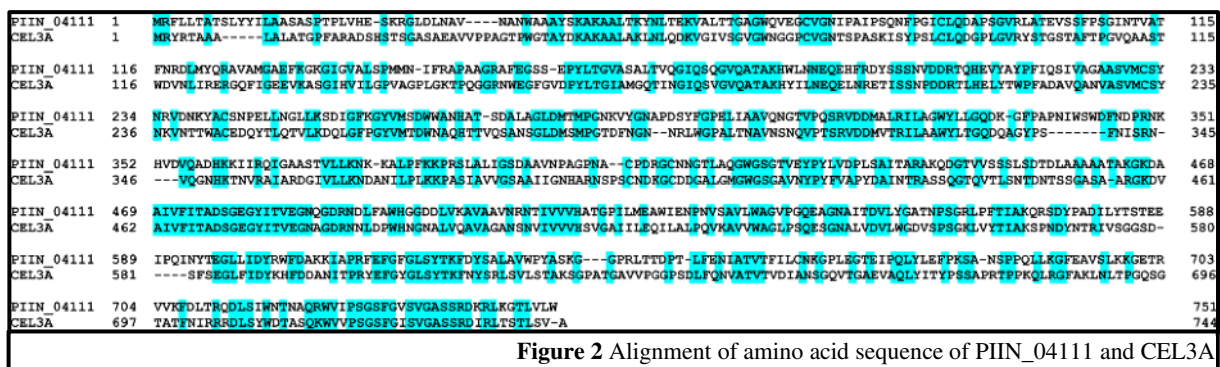


Figure 2 Alignment of amino acid sequence of PIIN_04111 and CEL3A

The *cycam* plants were generated by EMS (Ethyl Methanesulfonate) mutagenesis of pMAQ2 plants (Johnson et al., 2014). EMS treatment causes the introduction of many single-nucleotide polymorphisms (SNPs) in the genome (Johnson et al., 2014). The amount of unrelated mutations was drastically reduced by backcrossing (*cycam* x pMAQ2) and screening of the offspring from each crossing cycle. At the F2 generation, I pooled 25 backcrossed plants with a CT reactive phenotype and an equal amount of plants with the wild-type phenotype. Both pools were analysed by Illumina (100-bp paired-end) sequencing and the reads were mapped against the reference genome of *A. thaliana* (TAIR Version 10). Four SNPs unique to *cycam* and with a frequency of 100% were found. Interestingly, I identified neither a LysM-RLK nor a calcium channel. Instead I considered *AtPARN*, a Poly(A) specific Ribonuclease (At1G55870), as the most likely candidate. In *cycam* plants the point mutation in *AtPARN* causes an amino acid exchange (L135F) in the main RNA binding domain. Beside the CT-signalling phenotype, I showed that *cycam* plants show an irregular growth and have a higher level of endogenous ABA (Johnson et al., 2018). Interestingly, Nishimura et al. (2005) identified an *A. thaliana* mutant which has an unrelated mutation in the *PARN* gene and showed a similar growth phenotype as *cycam* (Nishimura et al., 2005). Since double knock-out lines of *AtPARN* are embryonal lethal (Thürich and Oelmüller, 2019), *cycam* plants were complemented using an 35S promotor with *AtPARN*. Complemented *cycam* plants showed the CT sensitive phenotype and a normal growth phenotype (Thürich and Oelmüller, 2019). In addition, pMAQ2 plants which were complemented with the same construct showed no abnormal phenotype (Figure 3) (Johnson et al., 2018). *P. indica* does not influence expression of *AtPARN* mRNA and neither PMAQ2 nor *cycam* plants show a different expression level of this gene (Thürich and Oelmüller, 2019). In conclusion, not the total amount of *AtPARN* mRNA is responsible for the *cycam* phenotype. Instead the activity or specificity of the ribonuclease seems to be

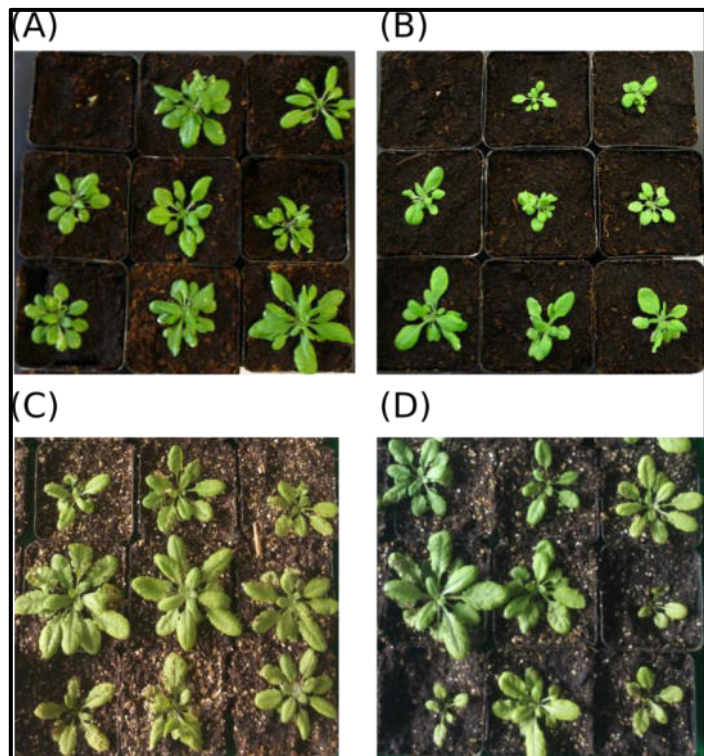


Figure 3 Parental lines (pMAQ2 (A) and *cycam* (B)) and lines complemented with the PARN construct (pMAQ2 (C) and *cycam* (D))

influenced by the point mutation. AtPARN is a highly conserved protein with homologues found in many species including *Homo sapiens*, *Caenorhabditis elegans*, and *Schizosaccharomyces pombe*. PARNs are involved in embryonical development and stress response by regulation of RNA metabolism (Thürich and Oelmüller, 2019). The role of PARN in *A. thaliana* and other plants is still unknown but some speculation of its function exist. It has been shown that the embryonic-specific gene *PROLIFERA* had a reduced poly(A) tail in non-viable seeds of a double knock-out mutant of *AtPARN* (Reverdatto et al., 2004). *PROLIFERA* is a DNA helicase which is critically involved in early seed development (Herridge et al., 2014). With the current knowledge, a role of *PROLIFERA* in CT-calcium signalling is unlikely. In line with previous work (Reverdatto et al., 2004), I did not observe any differences between the size of the poly(A) tail of the total RNA pool of *cycam* and pMAQ2 plants. This confirms the current theory of PARN being specific for a subset of RNAs (Reverdatto et al., 2004; Berndt et al., 2012; Virtanen et al., 2013; Zhang et al., 2015).

A role of AtPARN in mitochondrial processes, such as the regulation of mitochondrial mRNA, was proposed (Hirayama et al., 2013; Hirayama, 2014). Interestingly, while the aforementioned authors observed an approximately 1.5-fold increase of mitochondrial mRNA in *parn* mutants, this is not the case in *cycam* (Thürich and Oelmüller, 2019). Gene expression studies comparing *cycam* and pMAQ2 plants, showed for most mitochondrial genes no difference in the expression compared to the wild-type and for four genes a slight down regulation (Thürich and Oelmüller, 2019). Interestingly, three genes (two hypothetical proteins and a putative transcription factor) which possess a mitochondrial translocation sequence, are upregulated in *cycam* (Thürich and Oelmüller, 2019). Subsequently, it is unclear whether mitochondrial genes are the primary target of AtPARN or if my findings and those of others are only secondary effects.

Initially, an accumulation of PARN in the cytoplasm was reported (Reverdatto et al., 2004). In contrast, a partial co-localisation of PARN with mitochondria has later been reported (Hirayama et al., 2013). The construct used for the complementation assay was also used for stable transfection of wild-type *A. thaliana* plants. While a PARN-GFP version was detectable on protein level, no fluorescence was detectable. In future, new constructs will help to localise AtPARN within the cell.

Another possible role of AtPARN could be the regulation of small ncRNA. In mycorrhizal responsive plants miR171h indirectly regulates *RAM1*, which is required for AM formation (Diédhiou and Diouf, 2018). Interestingly, seven miRNAs were upregulated in *cycam* mutants (Table 2) (Thürich and Oelmüller, 2019). One possibility could be that one of these miRNAs is involved in the regulation components of the CT calcium signalling pathway.

Table 2 Differentially regulated miRNA in *cycam*

Accession number	Name	Function (according to Uniprot and TAIR)	regulation in <i>cycam</i>
AT4G03455.1	<i>mir447b</i>	targets several 2-phosphoglycerate kinase-related family members	8.0-fold up-regulated
AT3G26818.1	<i>mir169m</i>	targets several HAP2 family members.	8.0-fold up-regulated
AT5G62848.1	<i>mir420</i>	Not available	12.9-fold up-regulated
AT1G14071.1	<i>mir830a</i>	Not available	6.3-fold up-regulated
AT5G39693.1	<i>mir869a</i>	Not available	3.7-fold up-regulated
AT2G25011.1	<i>mir836a</i>	Not available	2.5-fold up-regulated
AT3G44444.1	<i>mir849a</i>	Not available	3.2-fold up-regulated

This thesis gave a first insight into the signal perception of CT, especially in the role of AtPARN. So far neither antibody-based approaches nor other methods such as Raman spectroscopy or imaging mass spectrometry were successful in visualizing CT. The development of new techniques for the production of antibodies against polysaccharides will help to answer questions about the production and localisation of CT (Rydahl et al., 2017). In the future, localisation experiments will also help to learn more about the function and the mode of action of the AtPARN protein. Co-immunoprecipitation experiments could help in the identification of interaction partners of AtPARN. Thanks to new techniques available, additional research can be performed on the role of RNA and in the plant-fungal interaction. Thus, targeted analysis of mRNA as well as untargeted approaches will help to study the effect of the PARN mutations on coding and ncRNAs. Especially the role of RNA with mitochondrial origin or mitochondrial translational sequences as well as miRNAs are promising targets.

III. Secretome Analysis

The establishment of a symbiosis requires a sophisticated communication between the respective partners. Hallmarks in the establishment of mycorrhiza are the regulation of plant defence and the modulation of cellular processes promoting colonisation. Typical signalling molecules are MAMPs such as chitin (Schmitz and Harrison, 2014), hormones such as auxin and cytokinin (Vadassery et al., 2008), defence-related hormones (Xu et al., 2018), and oligomers such as CT. In addition to these molecules, organisms release effector proteins which are essential for communication (Lo Presti and Kahmann, 2017; Liu et al., 2019).

Genome mining helped to identify the first symbiotic effector proteins, SP7 (Secreted Protein 7), produced by *R. irregularis* (Kloppholz et al., 2011) and MiSSP7 (Mycorrhiza induced Secreted Protein 7), from *L. bicolor* (Plett et al., 2011). Both small secreted proteins are translocated to the nucleus of host plants where they downregulate plant defence and subsequently enhance mycorrhiza. While SP7 interacts with ERF19 (Ethylene Response Factor 19) (Kloppholz et al., 2011), MiSSP7 interferes with JAZ (Jasmonate Zim-domain), a negative regulator of the JA pathway (Plett et al., 2011).

Gene expression data and *in silico* analyses were also used to predict effector proteins in *P. indica* (Zuccaro et al., 2011; Lahrmann and Zuccaro, 2012; Lahrmann et al., 2015). It was shown that *P. indicia* has approximately 1000 proteins with an N-terminal secretional sequence; more than half of these proteins are predicted effector proteins (Zuccaro et al., 2011; Rafiqi et al., 2013). Interestingly only 112 of these effector candidates are expressed during the colonisation of barley (Lahrmann et al., 2015). One of these genes, PIIN_08944, has been shown to be required for proper root colonisation; probably by interfering with the SA-dependent immune response (Akum et al., 2015). Some limitations exist for these *in silico*-based analyses, because only proteins which have certain features such as an N-terminal secretional sequence or a conserved motif (e.g. RXLR or DELD) are identified with this method (Liu et al., 2019). Since many of the proteins found in the secretome of plants do not possess these characteristics this can be a disadvantage for the identification of new effector proteins (Agrawal et al., 2010). In order to find new and unusual effector candidates, untargeted approaches are used. Proteome, transcriptome, and metabolome analyses produce a huge number of effector candidates, but it is unclear whether these proteins have a function outside the cell and whether they are transferred to their respective partner.

Furthermore, correlation between the transcriptome and proteome datasets can be quite weak. For example, Ghabooli et al. (2013) analysed the secretome of drought-stressed barley plants

and identified 37 differentially expressed proteins in the presence of *P. indica*. When the obtained proteome data were compared with RNA transcripts, a correlation for only two out of six of the studied genes was found (Ghabooli et al., 2013).

In order to overcome the limitation of untargeted -omics techniques and *in silico* analysis the focus of this thesis was the secretome of *P. indica* and *A. thaliana* (Thürich et al., 2018). The plant and the fungus were either cultivated alone or together in liquid media for three days (Figure 4). After filtration, the media were purified using solid phase extraction. Proteins were identified by liquid chromatography–tandem mass spectrometry. In total, 590 different *A. thaliana* and 164 *P. indica* proteins were identified in three biological replicates. While some proteins were found in all replicates, other were present only in one. Only proteins which were present in at least two out of three replicates and were found with a different frequency in the single and co-culture were used for further analyses. This was done in order to decrease the number of unspecific contaminants, such as the extremely abundant protein RuBisCo (Raven, 2013), which was found in all treatments. The fungal secretome contained 36 differentially secreted proteins out of which 34 were found predominantly in the co-culture. While some of them bear resemblance to degrading enzymes from other organisms, many of them have no predicted function and are uncharacterized to date. Thus, the list presented in this thesis is a starting point for future research on *P. indica* effector proteins. For example, PIIN_04899, was found in the co-culture, is a putative indole-3-acetaldehyde dehydrogenase, and might be involved in the formation of auxin. Another example is PIIN_05901: this uncharacterized protein is 260 amino acids long and was found in the co-culture. In transcriptome studies with barley it did not show any regulation (Zuccaro et al., 2011) but in a recent study with it was found in the secretome of the co-culture of *Brassica napus* and *P. indica* (Shrivastava et al., 2018).

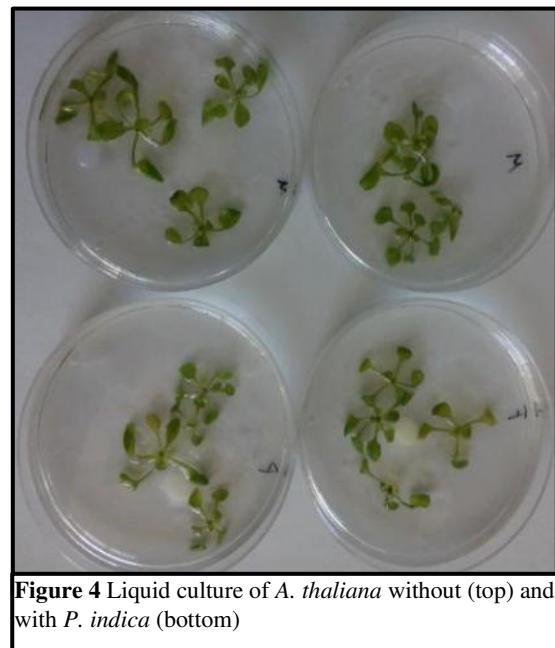
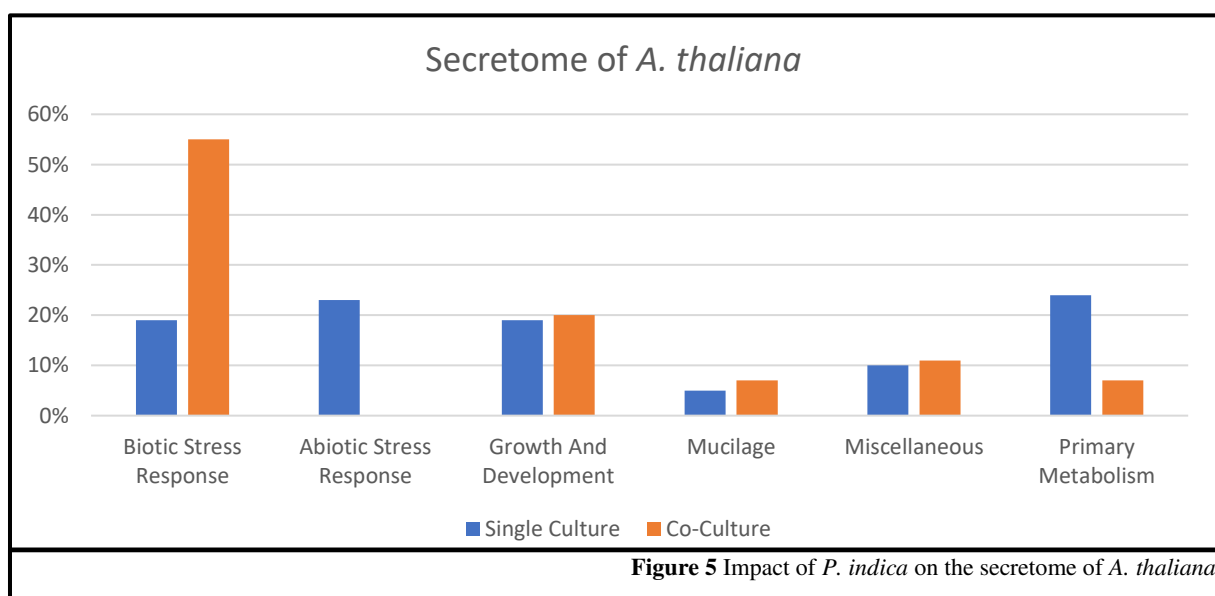


Figure 4 Liquid culture of *A. thaliana* without (top) and with *P. indica* (bottom)

Another main finding of this analysis was the strong impact of *P. indica* on *A. thaliana* plants cultivated with this fungus (Figure 5) (Thürich et al., 2018).

These results are in line with other studies that focused on the impact of *P. indica* on the transcriptome, proteome, or metabolome of the host (Schäfer et al., 2009; Alikhani et al., 2013; Kumar Bhuyan et al., 2015; Lahrmann et al., 2015). While almost no proteins associated with biotic stress were found in the single culture, many proteins with this function were found in the co-culture. Many of the proteins from the co-culture had a predicted secretional sequence and are associated with systemic acquired resistance (Thürich et al., 2018). Interestingly, several subtilisin-like proteases (SBT) and other proteins associated with mucilage were found in the supernatant of the co-culture. Mucilage is produced by plants and has diverse functions including maintenance of seed dormancy and lubrication during growth (Yang et al., 2012). In *M. truncatula*, expression of a subtilisin-like protease is induced by NOD factors (Taylor and Qiu, 2017). Furthermore, mucilage can induce branching of AMF hyphae or induce arbuscle formation (Nagahashi and Douds, 2004; Kaiser et al., 2015). The identification of mucilage associated proteins, such as SBT1.8, in the co-culture with *P. indica* will enable further insight into the role of mucilage in the non-mycorrhizal model plant *A. thaliana*.

In addition, several proteins associated with ER-bodies (Endoplasmic Reticulum) were found predominantly in the co-culture. ER-bodies are small structures which are derived from the ER network and are involved in innate defence reactions of *Brassicales* (Nakano et al., 2014). These rod-shaped organelles are found in specific tissues including epidermal, cortical, and endodermal cells of roots.



Inside ER-bodies huge quantities of the β -glucosidase PYK10 are found. Upon colonisation by nematodes and microbes PYK10 levels are increased in infected tissue. Interestingly, plants lacking PYK10 do not benefit from the interaction with *P. indica* compared to wild-type plants (Sherameti et al., 2008). Expression of *PYK10* is not influenced by *P. indica* and overaccumulation of *pyk10* mRNA does not influence colonisation of *P. indica* (Sherameti et al., 2008). Thus, it is unlikely that PYK10 itself is responsible for controlling growth. *In vitro* assays showed that PYK10 hydrolyses scopolin with highest specificity (Ahn et al., 2010). The coumarin scopolin and its aglycone scopoletin reduce growth of several pathogenic fungi including *F. oxysporum*, *Fusarium solani* (Peterson et al., 2003), and the endophytic fungus *P. indica* (Thürich et al., 2018). Furthermore, scopolin and scopoletin are involved in iron uptake (Nakano et al., 2014), shaping of the rhizosphere (Stringlis et al., 2018), and fine tuning of plant defence by scavenging of ROS (Kai et al., 2008; Ahn et al., 2010). The role of ROS as a key regulator in symbiosis with *P. indica* colonisation has been previously described (Jacobs et al., 2011; Nath et al., 2016). Another protein which was found in the secretome of the co-culture was PLAT1. PLAT1 is involved in the abiotic stress response and the protein has been shown to co-localise with ER-bodies (Hyun et al., 2015). The current hypothesis is that PLAT1 does not possess enzymatic activity on its own but supports other proteins, such as PYK10, by acting as a “docking-site” (Hyun et al., 2015). PLAT1 and its homologue PLAT2 are downregulated in roots colonised by *P. indica* at the 3rd and 7th dpi. In line with these results, *plat1* mutants are stronger colonised by *P. indica* at the 7th dpi (Thürich et al., 2018). Roots of wild-type plants colonised by *P. indica* have a significantly increased level of scopolin after two weeks, whereas this is not the case in *plat1* mutants (Thürich et al., 2018). Furthermore, the scopolin mutant *f6'h1* exhibited stronger colonisation by *P. indica*, which supports the hypothesis that scopolin controls the growth of the fungus. In order to confirm the hypothesis that PLAT1 and PYK10 are both involved in the formation of scopolin in ER-bodies, I studied the form and size of these organelles. While during the early phases of colonisation, no discernible difference was visible between colonised and mock-treated roots, a clear difference became apparent at the 7th dpi. ER-bodies in mock treated plants had the typical rod-shaped structure, while roots colonised by *P. indica* had ER-bodies with a dot-like structure and showed a diffuse fluorescence signal of an ER marker at the 7th dpi (Thürich et al., 2018). The diffuse signal could derive from dispersed ER-bodies. ER-bodies are formed locally and systemically after wounding in a JA dependent manner (Matsushima et al., 2002). A role of JA in AM has been proposed before (Hause et al., 2002) and the effect of *P. indica* on

phytohormones, in a phase-dependent manner, has been described as well (Lahrmann and Zuccaro, 2012).

The analysis of the secretome showed the impact of *P. indica* on *A. thaliana* plants cultivated with this fungus. This is in line with other studies that focused on the impact of *P. indica* on the transcriptome, proteome, or metabolome of the host (Schäfer et al., 2009; Alikhani et al., 2013; Kumar Bhuyan et al., 2015; Lahrmann et al., 2015). The analysis of selected proteins such as mucilage associated proteins can be fruitful for further experimental approaches. For example, I analysed the secretome after three days of co-cultivation in liquid media. An analysis of the secretome in solid media was not possible owing to the low amount of extractable proteins and technical constraints. New techniques, such as imaging mass spectrometry could help in further enquiries. In addition, a comparison of earlier and later time points during colonisation will be helpful to see the shift between the early recognition phase of both partners and the established symbiosis. Another possibility would be to alter the composition of the media for example by addition of a carbon source or plant-available phosphate, or the addition of additional pathogenic organisms.

The identification of ER-body associated proteins, such as PLAT1, in the secretome suggests that these organelles are involved in *P. indica* colonisation. Whether they are direct targets of the fungus or whether the observed effects are due to secondary effects should be analysed in future enquiries. Furthermore, the generation *plat1* and *plat2* double knock-out lines with GFP-tagged ER-bodies would help to study the connection between PLAT, ER-bodies and the defence compound scopolin.

Chapter 4:

Summary & Zusammenfassung

I Summary

The endophytic fungus *Piriformospora indica* can form beneficial interaction with many different plant species including *Arabidopsis thaliana*. This interaction has similarities to mycorrhiza, can improve the plant fitness, and can result in a higher biomass production. I focused on the perception of a novel signalling molecule, cellotriose, and the identification of symbiosis-specific (small) secreted proteins.

Cellotriose, a oligosaccharide which is most likely produced by *P. indica*, causes a strong and specific calcium signal in *A. thaliana*. I identified PARN, a poly(A) specific ribonuclease and showed that it is essential for calcium signal in response to cellotriose in *A. thaliana*. A single point mutation in the *PARN* gene completely abolishes the calcium response and the mutant phenotype is rescued after insertion of a function *PARN* gene into the *Arabidopsis* mutant. PARNs are conserved proteins which are involved in stress response and embryo development in animals, fungi, and plants.

In addition, I established a system to investigate the secretome of *P. indica* and *A. thaliana* during symbiosis. I identified plant and fungal proteins which are specifically secreted during the symbiosis and proteins which are no longer present in the secretome when the two symbionts grow together. Besides well well-known proteins involved in plant-microbial communication and biotic defence, I found several proteins which were not described in this context before. This includes proteins involved in the production of scopolin, the formation of the ER-body, and mucilage-related proteins. Using *Arabidopsis* mutants impaired in scopolin biosynthesis, I could show that the coumarin restricts growth of *P. indica* on agar plates, but the complete absence of this compound increases the colonisation level of the fungus in *Arabidopsis* roots. In addition, I showed that *P. indica* strongly affects the morphology of the ER-bodies, i.e. the organelles which are involved in the production of different defence-related secondary compounds including scopolin. I found, that during the early phase of colonisation, the ER-bodies have a reduced size. This effect is reversed once the interaction is established. Finally, symbiosis-specific exudate fractions contain elevated levels of plant-derived proteins involved in mucilage formation.

My investigation identified and initially characterised new players in the *P. indica* / *A. thaliana* root symbiosis which should be investigated in greater details to identify new ways of improving plant fitness.

II Zusammenfassung

Der endophytische Pilz *Piriformospora indica* bildet mykorrhiza-ähnliche Symbiosen mit verschiedenen Pflanzenarten. Kolonisierte Pflanzen können eine erhöhte Stressresistenz und eine höhere Biomasse haben. Ich habe die Interaktion zwischen *P. indica* und *Arabidopsis thaliana* untersucht und dabei besonderen Fokus auf die Erkennung und Weiterleitung von neuen Signalmoleküle, wie Cellotriose und die Identifikation von symbiosis-spezifischen sekretierten Proteinen gelegt. Cellotriose, ein Oligosaccharid welches vermutlich von *P. indica* produziert wird, induziert ein starkes und spezifisches Calcium-Signal in *A. thaliana*. Ich habe PARN, eine poly(A) spezifische Ribonuklease identifiziert und gezeigt, dass dieses Protein essenziell für die Kalziumsignalerkennung von Cellotriose ist. Eine einfache Punktmutation im *PARN* Gen kann diese spezifische Kalziumsignalweiterleitung komplett verhindern. Durch die Wiedereinführung des *PARN* Gens in das Genom von *A. thaliana* wird dieser Phänotyp wieder rückgängig gemacht. PARNs sind konservierte Proteine in Tieren, Pilzen und Pflanzen, die eine Rolle in Stressantwort und Embryonalentwicklung haben.

Weiterhin habe ich ein System etabliert, um das Sekretom von *P. indica* und *A. thaliana* während der gemeinsamen Kultivierung zu untersuchen. Ich habe viele Pflanzen- und Pilzproteine gefunden, die ausschließlich während der Symbiose sekretiert werden und Proteine die ausschließlich in der Einzelkultivierung von Pflanze und Pilz zu finden sind. Zusätzlich zu Proteinen, die für ihre Rolle in der biologischen Abwehr und der Kommunikation von Pflanzen mit Mikroben bekannt sind, habe ich weitere Proteine gefunden, die bisher nicht in diesem Kontext genannt wurden. Dazu gehören Proteine die in die Produktion von Scopolin, die Bildung von ER-Körpern involviert sind sowie mit Schleimstoffen interagieren. Mithilfe von *Arabidopsis* Mutanten, die in der Produktion von Scopolin gehemmt sind, konnte ich zeigen, dass dieses Kumarin *P. indica* nicht nur auf Agar-Platten hemmt, sondern auch das Wachstum des Pilzes in der Wurzel beeinflusst. Zusätzlich konnte ich zeigen, dass *P. indica* die Morphologie von ER-Körpern beeinflusst. Diese Organellen sind in die Bildung von Sekundärmetaboliten wie Scopolin involviert. Während der frühen Phase der Besiedlung durch *P. indica*, degradieren die ER-Körper– ein Prozess der später, sobald die Symbiose etabliert ist, revidiert wird. Außerdem enthält das Sekretom erhöhte Menge an Proteinen, die in die Bildung von Schleimstoffen involviert sind.

In dieser Arbeit habe ich verschiedene neue Komponenten identifiziert und untersucht die in die Interaktion zwischen *P. indica* und *A. thaliana* involviert sind und das Ziel für zukünftige Studien sein können.

References

- Agrawal, G.K., Jwa, N.-S., Lebrun, M.-H., Job, D., Rakwal, R., 2010. **Plant secretome: unlocking secrets of the secreted proteins**. *Proteomics* 10 (4), 799–827. 10.1002/pmic.200900514.
- Ahn, Y.O., Shimizu, B.-i., Sakata, K., Gantulga, D., Zhou, C., Zhou, Z., Bevan, D.R., Esen, A., 2010. **Scopolin-hydrolyzing beta-glucosidases in roots of Arabidopsis**. *Plant & cell physiology* 51 (1), 132–143. 10.1093/pcp/pcp174.
- Akum, F.N., Steinbrenner, J., Biedenkopf, D., Imani, J., Kogel, K.-H., 2015. **The *Piriformospora indica* effector PIIN_08944 promotes the mutualistic Sebacinalean symbiosis**. *Front Plant Sci* 6 (369), 1685. 10.3389/fpls.2015.00906.
- Alikhani, M., Khatabi, B., Sepehri, M., Nekouei, M.K., Mardi, M., Salekdeh, G.H., 2013. **A proteomics approach to study the molecular basis of enhanced salt tolerance in barley (*Hordeum vulgare* L.) conferred by the root mutualistic fungus *Piriformospora indica***. *Mol Biosyst* 9 (6), 1498–1510. 10.1039/c3mb70069k.
- Anith, K.N., Faseela, K.M., Archana, P.A., Prathapan, K.D., 2011. **Compatibility of *Piriformospora indica* and *Trichoderma harzianum* as dual inoculants in black pepper (*Piper nigrum* L.)**. *Symbiosis* 55 (1), 11–17. 10.1007/s13199-011-0143-1.
- Azcón-Aguilar, C., Barea, J.M., 1996. **Arbuscular mycorrhizas and biological control of soil-borne plant pathogens – an overview of the mechanisms involved**. *Mycorrhiza* (6), 457–464. 10.1007/s005720050147.
- Bakhshandeh, S., Corneo, P.E., Mariotte, P., Kertesz, M.A., Dijkstra, F.A., 2017. **Effect of crop rotation on mycorrhizal colonization and wheat yield under different fertilizer treatments**. *Agric Ecosyst Environ* 247, 130–136. 10.1016/j.agee.2017.06.027.
- Barazani, O., Benderoth, M., Groten, K., Kuhlemeier, C., Baldwin, I.T., 2005. ***Piriformospora indica* and *Sebacina vermifera* increase growth performance at the expense of herbivore resistance in *Nicotiana attenuata***. *Oecologia* 146 (2), 234–243. 10.1007/s00442-005-0193-2.
- Berndt, H., Harnisch, C., Rammelt, C., Stöhr, N., Zirkel, A., Dohm, J.C., Himmelbauer, H., Tavanez, J.-P., Hüttelmaier, S., Wahle, E., 2012. **Maturation of mammalian H/ACA box snoRNAs: PAPD5-dependent adenylation and PARN-dependent trimming**. *RNA* 18 (5), 958–972. 10.1261/rna.032292.112.
- Besserer, A., Puech-Pagès, V., Kiefer, P., Gomez-Roldan, V., Jauneau, A., Roy, S., Portais, J.-C., Roux, C., Bécard, G., Séjalon-Delmas, N., 2006. **Strigolactones stimulate arbuscular mycorrhizal fungi by activating mitochondria**. *PLoS Biol* 4 (7), e226. 10.1371/journal.pbio.0040226.
- Bonfante, P., Anca, I.-A., 2009. **Plants, mycorrhizal fungi, and bacteria: a network of interactions**. *Annu Rev Microbiol* 63, 363–383. 10.1146/annurev.micro.091208.073504.
- Bonfante, P., Genre, A., 2010. **Mechanisms underlying beneficial plant-fungus interactions in mycorrhizal symbiosis**. *Nat Commun* 1, 48. 10.1038/ncomms1046.
- Bonfante, P., Genre, A., 2015. **Arbuscular mycorrhizal dialogues: do you speak 'plantish' or 'fungish'?** *Trends Plant Sci* 20 (3), 150–154. 10.1016/j.tplants.2014.12.002.

- Bruisson, S., Maillot, P., Schellenbaum, P., Walter, B., Gindro, K., Deglène-Benbrahim, L., 2016. **Arbuscular mycorrhizal symbiosis stimulates key genes of the phenylpropanoid biosynthesis and stilbenoid production in grapevine leaves in response to downy mildew and grey mould infection.** *Phytochemistry* 131, 92–99. 10.1016/j.phytochem.2016.09.002.
- Cai, Q., Qiao, L., Wang, M., He, B., Lin, F.-M., Palmquist, J., Huang, S.-D., Jin, H., 2018. **Plants send small RNAs in extracellular vesicles to fungal pathogen to silence virulence genes.** *Science* 360 (6393), 1126–1129. 10.1126/science.aar4142.
- Chiapello, M., Perotto, S., Balestrini, R., 2015. **Symbiotic proteomics — state of the art in plant–mycorrhizal fungi interactions**, in: Magdeldin, S. (Ed.), *Recent Advances in Proteomics Research*. InTech, 10.5772/61331.
- Cook, C.E., Whichard, L.P., Turner, B., Wall, M.E., Egley, G.H., 1966. **Germination of witchweed (*Striga lutea* Lour.): isolation and properties of a potent stimulant.** *Science* 154 (3753), 1189–1190. 10.1126/science.154.3753.1189.
- Dakora, F.D., Phillips, D.A., 2002. **Root exudates as mediators of mineral acquisition in low-nutrient environments**, in: Adu-Gyamfi, J.J. (Ed.), *Food Security in Nutrient-Stressed Environments: Exploiting Plants' Genetic Capabilities*. Springer Netherlands, Dordrecht, pp. 201–213, 10.1023/A:1020809400075.
- Daneshkhah, R., Cabello, S., Rozanska, E., Sobczak, M., Grundler, F.M., Wieczorek, K., Hofmann, J., 2013. ***Piriformospora indica* antagonizes cyst nematode infection and development in Arabidopsis roots.** *J Exp Bot* 64 (12), 3763–3774. 10.1093/jxb/ert213.
- Das, A., Kamal, S., Shakil, N.A., Sherameti, I., Oelmüller, R., Dua, M., Tuteja, N., Johri, A.K., Varma, A., 2012. **The root endophyte fungus *Piriformospora indica* leads to early flowering, higher biomass and altered secondary metabolites of the medicinal plant, *Coleus forskohlii*.** *Plant Signal Behav* 7 (1), 103–112. 10.4161/psb.7.1.18472.
- Deshmukh, S.D., Hüchelhoven, R., Schäfer, P., Imani, J., Sharma, M., Weiss, M., Waller, F., Kogel, K.-H., 2006. **The root endophytic fungus *Piriformospora indica* requires host cell death for proliferation during mutualistic symbiosis with barley.** *Proc Natl Acad Sci U S A* 103 (49), 18450–18457. 10.1073/pnas.0605697103.
- Deshmukh, S.D., Kogel, K.-H., 2007. ***Piriformospora indica* protects barley from root rot caused by *Fusarium graminearum*.** *J Plant Dis Prot* (2006)114 (6), 263–268. 10.1007/BF03356227.
- Diédhiou, I., Diouf, D., 2018. **Transcription factors network in root endosymbiosis establishment and development.** *World J Microbiol Biotechnol* 34 (3), 37. 10.1007/s11274-018-2418-7.
- Dolatabadi, H.K., Goltapeh, E.M., Jaimand, K., Rohani, N., Varma, A., 2011. **Effects of *Piriformospora indica* and *Sebacina vermifera* on growth and yield of essential oil in fennel (*Foeniculum vulgare*) under greenhouse conditions.** *J Basic Microbiol* 51 (1), 33–39. 10.1002/jobm.201000214.
- Edel, K.H., Marchadier, E., Brownlee, C., Kudla, J., Hetherington, A.M., 2017. **The evolution of calcium-based signalling in plants.** *Curr Biol* 27 (13), R667-R679. 10.1016/j.cub.2017.05.020.

- Fakhro, A., Andrade-Linares, D.R., Bargen, S. von, Bandte, M., Büttner, C., Grosch, R., Schwarz, D., Franken, P., 2010. **Impact of *Piriformospora indica* on tomato growth and on interaction with fungal and viral pathogens.** Mycorrhiza 20 (3), 191–200. 10.1007/s00572-009-0279-5.
- Felle, H.H., Waller, F., Molitor, A., Kogel, K.-H., 2009. **The mycorrhiza fungus *Piriformospora indica* induces fast root-surface pH signaling and primes systemic alkalization of the leaf apoplast upon powdery mildew infection.** Mol Plant Microbe Interact 22 (9), 1179–1185. 10.1094/MPMI-22-9-1179.
- Fesel, P.H., Zuccaro, A., 2016. **Dissecting endophytic lifestyle along the parasitism/mutualism continuum in Arabidopsis.** Curr Opin Microbiol 32, 103–112. 10.1016/j.mib.2016.05.008.
- Franken, P., 2012. **The plant strengthening root endophyte *Piriformospora indica* : potential application and the biology behind.** Appl Microbiol Biotechnol 96 (6), 1455–1464. 10.1007/s00253-012-4506-1.
- Genre, A., Chabaud, M., Balzergue, C., Puech-Pagès, V., Novero, M., Rey, T., Fournier, J., Rochange, S., Bécard, G., Bonfante, P., Barker, D.G., 2013. **Short-chain chitin oligomers from arbuscular mycorrhizal fungi trigger nuclear Ca^{2+} spiking in *Medicago truncatula* roots and their production is enhanced by strigolactone.** New Phytol 198 (1), 190–202. 10.1111/nph.12146.
- Ghabooli, M., Khatabi, B., Ahmadi, F.S., Sepehri, M., Mirzaei, M., Amirkhani, A., Jorrín-Novo, J.V., Salekdeh, G.H., 2013. **Proteomics study reveals the molecular mechanisms underlying water stress tolerance induced by *Piriformospora indica* in barley.** J Proteomics 94, 289–301. 10.1016/j.jprot.2013.09.017.
- Glaeser, S.P., Imani, J., Alabid, I., Guo, H., Kumar, N., Kämpfer, P., Hardt, M., Blom, J., Goesmann, A., Rothballer, M., Hartmann, A., Kogel, K.-H., 2016. **Non-pathogenic *Rhizobium radiobacter* F4 deploys plant beneficial activity independent of its host *Piriformospora indica*.** ISME J 10 (4), 871–884. 10.1038/ismej.2015.163.
- Gobbato, E., Wang, E., Higgins, G., Bano, S.A., Henry, C., Schultze, M., Oldroyd, G.E.D., 2013. **RAM1 and RAM2 function and expression during arbuscular mycorrhizal symbiosis and *Aphanomyces euteiches* colonization.** Plant Signal Behav 8 (10), 10.4161/psb.26049.
- González-Guerrero, M., Azcón-Aguilar, C., Mooney, M., Valderas, A., MacDiarmid, C.W., Eide, D.J., Ferrol, N., 2005. **Characterization of a *Glomus intraradices* gene encoding a putative Zn transporter of the cation diffusion facilitator family.** Fungal Genet Biol 42 (2), 130–140. 10.1016/j.fgb.2004.10.007.
- Gough, C., Cottret, L., Lefebvre, B., Bono, J.-J., 2018. **Evolutionary history of plant LysM receptor proteins related to root endosymbiosis.** Front Plant Sci 9, 923. 10.3389/fpls.2018.00923.
- Govindarajulu, M., Pfeffer, P.E., Jin, H., Abubaker, J., Douds, D.D., Allen, J.W., Bücking, H., Lammers, P.J., Shachar-Hill, Y., 2005. **Nitrogen transfer in the arbuscular mycorrhizal symbiosis.** Nature 435 (7043), 819–823. 10.1038/nature03610.

- Guether, M., Neuhäuser, B., Balestrini, R., Dynowski, M., Ludewig, U., Bonfante, P., 2009. **A mycorrhizal-specific ammonium transporter from *Lotus japonicus* acquires nitrogen released by arbuscular mycorrhizal fungi.** *Plant Physiol* 150 (1), 73–83. 10.1104/pp.109.136390.
- Guo, B., Sato, N., Biely, P., Amano, Y., Nozaki, K., 2016. **Comparison of catalytic properties of multiple beta-glucosidases of *Trichoderma reesei*.** *Appl Microbiol Biotechnol* 100 (11), 4959–4968. 10.1007/s00253-016-7342-x.
- Hause, B., Maier, W., Miersch, O., Kramell, R., Strack, D., 2002. **Induction of jasmonate biosynthesis in arbuscular mycorrhizal barley roots.** *Plant Physiol* 130 (3), 1213–1220. 10.1104/pp.006007.
- Herridge, R.P., Day, R.C., Macknight, R.C., 2014. **The role of the MCM2-7 helicase complex during Arabidopsis seed development.** *Plant Mol Biol* 86 (1-2), 69–84. 10.1007/s11103-014-0213-x.
- Hilbert, M., Voll, L.M., Ding, Y., Hofmann, J., Sharma, M., Zuccaro, A., 2012. **Indole derivative production by the root endophyte *Piriformospora indica* is not required for growth promotion but for biotrophic colonization of barley roots.** *New Phytol* 196 (2), 520–534. 10.1111/j.1469-8137.2012.04275.x.
- Hildebrandt, U., Janetta, K., Bothe, H., 2002. **Towards growth of arbuscular mycorrhizal fungi independent of a plant host.** *Appl Environ Microbiol* 68 (4), 1919–1924. 10.1128/AEM.68.4.1919-1924.2002.
- Hirayama, T., 2014. **A unique system for regulating mitochondrial mRNA poly(A) status and stability in plants.** *Plant Signal Behav* 9 (10), e973809. 10.4161/15592324.2014.973809.
- Hirayama, T., Matsuura, T., Ushiyama, S., Narusaka, M., Kurihara, Y., Yasuda, M., Ohtani, M., Seki, M., Demura, T., Nakashita, H., Narusaka, Y., Hayashi, S., 2013. **A poly(A)-specific ribonuclease directly regulates the poly(A) status of mitochondrial mRNA in Arabidopsis.** *Nat Commun* 4, 2247. 10.1038/ncomms3247.
- Hirsch, A.M., Bauer, W.D., Bird, D.M., Cullimore, J., Tyler, B., Yoder, J.I., 2003. **Molecular signals and receptors: controlling rhizosphere interactions between plants and other organisms.** *Ecology* 84 (4), 858–868. 10.1890/0012-9658(2003)084[0858:MSARCR]2.0.CO;2.
- Hui, F., Liu, J., Gao, Q., Lou, B., 2015. ***Piriformospora indica* confers cadmium tolerance in *Nicotiana tabacum*.** *J Environ Sci (China)* 37, 184–191. 10.1016/j.jes.2015.06.005.
- Husaini, A.M., Abdin, M.Z., Khan, S., Xu, Y.W., Aquil, S., Anis, M., 2012. **Modifying strawberry for better adaptability to adverse impact of climate change.** *Curr Sci India* (102), 1660–1673.
- Hyun, T.K., Albacete, A., van der Graaff, E., Eom, S.H., Grosskinsky, D.K., Bohm, H., Janschek, U., Rim, Y., Ali, W.W., Kim, S.Y., Roitsch, T., 2015. **The Arabidopsis PLAT domain protein1 promotes abiotic stress tolerance and growth in tobacco.** *Transgenic Res* 24 (4), 651–663. 10.1007/s11248-015-9868-6.

- Jacobs, S., Zechmann, B., Molitor, A., Trujillo, M., Petutschnig, E., Lipka, V., Likpa, V., Kogel, K.-H., Schäfer, P., 2011. **Broad-spectrum suppression of innate immunity is required for colonization of Arabidopsis roots by the fungus *Piriformospora indica***. Plant Physiol 156 (2), 726–740. 10.1104/pp.111.176446.
- Javot, H., Penmetsa, R.V., Terzaghi, N., Cook, D.R., Harrison, M.J., 2007a. **A *Medicago truncatula* phosphate transporter indispensable for the arbuscular mycorrhizal symbiosis**. Proc Natl Acad Sci U S A 104 (5), 1720–1725. 10.1073/pnas.0608136104.
- Javot, H., Pumplin, N., Harrison, M.J., 2007b. **Phosphate in the arbuscular mycorrhizal symbiosis: transport properties and regulatory roles**. Plant Cell Environ 30 (3), 310–322. 10.1111/j.1365-3040.2006.01617.x.
- Johnson, J.M., 2009. ***Piriformospora indica* released factors and its role in the molecular interaction with Arabidopsis thaliana**. Dissertation, Universität Jena
- Johnson, J.M., Sherameti, I., Ludwig, A., Nongbri, P.L., Sun, C., Lou, B., Varma, A., Oelmüller, R., 2011. **Protocols for Arabidopsis thaliana and Piriformospora indica co-cultivation – a model system to study plant beneficial traits**. Endocytobiosis Cell Res, 101–113.
- Johnson, J.M., Thürich, J., Petutschnig, E.K., Altschmied, L., Meichsner, D., Sherameti, I., Dindas, J., Mrozinska, A., Paetz, C., Scholz, S.S., Furch, A.C., Lipka, V., Hedrich, R., Schneider, B., Svatoš, A., Oelmüller, R., 2018. **A poly(A) ribonuclease controls the cellotriose-based interaction between Piriformospora indica and its host Arabidopsis**. Plant Physiol. 10.1104/pp.17.01423.
- Kai, K., Mizutani, M., Kawamura, N., Yamamoto, R., Tamai, M., Yamaguchi, H., Sakata, K., Shimizu, B.-i., 2008. **Scopoletin is biosynthesized via ortho-hydroxylation of feruloyl CoA by a 2-oxoglutarate-dependent dioxygenase in Arabidopsis thaliana**. Plant J 55 (6), 989–999. 10.1111/j.1365-313X.2008.03568.x.
- Kaiser, C., Kilburn, M.R., Clode, P.L., Fuchslueger, L., Koranda, M., Cliff, J.B., Solaiman, Z.M., Murphy, D.V., 2015. **Exploring the transfer of recent plant photosynthates to soil microbes: mycorrhizal pathway vs direct root exudation**. New Phytol 205 (4), 1537–1551. 10.1111/nph.13138.
- Kaldorf, M., Koch, B., Rexer, K.-H., Kost, G., Varma, A., 2005. **Patterns of interaction between populus Esch5 and Piriformospora indica : a transition from mutualism to antagonism**. Plant Biol (Stuttg) 7 (2), 210–218. 10.1055/s-2005-837470.
- Kari Dolatabadi, H., Mohammadi Goltapeh, E., Mohammadi, N., Rabiey, M., Rohani, N., Varma, A., 2012. **Biocontrol potential of root endophytic fungi and trichoderma species against fusarium wilt of lentil under in vitro and greenhouse conditions**. J. Agric. Sci. Technol 14 (2), 407–420.
- Kloppholz, S., Kuhn, H., Requena, N., 2011. **A secreted fungal effector of Glomus intraradices promotes symbiotic biotrophy**. Curr Biol 21 (14), 1204–1209. 10.1016/j.cub.2011.06.044.

- Kosuta, S., Chabaud, M., Loughon, G., Gough, C., Dénarié, J., Barker, D.G., Bécard, G., 2003. **A diffusible factor from arbuscular mycorrhizal fungi induces symbiosis-specific MtENOD11 expression in roots of *Medicago truncatula***. *Plant Physiol* 131 (3), 952–962. 10.1104/pp.011882.
- Kosuta, S., Hazledine, S., Sun, J., Miwa, H., Morris, R.J., Downie, J.A., Oldroyd, G.E.D., 2008. **Differential and chaotic calcium signatures in the symbiosis signaling pathway of legumes**. *Proc Natl Acad Sci U S A* 105 (28), 9823–9828. 10.1073/pnas.0803499105.
- Kumar, M., Yadav, V., Kumar, H., Sharma, R., Singh, A., Tuteja, N., Johri, A.K., 2014. ***Piriformospora indica* enhances plant growth by transferring phosphate**. *Plant Signal Behav* 6 (5), 723–725. 10.4161/psb.6.5.15106.
- Kumar, M., Yadav, V., Tuteja, N., Johri, A.K., 2009. **Antioxidant enzyme activities in maize plants colonized with *Piriformospora indica***. *Microbiology* 155 (Pt 3), 780–790. 10.1099/mic.0.019869-0.
- Kumar, V., Sarma, M.V.R.K., Saharan, K., Srivastava, R., Kumar, L., Sahai, V., Bisaria, V.S., Sharma, A.K., 2012. **Effect of formulated root endophytic fungus *Piriformospora indica* and plant growth promoting rhizobacteria fluorescent pseudomonads R62 and R81 on *Vigna mungo***. *World J Microbiol Biotechnol* 28 (2), 595–603. 10.1007/s11274-011-0852-x.
- Kumar Bhuyan, S., Bandyopadhyay, P., Kumar, P., Kumar Mishra, D., Prasad, R., Kumari, A., Chandra Upadhyaya, K., Varma, A., Kumar Yadava, P., 2015. **Interaction of *Piriformospora indica* with *Azotobacter chroococcum***. *Sci Rep* 5, 13911. 10.1038/srep13911.
- Lahrmann, U., Ding, Y., Banhara, A., Rath, M., Hajirezaei, M.R., Dohlemann, S., Wiren, N. von, Parniske, M., Zuccaro, A., 2013. **Host-related metabolic cues affect colonization strategies of a root endophyte**. *Proc Natl Acad Sci U S A* 110 (34), 13965–13970. 10.1073/pnas.1301653110.
- Lahrmann, U., Strehmel, N., Langen, G., Frerigmann, H., Leson, L., Ding, Y., Scheel, D., Herklotz, S., Hilbert, M., Zuccaro, A., 2015. **Mutualistic root endophytism is not associated with the reduction of saprotrophic traits and requires a noncompromised plant innate immunity**. *New Phytol.* 10.1111/nph.13411.
- Lahrmann, U., Zuccaro, A., 2012. **Opprimo ergo sum - evasion and suppression in the root endophytic fungus *Piriformospora indica***. *Mol Plant Microbe Interact* 25 (6), 727–737. 10.1094/MPMI-11-11-0291.
- Lee, Y.C., Johnson, J.M., Chien, C.T., Sun, C., Cai, D., Lou, B., Oelmüller, R., Yeh, K.W., 2011. **Growth promotion of Chinese cabbage and *Arabidopsis* by *Piriformospora indica* is not stimulated by mycelium-synthesized auxin**. *Mol Plant Microbe Interact* 24 (4), 421–431. 10.1094/MPMI-05-10-0110.
- Lelandais-Brière, C., Moreau, J., Hartmann, C., Crespi, M., 2016. **Noncoding RNAs, emerging regulators in root endosymbioses**. *Mol Plant Microbe Interact* 29 (3), 170–180. 10.1094/MPMI-10-15-0240-FI.

- Lenoir, I., Fontaine, J., Lounès-Hadj Sahraoui, A., 2016. **Arbuscular mycorrhizal fungal responses to abiotic stresses: a review**. *Phytochemistry* 123, 4–15. 10.1016/j.phytochem.2016.01.002.
- Li, L., Li, L., Wang, X., Zhu, P., Wu, H., Qi, S., 2017. **Plant growth-promoting endophyte *Piriformospora indica* alleviates salinity stress in *Medicago truncatula***. *Plant Physiol Biochem* 119, 211–223. 10.1016/j.plaphy.2017.08.029.
- Liang, Y., Tóth, K., Cao, Y., Tanaka, K., Espinoza, C., Stacey, G., 2014. **Lipochitooligosaccharide recognition: an ancient story**. *New Phytol* 204 (2), 289–296. 10.1111/nph.12898.
- Liu, L., Le Xu, Jia, Q., Pan, R., Oelmüller, R., Zhang, W., Wu, C., 2019. **Arms race: diverse effector proteins with conserved motifs**. *Plant Signal Behav* 14 (2), 1557008. 10.1080/15592324.2018.1557008.
- Liu, T., Liu, Z., Song, C., Hu, Y., Han, Z., She, J., Fan, F., Wang, J., Jin, C., Chang, J., Zhou, J.-M., Chai, J., 2012. **Chitin-induced dimerization activates a plant immune receptor**. *Science* 336 (6085), 1160–1164. 10.1126/science.1218867.
- Liu, Y., Feng, X., Gao, P., Li, Y., Christensen, M.J., Duan, T., 2018. **Arbuscular mycorrhiza fungi increased the susceptibility of *Astragalus adsurgens* to powdery mildew caused by *Erysiphe pisi***. *Mycology* 9 (3), 223–232. 10.1080/21501203.2018.1477849.
- Lo Presti, L., Kahmann, R., 2017. **How filamentous plant pathogen effectors are translocated to host cells**. *Curr Opin Plant Biol* 38, 19–24. 10.1016/j.pbi.2017.04.005.
- Maillet, F., Poinot, V., André, O., Puech-Pagès, V., Haouy, A., Gueunier, M., Cromer, L., Giraudet, D., Formey, D., Niebel, A., Martinez, E.A., Driguez, H., Bécard, G., Dénarié, J., 2011. **Fungal lipochitooligosaccharide symbiotic signals in arbuscular mycorrhiza**. *Nature* 469 (7328), 58–63. 10.1038/nature09622.
- Mandal, S.M., Chakraborty, D., Dey, S., 2010. **Phenolic acids act as signaling molecules in plant-microbe symbioses**. *Plant Signal Behav* 5 (4), 359–368. 10.4161/psb.5.4.10871.
- Mariotte, P., Mehrabi, Z., Bezemer, T.M., Deyn, G.B. de, Kulmatiski, A., Drigo, B., Veen, G.F.C., van der Heijden, M.G.A., Kardol, P., 2018. **Plant-soil feedback: bridging natural and agricultural sciences**. *Trends Ecol Evol* 33 (2), 129–142. 10.1016/j.tree.2017.11.005.
- Martin, F., Nehls, U., 2009. **Harnessing ectomycorrhizal genomics for ecological insights**. *Curr Opin Plant Biol* 12 (4), 508–515. 10.1016/j.pbi.2009.05.007.
- Martin, J.K., Merckx, R., 1992. **The partitioning of photosynthetically fixed carbon within the rhizosphere of mature wheat**. *Soil Biol Biochem* 24 (11), 1147–1156. 10.1016/0038-0717(92)90065-6.
- Matsushima, R., Hayashi, Y., Kondo, M., Shimada, T., Nishimura, M., Hara-Nishimura, I., 2002. **An endoplasmic reticulum-derived structure that is induced under stress conditions in *Arabidopsis***. *Plant Physiol* 130 (4), 1807–1814. 10.1104/pp.009464.

- Meena, K.K., Mesapogu, S., Kumar, M., Yandigeri, M.S., Singh, G., Saxena, A.K., 2010. **Co-inoculation of the endophytic fungus *Piriformospora indica* with the phosphate-solubilising bacterium *Pseudomonas striata* affects population dynamics and plant growth in chickpea.** Biol Fertil Soils 46 (2), 169–174. 10.1007/s00374-009-0421-8.
- Meimoun, P., Vidal, G., Bohrer, A.-S., Lehner, A., Tran, D., Briand, J., Bouteau, F., Rona, J.-P., 2009. **Intracellular Ca^{2+} stores could participate to abscisic acid-induced depolarization and stomatal closure in *Arabidopsis thaliana*.** Plant Signal Behav 4 (9), 830–835.
- Michal Johnson, J., Reichelt, M., Vadassery, J., Gershenzon, J., Oelmuller, R., 2014. **An *Arabidopsis* mutant impaired in intracellular calcium elevation is sensitive to biotic and abiotic stress.** BMC Plant Biol 14, 162. 10.1186/1471-2229-14-162.
- Miller, R.M., Jastrow, J.D., Reinhardt, D.R., 1995. **External hyphal production of vesicular-arbuscular mycorrhizal fungi in pasture and tallgrass prairie communities.** Oecologia 103 (1), 17–23. 10.1007/BF00328420.
- Miransari, M., 2010. **Contribution of arbuscular mycorrhizal symbiosis to plant growth under different types of soil stress.** Plant Biol (Stuttg) 12 (4), 563–569. 10.1111/j.1438-8677.2009.00308.x.
- Musselman, L.J., 1980. **The biology of striga, orobanche, and other root-parasitic weeds.** Annu Rev Phytopathol 18 (1), 463–489. 10.1146/annurev.py.18.090180.002335.
- Mustafa, G., Khong, N.G., Tisserant, B., Randoux, B., Fontaine, J., Magnin-Robert, M., Reignault, P., Sahraoui, A.L.-H., 2017. **Defence mechanisms associated with mycorrhiza-induced resistance in wheat against powdery mildew.** Funct Plant Biol. 44 (4), 443. 10.1071/FP16206.
- Nagahashi, G., Douds, D.D., 2004. **Isolated root caps, border cells, and mucilage from host roots stimulate hyphal branching of the arbuscular mycorrhizal fungus, *Gigaspora gigantea*.** Mycol Res 108 (Pt 9), 1079–1088.
- Nakano, R.T., Yamada, K., Bednarek, P., Nishimura, M., Hara-Nishimura, I., 2014. **ER bodies in plants of the Brassicales order: biogenesis and association with innate immunity.** Front Plant Sci 5, 73. 10.3389/fpls.2014.00073.
- Nanda, R., Agrawal, V., 2018. ***Piriformospora indica*, an excellent system for heavy metal sequestration and amelioration of oxidative stress and DNA damage in *Cassia angustifolia* Vahl under copper stress.** Ecotoxicol Environ Saf 156, 409–419. 10.1016/j.ecoenv.2018.03.016.
- Narayan, O.P., Verma, N., Singh, A.K., Oelmuller, R., Kumar, M., Prasad, D., Kapoor, R., Dua, M., Johri, A.K., 2017. **Antioxidant enzymes in chickpea colonized by *Piriformospora indica* participate in defense against the pathogen *Botrytis cinerea*.** Sci Rep 7 (1), 13553. 10.1038/s41598-017-12944-w.
- Nath, M., Bhatt, D., Prasad, R., Gill, S.S., Anjum, N.A., Tuteja, N., 2016. **Reactive oxygen species generation-scavenging and signaling during plant-arbuscular mycorrhizal and *Piriformospora indica* interaction under stress condition.** Front Plant Sci 7, 1574. 10.3389/fpls.2016.01574.

- Nautiyal, C.S., Chauhan, P.S., DasGupta, S.M., Seem, K., Varma, A., Staddon, W.J., 2010. **Tripartite interactions among *Paenibacillus lentimorbus* NRRL B-30488, *Piriformospora indica* DSM 11827, and *Cicer arietinum* L.** World J Microbiol Biotechnol 26 (8), 1393–1399. 10.1007/s11274-010-0312-z.
- Navazio, L., Moscatiello, R., Genre, A., Novero, M., Baldan, B., Bonfante, P., Mariani, P., 2007. **A diffusible signal from arbuscular mycorrhizal fungi elicits a transient cytosolic calcium elevation in host plant cells.** Plant Physiol 144 (2), 673–681. 10.1104/pp.106.086959.
- Nishimura, N., Kitahata, N., Seki, M., Narusaka, Y., Narusaka, M., Kuromori, T., Asami, T., Shinozaki, K., Hirayama, T., 2005. **Analysis of ABA hypersensitive germination2 revealed the pivotal functions of PARN in stress response in Arabidopsis.** Plant J 44 (6), 972–984. 10.1111/j.1365-313X.2005.02589.x.
- Nongbri, P.L., Vahabi, K., Mrozinska, A., Seebald, E., Sun, C., Sherameti, I., Johnson, J.M., Oelmüller, R., 2012. **Balancing defense and growth – analyses of the beneficial symbiosis between *Piriformospora indica* and *Arabidopsis thaliana*.** Symbiosis 58 (1-3), 17–28. 10.1007/s13199-012-0209-8.
- Ohtaka, N., Narisawa, K., 2008. **Molecular characterization and endophytic nature of the root-associated fungus *Meliniomyces variabilis* (LtVB3).** J Gen Plant Pathol 74 (1), 24–31. 10.1007/s10327-007-0046-4.
- Oláh, B., Brière, C., Bécard, G., Dénarié, J., Gough, C., 2005. **Nod factors and a diffusible factor from arbuscular mycorrhizal fungi stimulate lateral root formation in *Medicago truncatula* via the DMI1/DMI2 signalling pathway.** Plant J 44 (2), 195–207. 10.1111/j.1365-313X.2005.02522.x.
- Oldroyd, G.E.D., 2013. **Speak, friend, and enter: signalling systems that promote beneficial symbiotic associations in plants.** Nat Rev Microbiol 11 (4), 252–263. 10.1038/nrmicro2990.
- Parniske, M., 2008. **Arbuscular mycorrhiza: The mother of plant root endosymbioses.** Nat Rev Microbiol 6 (10), 763–775. 10.1038/nrmicro1987.
- Peck, M.C., Fisher, R.F., Long, S.R., 2006. **Diverse flavonoids stimulate NodD1 binding to nod gene promoters in *Sinorhizobium meliloti*.** J Bacteriol 188 (15), 5417–5427. 10.1128/JB.00376-06.
- Perotto, S., Daghino, S., Martino, E., 2018. **Ericoid mycorrhizal fungi and their genomes: another side to the mycorrhizal symbiosis?** New Phytol 220 (4), 1141–1147. 10.1111/nph.15218.
- Peskan-Berghofer, T., Shahollari, B., Giong, P.H., Hehl, S., Markert, C., Blanke, V., Kost, G., Varma, A., Oelmüller, R., 2004. **Association of *Piriformospora indica* with *Arabidopsis thaliana* roots represents a novel system to study beneficial plant-microbe interactions and involves early plant protein modifications in the endoplasmic reticulum and at the plasma membrane.** Physiol Plant 122 (4), 465–477. 10.1111/j.1399-3054.2004.00424.x.

- Peskan-Berghöfer, T., Vilches-Barro, A., Müller, T.M., Glawischnig, E., Reichelt, M., Gershenzon, J., Rausch, T., 2015. **Sustained exposure to abscisic acid enhances the colonization potential of the mutualist fungus *Piriformospora indica* on *Arabidopsis thaliana* roots.** New Phytol. 10.1111/nph.13504.
- Peterson, J.K., Harrison, H.F., Jackson, D.M., Snook, M.E., 2003. **Biological activities and contents of scopolin and scopoletin in sweetpotato clones.** HortScience 38 (6), 1129–1133.
- Petrini O. (1991) **Fungal Endophytes of Tree Leaves.** In: Andrews J.H., Hirano S.S. (eds) Microbial Ecology of Leaves. Brock/Springer Series in Contemporary Bioscience. Springer, New York, NY. 10.1007/978-1-4612-3168-4_9
- Pinochet, J., Calvet, C., Camprubl A. and C. FernAndez, 1996. **Interactions between migratory endoparasitic nematodes and arbuscular mycorrhizal fungi in perennial crops: A review.** Plant Soil (185), 183–190. 10.1007/BF02257523.
- Plett, J.M., Kemppainen, M., Kale, S.D., Kohler, A., Legué, V., Brun, A., Tyler, B.M., Pardo, A.G., Martin, F., 2011. **A secreted effector protein of *Laccaria bicolor* is required for symbiosis development.** Curr Biol 21 (14), 1197–1203. 10.1016/j.cub.2011.05.033.
- Rafiqi, M., Jelonek, L., Akum, N.F., Zhang, F., Kogel, K.-H., 2013. **Effector candidates in the secretome of *Piriformospora indica* , a ubiquitous plant-associated fungus.** Front Plant Sci 4, 228. 10.3389/fpls.2013.00228.
- Rai, M., Acharya, D., Singh, A., Varma, A., 2001. **Positive growth responses of the medicinal plants *Spilanthes calva* and *Withania somnifera* to inoculation by *Piriformospora indica* in a field trial.** Mycorrhiza 11 (3), 123–128. 10.1007/s005720100115.
- Rai, M., Varma, A., 2005. **Arbuscular mycorrhiza-like biotechnological potential of *Piriformospora indica* , which promotes the growth of *Adhatoda vasica* Nees.** Electron J Biotechnol 8 (1). 10.2225/vol8-issue1-fulltext-5.
- Rathod, P.D., Shao, H., Brestic, M., 2011. **Chlorophyll A fluorescence determines the drought resistance capabilities in two varieties of mycorrhized and non-mycorrhized *Glycine max* Linn.** Afr J Microbiol Res. 5 (24). 10.5897/AJMR11.737.
- Raven, J.A., 2013. **RuBisco: still the most abundant protein of Earth?** New Phytol 198 (1), 1–3. 10.1111/nph.12197.
- Redecker, D., 2000. **Glomalean fungi from the ordovician.** Science 289 (5486), 1920–1921. 10.1126/science.289.5486.1920.
- Remy, W., Taylor, T.N., Hass, H., Kerp, H., 1994. **Four hundred-million-year-old vesicular arbuscular mycorrhizae.** Proc Natl Acad Sci U S A 91 (25), 11841–11843. 10.1073/pnas.91.25.11841.
- Reverdatto, S.V., Dutko, J.A., Chekanova, J.A., Hamilton, D.A., Belostotsky, D.A., 2004. **mRNA deadenylation by PARN is essential for embryogenesis in higher plants.** RNA 10 (8), 1200–1214. 10.1261/rna.7540204.
- Rich, M.K., Nouri, E., Courty, P.-E., Reinhardt, D., 2017. **Diet of arbuscular mycorrhizal fungi: bread and butter?** Trends Plant Sci 22 (8), 652–660. 10.1016/j.tplants.2017.05.008.

- Ruyter-Spira, C., Al-Babili, S., van der Krol, S., Bouwmeester, H., 2013. **The biology of strigolactones**. Trends Plant Sci 18 (2), 72–83. 10.1016/j.tplants.2012.10.003.
- Rydahl, M.G., Krac Un, S.K., Fangel, J.U., Michel, G., Guillouzo, A., Génicot, S., Mravec, J., Harholt, J., Wilkens, C., Motawia, M.S., Svensson, B., Tranquet, O., Ralet, M.-C., Jørgensen, B., Domozych, D.S., Willats, W.G.T., 2017. **Development of novel monoclonal antibodies against starch and ulvan - implications for antibody production against polysaccharides with limited immunogenicity**. Sci Rep 7 (1), 9326. 10.1038/s41598-017-04307-2.
- Saddique, M.A.B., Ali, Z., Khan, A.S., Rana, I.A., Shamsi, I.H., 2018. **Inoculation with the endophyte *Piriformospora indica* significantly affects mechanisms involved in osmotic stress in rice**. Rice (N Y) 11 (1), 34. 10.1186/s12284-018-0226-1.
- Sarma, M.V.R.K., Kumar, V., Saharan, K., Srivastava, R., Sharma, A.K., Prakash, A., Sahai, V., Bisaria, V.S., 2011. **Application of inorganic carrier-based formulations of fluorescent pseudomonads and *Piriformospora indica* on tomato plants and evaluation of their efficacy**. J Appl Microbiol 111 (2), 456–466. 10.1111/j.1365-2672.2011.05062.x.
- Satheesan, J., Narayanan, A.K., Sakunthala, M., 2012. **Induction of root colonization by *Piriformospora indica* leads to enhanced asiaticoside production in *Centella asiatica***. Mycorrhiza 22 (3), 195–202. 10.1007/s00572-011-0394-y.
- Schäfer, P., Pfiffi, S., Voll, L.M., Zajic, D., Chandler, P.M., Waller, F., Scholz, U., Pons-Kühnemann, J., Sonnewald, S., Sonnewald, U., Kogel, K.-H., 2009. **Manipulation of plant innate immunity and gibberellin as factor of compatibility in the mutualistic association of barley roots with *Piriformospora indica***. Plant J 59 (3), 461–474. 10.1111/j.1365-313X.2009.03887.x.
- Schlegel, M., Münsterkötter, M., Güldener, U., Bruggmann, R., Duò, A., Hainaut, M., Henrissat, B., Sieber, C.M.K., Hoffmeister, D., Grünig, C.R., 2016. **Globally distributed root endophyte *Phialocephala subalpina* links pathogenic and saprophytic lifestyles**. BMC Genomics 17 (1), 1015. 10.1186/s12864-016-3369-8.
- Schmitz, A.M., Harrison, M.J., 2014. **Signaling events during initiation of arbuscular mycorrhizal symbiosis**. J Integr Plant Biol 56 (3), 250–261. 10.1111/jipb.12155.
- Serfling, A., Wirsal, Stefan G.R., Lind, V., Deising, H.B., 2007. **Performance of the biocontrol fungus *Piriformospora indica* on wheat under greenhouse and field conditions**. Phytopathology 97 (4), 523–531. 10.1094/PHYTO-97-4-0523.
- Sharma, G., Agrawal, V., 2013. **Marked enhancement in the artemisinin content and biomass productivity in *Artemisia annua* L. shoots co-cultivated with *Piriformospora indica***. World J Microbiol Biotechnol 29 (6), 1133–1138. 10.1007/s11274-013-1263-y.
- Sherameti, I., Shahollari, B., Venus, Y., Altschmied, L., Varma, A., Oelmüller, R., 2005. **The endophytic fungus *Piriformospora indica* stimulates the expression of nitrate reductase and the starch-degrading enzyme glucan-water dikinase in tobacco and Arabidopsis roots through a homeodomain transcription factor that binds to a conserved motif in their promoters**. J Biol Chem 280 (28), 26241–26247. 10.1074/jbc.M500447200.

- Sherameti, I., Venus, Y., Drzewiecki, C., Tripathi, S., Dan, V.M., Nitz, I., Varma, A., Grundler, F.M., Oelmüller, R., 2008. **PYK10, a beta-glucosidase located in the endoplasmatic reticulum, is crucial for the beneficial interaction between *Arabidopsis thaliana* and the endophytic fungus *Piriformospora indica*.** Plant J 54 (3), 428–439. 10.1111/j.1365-3113X.2008.03424.x.
- Shinohara, N., Taylor, C., Leyser, O., 2013. **Strigolactone can promote or inhibit shoot branching by triggering rapid depletion of the auxin efflux protein PIN1 from the plasma membrane.** PLoS Biol 11 (1), e1001474. 10.1371/journal.pbio.1001474.
- Shrivastava, N., Jiang, L., Li, P., Sharma, A.K., Luo, X., Wu, S., Pandey, R., Gao, Q., Lou, B., 2018. **Proteomic approach to understand the molecular physiology of symbiotic interaction between *Piriformospora indica* and *Brassica napus*.** Sci Rep 8 (1), 5773. 10.1038/s41598-018-23994-z.
- Simard, S.W., Perry, D.A., Jones, M.D., Myrold, D.D., Durall, D.M., Molina, R., 1997. **Net transfer of carbon between ectomycorrhizal tree species in the field.** Nature 388, 579 EP - . 10.1038/41557.
- Stec, N., Banasiak, J., Jasiński, M., 2016. **Absciscic acid - an overlooked player in plant-microbe symbioses formation?** Acta Biochim Pol 63 (1), 53–58. 10.18388/abp.2015_1210.
- Stein, E., Molitor, A., Kogel, K.-H., Waller, F., 2008. **Systemic resistance in *Arabidopsis* conferred by the mycorrhizal fungus *Piriformospora indica* requires jasmonic acid signaling and the cytoplasmic function of NPR1.** Plant Cell Physiol 49 (11), 1747–1751. 10.1093/pcp/pcn147.
- Stringlis, I.A., Yu, K., Feussner, K., Jonge, R. de, van Bentum, S., van Verk, M.C., Berendsen, R.L., Bakker, P.A.H.M., Feussner, I., Pieterse, C.M.J., 2018. **MYB72-dependent coumarin exudation shapes root microbiome assembly to promote plant health.** Proc Natl Acad Sci U S A 115 (22), E5213-E5222. 10.1073/pnas.1722335115.
- Sun, C., Johnson, J.M., Cai, D., Sherameti, I., Oelmüller, R., Lou, B., 2010. ***Piriformospora indica* confers drought tolerance in Chinese cabbage leaves by stimulating antioxidant enzymes, the expression of drought-related genes and the plastid-localized CAS protein.** J Plant Physiol 167 (12), 1009–1017. 10.1016/j.jplph.2010.02.013.
- Sun, C., Shao, Y., Vahabi, K., Lu, J., Bhattacharya, S., Dong, S., Yeh, K.W., Sherameti, I., Lou, B., Baldwin, I.T., Oelmüller, R., 2014. **The beneficial fungus *Piriformospora indica* protects *Arabidopsis* from *Verticillium dahliae* infection by downregulation plant defense responses.** BMC Plant Biol 14 (1), 268. 10.1186/s12870-014-0268-5.
- Taylor, A., Qiu, Y.-L., 2017. **Evolutionary history of subtilases in land plants and their involvement in symbiotic interactions.** Mol Plant Microbe Interact 30 (6), 489–501. 10.1094/MPMI-10-16-0218-R.
- Tedersoo, L., May, T.W., Smith, M.E., 2010. **Ectomycorrhizal lifestyle in fungi: global diversity, distribution, and evolution of phylogenetic lineages.** Mycorrhiza 20 (4), 217–263. 10.1007/s00572-009-0274-x.

- Thürich, J., Meichsner, D., Furch, A.C.U., Pfalz, J., Krüger, T., Kniemeyer, O., Brakhage, A., Oelmüller, R., 2018. ***Arabidopsis thaliana* responds to colonisation of *Piriformospora indica* by secretion of symbiosis-specific proteins.** PloS One 13 (12), e0209658. 10.1371/journal.pone.0209658.
- Thürich, J., Oelmüller, R., 2019. **How does AtPARN connect RNA metabolism with calcium signalling?** In preparation
- Trappe, J.M., 2005. **A.B. Frank and mycorrhizae: the challenge to evolutionary and ecologic theory.** Mycorrhiza 15 (4), 277–281. 10.1007/s00572-004-0330-5.
- Vadassery, J., Oelmüller, R., 2009. **Calcium signaling in pathogenic and beneficial plant microbe interactions.** Plant Signal Behav 4 (11), 1024–1027. 10.4161/psb.4.11.9800.
- Vadassery, J., Ritter, C., Venus, Y., Camehl, I., Varma, A., Shahollari, B., Novak, O., Strnad, M., Ludwig-Muller, J., Oelmüller, R., 2008. **The role of auxins and cytokinins in the mutualistic interaction between *Arabidopsis* and *Piriformospora indica*.** Mol Plant Microbe Interact 21 (10), 1371–1383. 10.1094/MPMI-21-10-1371.
- Vahabi, K., Sherameti, I., Bakshi, M., Mrozinska, A., Ludwig, A., Reichelt, M., Oelmüller, R., 2015. **The interaction of *Arabidopsis* with *Piriformospora indica* shifts from initial transient stress induced by fungus-released chemical mediators to a mutualistic interaction after physical contact of the two symbionts.** BMC Plant Biol 15, 58. 10.1186/s12870-015-0419-3.
- van der Heijden, M.G.A., Martin, F.M., Selosse, M.-A., Sanders, I.R., 2015. **Mycorrhizal ecology and evolution: the past, the present, and the future.** New Phytol 205 (4), 1406–1423. 10.1111/nph.13288.
- Varma, A., Savita, V., Sudha S., Sahay, N., Butehorn, B., Franken, P., 1999. ***Piriformospora indica*, a cultivable plant-growth-promoting root endophyte.** Appl Environ Microbiol 65 (6), 2741–2744.
- Veiga, R.S.L., Faccio, A., Genre, A., Pieterse, C.M.J., Bonfante, P., van der Heijden, M.G.A., 2013. **Arbuscular mycorrhizal fungi reduce growth and infect roots of the non-host plant *Arabidopsis thaliana*.** Plant Cell Environ 36 (11), 1926–1937. 10.1111/pce.12102.
- Verma, S., Varma, A., Rexer, K.-H., Hassel, A., Kost, G., Sarbhoy, A., Bisen, P., Butehorn, B., Franken, P., 1998. ***Piriformospora indica*, gen. et sp. nov., a new root-colonizing fungus.** Mycologia 90 (5), 896. 10.2307/3761331.
- Virtanen, A., Henriksson, N., Nilsson, P., Nissbeck, M., 2013. **Poly(A)-specific ribonuclease (PARN): an allosterically regulated, processive and mRNA cap-interacting deadenylase.** Crit Rev Biochem Mol Biol 48 (2), 192–209. 10.3109/10409238.2013.771132.
- Volpe, V., Chitarra, W., Cascone, P., Volpe, M.G., Bartolini, P., Moneti, G., Pieraccini, G., Di Serio, C., Maserti, B., Guerrieri, E., Balestrini, R., 2018. **The association with two different arbuscular mycorrhizal fungi differently affects water stress tolerance in tomato.** Front Plant Sci 9. 10.3389/fpls.2018.01480.

- Waller, F., Achatz, B., Baltruschat, H., Fodor, J., Becker, K., Fischer, M., Heier, T., Hückelhoven, R., Neumann, C., Wettstein, D. von, Franken, P., Kogel, K.-H., 2005. **The endophytic fungus *Piriformospora indica* reprograms barley to salt-stress tolerance, disease resistance, and higher yield.** Proc Natl Acad Sci U S A 102 (38), 13386–13391. 10.1073/pnas.0504423102.
- Weiß, M., Waller, F., Zuccaro, A., Selosse, M.-A., 2016. **Sebacinales - one thousand and one interactions with land plants.** New Phytol 211 (1), 20–40. 10.1111/nph.13977.
- Xu, L., Wu, C., Oelmüller, R., Zhang, W., 2018. **Role of phytohormones in *Piriformospora indica*-induced growth promotion and stress tolerance in plants: more questions than answers.** Front Microbiol 9, 1646. 10.3389/fmicb.2018.01646.
- Yang, X., Baskin, J.M., Baskin, C.C., Huang, Z., 2012. **More than just a coating: ecological importance, taxonomic occurrence and phylogenetic relationships of seed coat mucilage.** Perspect Plant Ecol Syst 14 (6), 434–442. 10.1016/j.ppees.2012.09.002.
- Zhang, X., Devany, E., Murphy, M.R., Glazman, G., Persaud, M., Kleiman, F.E., 2015. **PARN deadenylase is involved in miRNA-dependent degradation of *tp53* mRNA in mammalian cells.** Nucleic Acids Res 43 (22), 10925–10938. 10.1093/nar/gkv959.
- Zipfel, C., Oldroyd, G.E.D., 2017. **Plant signalling in symbiosis and immunity.** Nature 543 (7645), 328–336. 10.1038/nature22009.
- Zuccaro, A., Lahrmann, U., Güldener, U., Langen, G., Pfiffi, S., Biedenkopf, D., Wong, P., Samans, B., Grimm, C., Basiewicz, M., Murat, C., Martin, F., Kogel, K.-H., 2011. **Endophytic life strategies decoded by genome and transcriptome analyses of the mutualistic root symbiont *Piriformospora indica*.** PLoS Pathog 7 (10), e1002290. 10.1371/journal.ppat.1002290.

Supplementary Material

Acknowledgment

First of all, I would like to thank Prof. Oelmüller from the Matthias Schleiden Institute – Department of Plant Physiology and Prof. Brakhage from the Leibniz Institute for Natural Product Research and Infection Biology – Hans Knöll Institute for giving me the opportunity to work with them and learn much about plant-microbial interaction.

Furthermore, I would like to thank my former co-workers for their valuable input and support. In addition, I would like to thank my external partner from which I learned a lot as well.

A special thanks goes out to the other members of ChemBioSys. Many fruitful discussions and the possibility to simply try new techniques and ideas was incredibly rewarding.

Last, but definitely not least: Thank you Juer and Veronika for everything. Also, thanks to all of my family and friends which supported me a lot.

Ehrenwörtliche Erklärung

Hiermit erkläre ich, dass mir die Promotionsordnung der Biologisch-Pharmazeutischen Fakultät der Friedrich-Schiller-Universität bekannt ist und ich insbesondere die Anforderungen entsprechend §5 4 erfülle. Das heißt, dass ich die Dissertation selbst angefertigt habe. Textabschnitte Dritter sowie eigene Arbeiten habe ich nicht ohne Kennzeichnung übernommen und alle von mir benutzten Hilfsmittel, persönliche Mitteilungen und Quellen angegeben. Personen, die mich bei der Auswahl und Auswertung des Materials und des Manuskripts unterstützt haben, wurden genannt. Weder wurde die Hilfe eines Promotionsberaters in Anspruch genommen, noch haben Dritte unmittelbare oder mittelbare geldwerte Leistungen für Arbeiten erhalten, die im Zusammenhang mit dem Inhalt dieser Dissertation stehen. Schlussendlich wurde diese Arbeit oder Teile davon nicht zuvor an der Uni Jena noch an anderen Hochschulen als Prüfung oder Dissertation eingereicht.

Jena, 18.06.2020

A handwritten signature in blue ink, reading "Johannes Thürich". The signature is written in a cursive style with a blue ink stamp or background behind it.

Johannes Thürich